

DOT HS 807 034
Final Report

August 1986

Preliminary Development -- Head-Neck Simulator

Volume I: Analysis Volunteer Tests



The United States Government does not endorse products or manufacturers. Trade or manufacturers' names appear only because they are considered essential to the object of this report.

1. Report No. DOT HS 807 034		2. Government Accession No.		3. Recipient's Catalog No.	
4. Title and Subtitle ✓ Preliminary Development, Head-Neck Simulator, ✓ VOLUME I: Analysis Volunteer Tests		5. Report Date August 1986		6. Performing Organization Code	
7. Author(s) Wismans, J. S. H. M.		8. Performing Organization Report No. 700560478-A		9. Performing Organization Name and Address Research Institute for Road Vehicles TNO Delft, The Netherlands	
10. Work Unit No. (TRAIS)		11. Contract or Grant No.		12. Sponsoring Agency Name and Address Vehicle Research and Test Center National Highway Traffic Safety Admin. 400 7th Street, S.W. Washington, D.C. 20590	
13. Type of Report and Period Covered Sept. 82 - Oct. 84 FINAL REPORT		14. Sponsoring Agency Code Project SRL-59		15. Supplementary Notes	
16. Abstract This report documents the initial work of an ongoing research program of which the objective is to develop a head-neck simulator with omni-directional biofidelity. The report is composed of two volumes: VOLUME I: Analysis Volunteer Tests and VOLUME II: Mathematical Simulations. In VOLUME I, a detailed analysis is presented of a large number of human volunteer tests conducted by the Naval Biodynamics Laboratory in New Orleans. These human subjects were exposed to frontal, lateral and oblique impacts with an impact severity up to 15 g and 17 m/s. This analysis results for each impact direction in a simple analog system that completely specifies the observed dynamical behavior. VOLUME II documents the validation of the proposed analog systems and compares the behavior of the Part 572 and Hybrid III head-neck systems with the human volunteer behavior. It follows that both neck designs are stiffer than any of the volunteers in the impact ranges tested. Preliminary results are presented of computer aided design activities in order to improve existing designs in view of these new findings.					
17. Key Words Head-Neck Simulator MADYMO Part 572 Dummy Hybrid III Dummy Anthropomorphic Test Device			18. Distribution Statement Document is available to the public from the National Technical Information Service, Springfield, VA 22161		
19. Security Classif. (of this report) Unclassified		20. Security Classif. (of this page) Unclassified		21. Na. of Pages	
				22. Price	

ABSTRACT

This report documents the work conducted in phase I of an ongoing research program of which the objective is to develop a head-neck simulator with omni-directional biofidelity. The report is composed of two volumes:

Vol. I : Analysis volunteer tests

Vol. II : Mathematical simulations

In Vol. I a detailed analysis is carried out of a large number of human volunteer tests conducted by the Naval Biodynamics Laboratory in New Orleans. These human subjects were exposed to frontal, lateral and oblique impacts with an impact severity up to 15 g and 17 m/s. This analysis results for each impact direction in a simple analog system that completely specifies the observed dynamical behaviour.

Vol. II documents the validation of the proposed analog systems and compares the behaviour of the Part 572 and Hybrid III head-neck systems with the human volunteer behaviour. It follows that both neck designs are stiffer than any of the volunteers in the impact ranges tested. Preliminary results are presented of computer aided design activities in order to improve existing designs in view of these new findings.



TABLE OF CONTENTS

ABSTRACT	iii
LIST OF TABLES	vii
LIST OF FIGURES	viii
CHAPTER	
1. INTRODUCTION	i
1.1 Project description and objectives	1
1.2 Summary research program: analysis of volunteer tests	2
1.3 Performance Requirements	3
1.4 Literature review: Human volunteer tests conducted by NBDL	6
2. DATABASE DESCRIPTION (SUBJECT H00083 AND H00093)	9
2.1 Test method	9
2.2 Instrumentation	9
2.3 Processed data obtained from NBDL	11
2.4 Test conditions of 30 selected tests	14
3. COORDINATE SYSTEMS AND HUMAN SUBJECT ANTROPOMETRY	17
3.1 Introduction	17
3.2 Head and T1 anatomical coordinate systems	17
3.3 Laboratory and sled coordinate systems	18
3.4 Human subject anthropometric measurements	20
3.5 Head mass and moments of inertia	20
3.6 Location of center of gravity and occipital condyles	22
4. ANALYSIS OF T1 MOTION AND CORRECTION OF T1 COORDINATE SYSTEM	25
4.1 Introduction	25
4.2 T1 motion in the plane of impact and T1 initial orientation	25
4.3 The initial neck length	28
4.4 Correction of T1 coordinate system	28
5. ANALYSIS OF RELATIVE HEAD MOTION	33
5.1 General	33
5.2 Head trajectories and displacements of the head anatomical z-axis in the impact plane	34
5.3 Geometrical properties of the linkage mechanism	34
5.4 Head torsion and neck link rotation as function of head flexion	35

6.	LOAD CALCULATIONS	43
6.1	Introduction	43
6.2	Occipital condyle and T1 torques	44
7.	PERFORMANCE REQUIREMENTS BASED ON NBDL TESTS WITH TWO SUBJECTS	51
7.1	Introduction	51
7.2	Literature review linkage mechanisms for head-neck motion	52
7.3	The analog system	53
8.	ANALYSIS OF ADDITIONAL TESTS WITH OTHER SUBJECTS	57
8.1	Introduction	57
8.2	Frontal impact tests	57
8.3	Lateral impact tests	60
9.	DISCUSSION AND CONCLUSIONS	65
	ACKNOWLEDGEMENT	69
	REFERENCES	71

APPENDIX A - Comparison of sled acceleration and horizontal T1 acceleration
in 30 selected tests with subject H00083 and H00093

APPENDIX B - Relative head motions in 30 selected tests in plane of impact

LIST OF TABLES

TABLE		PAGE
1	Test results for the head, T1 and sled motions available on the NBDL data tapes	12
2	Selected set of kinematic variables on NBDL data tapes	13
3	Test characteristics of 30 selected runs with 2 human volunteers (H00083 and H00093)	15
4	Selected Human Subject Anthropometry	20
5	Coefficients in regression eqs. (2-5)	21
6	Estimations for Masses and Moments of Inertia	22
7	Location of center of gravity and occipital condyles with respect to head anatomical coordinate system	23
8	Location of lower pivot relative to corrected T1 coordinate systems for a neck link length of 0.125 m	38
9	Initial and maximum values in degrees for head flexion ϕ , head torsion ψ and neck link rotation θ	41
10	Linkage parameters for the loading phase based on 30 impact tests with two subjects (H00083 and H00093)	56
11	Test characteristics of earlier test with 10 different subjects in frontal impacts (7)	58
12	Selection of test results provided in reference (7)	59
13	Initial and maximum values for the head rotation ϕ and the link rotation θ (in degrees)	59
14	Test characteristics of 16 selected runs with 6 human volunteers in lateral flexion	61
15	Initial and maximum head flexion ϕ and neck link rotation θ (in degrees) in lateral flexion	61

LIST OF FIGURES

FIGURE NO.		PAGE
1	Head-neck response envelopes for the loading phase according to Mertz et al. (2).	4
2	A preliminary torque rotation response corridor for lateral flexion according to Patrick and Chou (5).	5
3	Six-accelerometer system 3-2-1 configuration (12).	10
4	Instrumented human volunteer (9).	11
5	Comparison of sled accelerations in the most severe frontal, lateral and oblique test.	16
6	Location of head and T1 anatomical coordinate systems (o.c. = occipital condyles, c.g. = center of gravity).	18
7	Rough orientation of head and T1 anatomical coordinate systems relative to laboratory and sled coordinate system in case of frontal, oblique and lateral impacts.	19
8	Displacement of T1 anatomical origin relative to sled in plane of impact. Vertical line segments indicate position of T1 z-axis at different time frames.	26
9	Typical examples of horizontal T1 and sled acceleration as function of time in three different impact directions. —— = T1;----- = sled.	27
10	Initial neck length (i.e. distance between head and T1 anatomical origin at time = 0) in 85 tests with subjects H00083 and H00093.	30
11	Initial vertical position of the head and T1 anatomical origin relative to the sled coordinate system as a function of the initial neck length.	31
12	Head displacements relative to corrected T1 coordinate system for three impact directions. Upper curves: head anatomical origin. Lower curves: occipital condyles. Stick figures: head z-axis at 50, 100 and 150 ms.	35
13	Two-pivot linkage mechanism.	36
14	Neck link rotation ($\theta - \theta_0$) as function of head flexion ($\phi - \phi_0$) in 30 tests with 2 subjects.	40
15	Head torsion ($\psi - \psi_0$) as function of head flexion ($\phi - \phi_0$) in 19 tests with 2 subjects.	42

16	Torque M_ϕ near occipital condyles about an axis perpendicular to the plane of impact as function of head flexion $(\phi - \phi_0)$.	45
17	Torque M_ϕ near occipital condyles about an axis perpendicular to the plane of impact as function of the relative angle between head and neck link $(\theta - \theta_0) - (\phi - \phi_0)$.	46
18	Torque M_ψ near occipital condyles about the head anatomical z-axis as function of head torsion $(\psi - \psi_0)$.	47
19	Torque M_θ near the corrected T1 origin about an axis perpendicular to the plane of impact as function of neck rotation $(\theta - \theta_0)$.	49
20	Three-dimensional linkage according to Becker (41,42).	54
21	Comparison of sled accelerations.	58
22	Neck link flexion $(\theta - \theta_0)$ and head link torsion $(\psi - \psi_0)$ as function of head flexion $(\phi - \phi_0)$ in 16 lateral impacts with subjects H00044, H00064, H00065, H00067, H00083 and H00093.	63



CHAPTER 1

INTRODUCTION

1.1 Project description and objectives

The National Highway Traffic Safety Administration (NHTSA) has available large quantities of test data on the head and neck response of human volunteer subjects in frontal, oblique and lateral sled tests. The Vehicle Research and Test Center (VRTC) will use this data for the development of an improved head/neck motion simulator. Where possible, this human test data will be supplemented by data of human cadavers tested at exposure levels beyond those generally acceptable for human volunteers.

One or more candidate mechanical systems will be identified to reproduce observed head/neck motions. Existing models will form the basis for this analysis but the study will not necessarily be limited to such models. The performance of candidate mechanical neck simulators will be analyzed and optimized using mathematical model simulations resulting finally in design specification for an improved dummy neck.

This report presents the results of phase I of this ongoing research program. The report is composed of two volumes:

Volume I : Analysis volunteer tests

Volume II: Mathematical simulations.

In Vol. I an analysis is presented of a number of human volunteer tests in three different impact directions conducted at the Naval Biodynamics Laboratory (NBDL)*. This analysis results for each impact direction in an analog system that completely specifies the observed dynamical behaviour.

Vol. II documents the validation of the proposed analog systems by means of mathematical simulations and presents a number of preliminary computer aided design activities in order to improve existing dummy necks in view of these new findings.

* NBDL: Naval Biodynamics Laboratory in New Orleans; Previously Naval Aerospace Medical Research Laboratory Detachment (NAMRLD).

1.2 Summary research program: analyses of volunteer tests

Realistic simulation of the neck response in a dummy is of vital importance to get a humanlike dynamical behaviour of the head. Trajectories of the head and the nature of the head contact with vehicle interior or exterior are critically dependent on the dummy's neck design. In literature neck performance criteria are limited to the neck response in forward flexion and extension. Section 1.3 will review these requirements and it will be shown that the present requirements are not sufficient conditions to ensure humanlike response in frontal impact direction. Moreover, increasing research activities in the field of side impact and pedestrian protection clearly show the need for additional requirements in lateral and oblique direction.

In the past years the Naval Biodynamics Laboratory (NBDL) has conducted an extensive research program to determine the dynamic head-neck response of volunteer subjects under various test conditions and impact directions. In section 1.4 a brief review will be presented of relevant literature in this respect. Up to now no concrete recommendations for performance requirements have been based on these NBDL tests.

The analysis of the human volunteer tests in this study is based on detailed test results on magnetic tape, obtained from NBDL. Chapter 2 will summarize the NBDL test methodology, test conditions and the instrumentation used in the tests. A description will be given of the type of test parameters available on the magnetic tapes and of the selected test data used in our study. Coordinate system definitions by NBDL and the human subject antropometry will be described in chapter 3.

A computer program was developed that allows visualisation of the head and T1 displacements on the basis of the test results available on magnetic tape. Chapter 4 will present results for the T1 displacements and chapter 5 for the relative head motion. Significant variations can be observed in the initial neck length in different tests with the same subject (see chapter 4). It will be shown that these variations are mainly due to errors in the specification of the T1 coordinate system. A method will be proposed to correct for these errors.

From the analysis of the relative head displacements in chapter 5 it follows that the motions in frontal, lateral as well as oblique impacts can be quite realistically approximated by means of a 2-pivot linkage with 2 degrees of freedom in frontal impacts and 3 degrees of freedom in lateral and oblique impacts.

Chapter 6 deals with the calculation of loads applied by the neck to the head near the occipital condyles and the T1 origin. For frontal impacts, results of these calculations are compared with the response corridors proposed by Mertz et al. On the basis of these load calculations dynamical elements (joint properties) for the 2-pivot linkage will be defined (chapter 7). Chapter 8 briefly discusses an evaluation of some of the earlier tests conducted by NBDL and a comparison with our findings.

The major findings and conclusions of this research program as far as the analysis of the human volunteer tests is concerned, are discussed and summarized in Chapter 9.

1.3 Literature review: performance requirements

In the early seventies performance requirements for dynamical head-neck behaviour in frontal impacts were proposed by Mertz et al. (1,2), based on static and dynamical tests with volunteers and human cadavers. Neck response was defined by the relation between the torque about the occipital condyles and the angular position of the head. Resulting performance corridors specifically for the loading phase are shown in Fig. 1. For unloading motion a ratio was defined for the area under the unloading curve with respect to the area under the loading curve. Separate corridors for flexion and extension motions were developed. Human volunteer dynamical tests in this study were limited to one subject, partly tested with an additional weight attached to the head. An evaluation of several neck designs with respect to these requirements is incorporated in ref.(2).

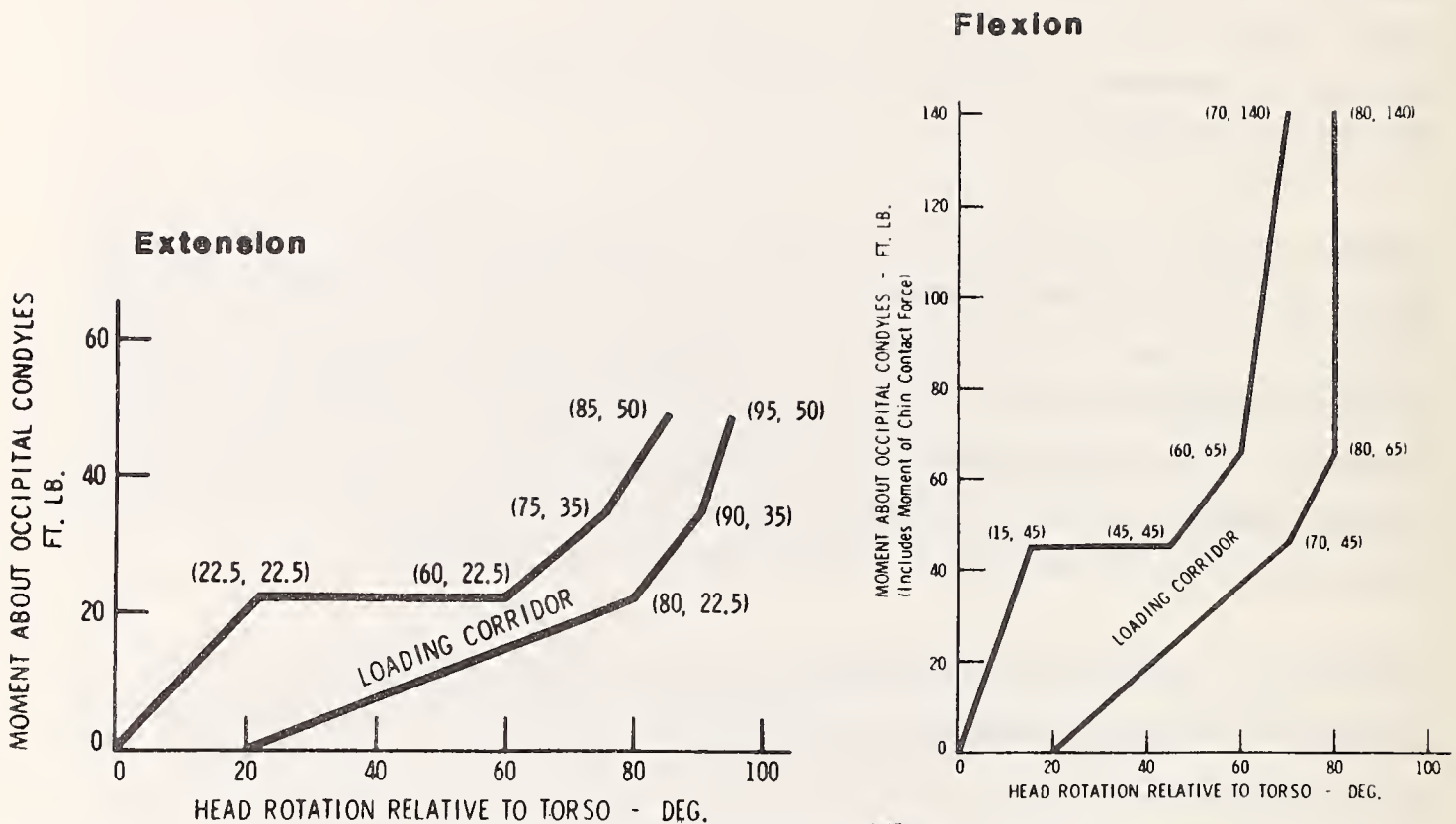


Fig. 1 Head-neck response envelopes for the loading phase according to Mertz et al. (2).

Such requirements, however, are not sufficient conditions to ensure human-like response (2). Both Mertz et al. (2) and Melvin et al. (3) discuss additional displacement requirements such as a center of gravity trajectory, but concrete recommendations in this respect have not been formulated.

A more recent paper by Muzzy and Lustick (4) illustrates the need for these type of requirements. In their study displacements of the Hybrid II head-neck system were compared with human volunteers in 10 g frontal impacts. The complete dummy was tested in a restraint system similar to that of the human volunteers. Significant differences in the displacements of the head center of gravity and the head angle relative to the torso were observed: the Hybrid II neck was found to be stiffer than the volunteer.

A preliminary torque rotation response corridor for lateral flexion was proposed by Patrick and Chou (5). This corridor which is shown in Fig. 2,

was based on 4 dynamic tests with 2 human volunteers. Torque-rotation curves with respect to the occipital condyles for the individual tests are included in Fig. 2. Considerable differences between both volunteers can be observed.

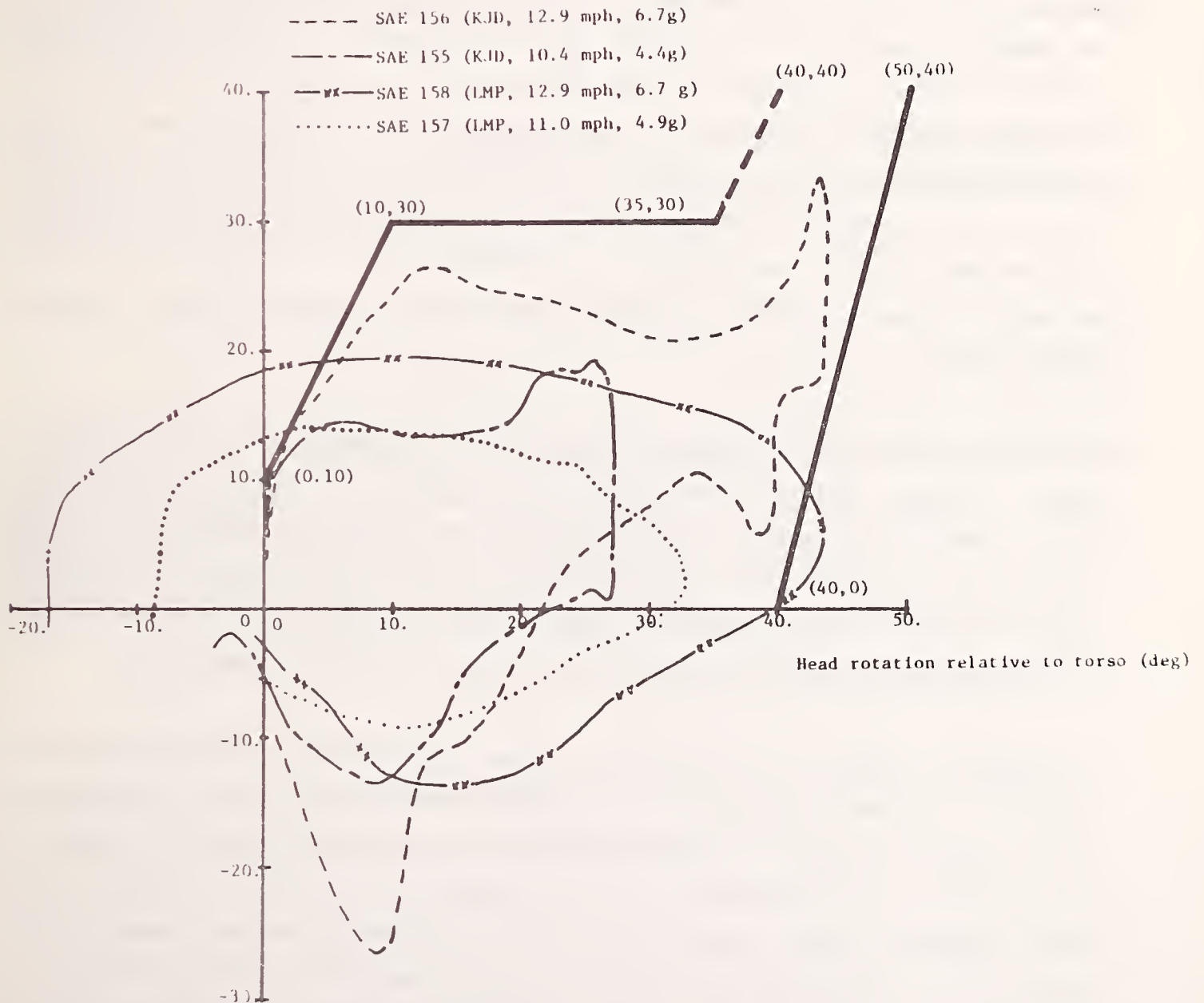


Fig. 2 A preliminary torque rotation response corridor for lateral flexion according to Patrick and Chou (5).

Neck performance requirements used in a recent evaluation of four side impact dummies were limited to the maximum head lateral flexion as observed in volunteer and cadaver tests neglecting the typical three-dimensional nature of lateral head neck motions in a dynamical environment (6).

In contrast to frontal and lateral impacts, for oblique motion no response requirements are reported in literature.

1.4 Literature review: human volunteer tests conducted by NBDL

A detailed description of the test methodology in the NBDL tests is provided in references (7-12) and will be summarized in section 2.1 (test method). The first experiments in the NBDL test program were conducted on the WHAM II accelerator at Wayne State University in the period between 1967 and 1969. In total 236 experiments with 15 subjects in frontal flexion were conducted. Head and T1 accelerations and velocity time histories of 18 representative runs involving 6 subjects are presented in references (13-15). More detailed results including head displacement-time histories with respect to T1, can be found in reference (7). As a part of our study an analysis has been made of displacement data provided in this reference (see chapter 8).

By Ewing and Thomas (16) torque-angular displacement characteristics for some of these tests were determined and compared with data of Mertz et al. (1,2). Due to different instrumentation and measuring techniques several differences were noted, in particular in the initial phase of the motion where the sign of the occipital torque was the opposite of the Mertz data. For larger head excursions torque data were found to be comparable.

A subsequent series of 100 frontal impact runs with 13 volunteers was conducted in the early seventies on the HYGE accelerator of the laboratory of NBDL. Newly developed instrumentation and photographic mount were used. The main objective of this study was the analysis of the effect of the initial head position on head linear and angular accelerations and angular velocities (17). A considerable influence of the head-neck initial position was reported. In an additional test program of 75 tests, the effect of sled pulse duration, rate of onset and peak acceleration on head accelerations and head velocities was evaluated (18). The experimental results were found to be affected considerably by these changes in experimental conditions.

The pelvic response in these type of impacts was measured in a test program with one subject. Significant differences were observed between T1 and pelvis acceleration-time histories due to relatively larger motion of T1 permitted by the restraint system and due to chest deformation (19).

More recently a large number of lateral and oblique tests were conducted by NBDL. A detailed description of test method and test results for the first serie of lateral tests (i.e. 34 experiments with 6 subjects) is provided in ref. (10). Based on additional test data obtained from NBDL, in our study an analysis was made of some of the most severe tests in this test program (see chapter 8).

Ref. (20) presents for a subsequent test series with 5 subjects, head accelerations and velocities as function of time. Various sled acceleration profiles were used with peak values up to 11 g.

In ref. (21) the effect of initial head-neck position on head accelerations, velocities and displacements for 100 lateral tests with 6 human subjects, was evaluated. Peak sled accelerations in these experiments ranged from 2-7 g. As with for the frontal impacts a significant effect of the initial head-neck position was observed. One of the subjects incorporated in this test program i.e. subject H00083, is also incorporated in the database to be analysed in the present study.



CHAPTER 2

DATABASE DESCRIPTION (SUBJECTS H00083 AND H00093)

2.1 Test method

In the tests conducted at NBDL the subjects are seated on a Bendix HYGE pneumatically driven 0.3048 diameter accelerator. The sled mass is 1669 kg and the acceleration stroke is limited to 1.52 m (12). In the frontal impact tests the subjects are in an upright position restrained by shoulder straps, a lap belt and an inverted V-pelvic strap tied to the lap belt. Upper arm and wrist restraints are used to prevent flailing (12). In addition a loose safety belt around the chest is employed. The same restraint system is used in lateral and oblique tests. In addition a lightly padded wooden board is placed against the right shoulder of the subject to limit the upper torso motion.

In frontal impacts the thrust vector is nominally directed from chest to back and in lateral impacts from the right to the left shoulder (Fig. 7). In oblique tests the thrust vector is directed from right-front to left-back (angle between thrust vector and left-right axis is 45 degrees).

2.2 Instrumentation

The resulting three-dimensional motions of the head and first thoracic vertebral body (T1) are monitored by anatomically mounted clusters of accelerometers and photographic targets. Both the head and T1 are equipped with six piezo-resistive accelerometers mounted on a T-shaped plate at the mouth and at the spinous process of T1 (Fig. 3). The configuration of the accelerometers and the error propagation associated with this method for determining kinematic quantities has been described by Becker and Willems (9). More recently the application of a nine-accelerator configurations at NBDL has also been reported (22).

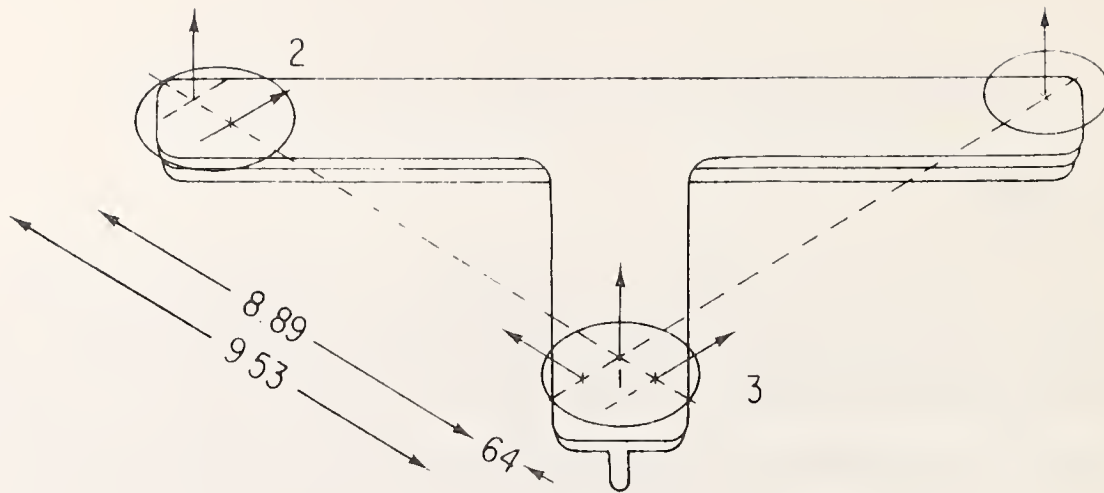


Fig. 3 Six-accelerometer system 3-2-1 configuration (12).

In addition to the accelerometers, a two axis rate gyroscope is mounted on both T plates. The resulting data are used as an independent measurement of two components of the angular velocity of the head and neck (12). Test data, obtained within the present study from NBDL, did not include this type of gyroscopic based data.

Groups of black and white phototargets are connected to the T plates carried by head and T1 (Fig. 4). Cinephotographic coverage of these targets is provided by sled mounted camera's (pin-registered 16 mm, 500 frames per second), situated orthogonally to each other at approximately one meter from the subject (8,12). This method permits three-dimensional displacements of head and T1 to be determined relative to the sled.

In order to compare subjects at similar points in the anatomy, it is necessary to define head and T1 anatomical coordinate system (see chapter 3). These antropometric coordinate systems are related to instrumentation coordinate systems by means of three-dimensional X-ray techniques (11).



Fig. 4 Instrumented human volunteer (9).

2.3 Processed data obtained from NBDL

Data processing by NBDL includes conversion of photo and sensor data into kinematics of the head and T1 anatomical coordinate systems. The solution for the kinematic variables derived from accelerometer data requires initialisation of location and orientation from photo derived data and integration of the non-linear differential equations defined by expressions for the accelerometer measurements (9). The solution for displacements and angular rotations is obtained by a least square algorithm, which makes use of measurements in the film plane from two different cameras (8). Successive differentiation is used to determine velocity components from the photo derived displacements.

In this way for each test 91 kinematic variables as function of time are available on the tapes obtained from NBDL. Table 1 provides a summary of this data. Components of rotations, translations, linear velocities and linear accelerations are all expressed with respect to the laboratory or sled coordinate system while components of angular velocities and accelerations are given with respect to anatomical coordinate systems.

Table 1 - Test results for the head, T1 and sled motions
available on the NBDL data tapes

- Translations and linear velocities of the head and T1 anatomical origins with respect to the sled, derived from photographic as well as accelerometer data (24)*.
- Translations, linear velocities and linear accelerations of head and T1 anatomical origins with respect to the laboratory, derived from accelerometer data (18).
- Angular velocities of the head and T1 about the anatomical coordinate axes derived from photographic as well as accelerometer data (12).
- Angular accelerations of the head and T1 about the anatomical coordinate axes, derived from accelerometer data (6).
- Rotations of the head and T1 expressed in euler angles as well as quaternions with respect to the laboratory, derived from photographic as well as accelerometer data (28).
- Acceleration, velocity and displacement of the sled with respect to the x-axis of the laboratory (3).

* Number of variables in this category.

Some of the kinematic variables are derived independently from accelerometer as well as photographic measurements (i.e. linear translations and linear velocities relative to the sled, rotations and angular velocities). A comparison between these data showed discrepancies in a number of cases particularly in some of the tests with large three-dimensional motions (head motion in lateral and oblique impacts). Such differences also have been reported by NBDL (23). Optimal combination of the results from both sets of measurements into one consistent set of kinematic variables is one of the objects of the NBDL research program (23).

Our further analysis will be based on a subset out of the 91 NBDL variables. Table 2 summarizes these variables together with a code defined by NBDL to identify these variables on the tapes. A complete description of all 91 variables is provided in ref. (10). The displacements data (translations and rotations) in this subset are derived from photographic data while the accelerations are derived from accelerometer data. Head angular velocities which are required for the load calculations described in chapter 6, are based on accelerometer data.

Table 2 Selected set of kinematic variables on NBDL data tapes

NBDL Definition	Description
AAXXOS AAYXOS AAZXOS	Linear accelerations of the head anatomical origin along the x-axis (AAXXOS), the y-axis (AAYXOS) and the z-axis (AAZXOS) respectively of the laboratory coordinate system with respect to the fixed laboratory coordinate system as derived from accelerometer data.
ANXXOS ANYXOS ANZXOS	Linear accelerations of the T1 anatomical origin defined corresponding to the linear head accelerations AAXXOS, AAYXOS and AAZXOS.
QHAOXS QHBOXS QHCOXS	Angular accelerations of the head about the x-axis (QHAOXS), y-axis (QHBOXS) and z-axis (QHCOXS) respectively of the head anatomical coordinate system as derived from accelerometer data.
QNAOXS QNBOXS QNCOXS	Angular accelerations of T1 about the x-axis (QNAOXS), y-axis (QNBOXS) and z-axis (QNCOXS) respectively of the T1 anatomical coordinate system as derived from accelerometer data.
RHAOXS RHBOXS RHCOXS	Angular velocities of the head about the x-axis (RHAOXS), the y-axis (RHBOXS) and the z-axis (RHCOXS) respectively of the head anatomical coordinate system as derived from accelerometer data.
ACXXOS VCXXOS	Linear acceleration (ACXXOS) and linear velocity (VCXXOS) of the sled along the x-axis of the laboratory coordinate system with respect to the fixed laboratory coordinate systems as derived from sled mounted accelerometer data.
DAXSOP DAYSOP DAZSOP	Linear displacements of the head anatomical origin along the x-axis (DAXSOP), the y-axis (DAYSOP) and the z-axis (DAZSOP) respectively of the sled coordinate system with respect to the sled coordinate system as derived from photo target data.
DNXSOP DNYSOP DNZSOP	Linear displacements of the T1 anatomical origin defined corresponding to the linear head displacements DAXSOP, DAYSOP and DAZSOP.
4H001P 4H002P 4H003P 4H004P	Quaternions - The four variables which define the angular orientation of the head anatomical coordinate system relative to the laboratory coordinate system as derived from photo target data (see eq. (1)).
4N001P 4N002P 4N003P 4N004P	Quaternions - The four variables which define the angular orientation of the T1 anatomical coordinate system relative to the laboratory coordinate system as derived from photo target data.
PHC03P	Angle of rotation (euler angle) of the head about the z-axis of the head anatomical coordinate system as derived from photo target. (Head anatomical coordinate system is initially aligned with the laboratory coordinate system).

Quarternians will be used to define the angular orientation of head and Tl. The transformation matrix to transform a vector from the anatomical coordinate system to the laboratory coordinate system in terms of quarternians is as follows (10):

$$A = \begin{vmatrix} q_4^2 + q_1^2 - q_2^2 - q_3^2 & 2(q_1q_2 - q_3q_4) & 2(q_1q_3 + q_4q_2) \\ 2(q_4q_3 + q_1q_2) & q_4^2 + q_2^2 - q_1^2 - q_3^2 & 2(q_2q_3 - q_4q_1) \\ 2(q_1q_3 - q_4q_2) & (2q_1q_4 + q_3q_2) & q_4^2 + q_3^2 - q_1^2 - q_2^2 \end{vmatrix} \quad (1)$$

where: $q_1 = 4H001P$ (4N001P)

$q_2 = 4H002P$ (4N002P)

$q_3 = 4H003P$ (4N003P)

$q_4 = 4H004P$ (4N004P)

In addition to quarternians euler angles are also provided on tape. These angles are defined by NBDL as follows: The angular orientation of a body is thought to be the result of three successive rotations. Before the first rotation the coordinate system of the body (head or Tl) coincides with the laboratory (sled) coordinate system. The first rotation is carried out about the x-axis. The second rotation is performed about the carried y-axis of the body and the third rotation about the carried z-axis. The third euler angle for the head (denoted by PHC03P in Table 2) will be used here for evaluation of the head twist in lateral and oblique impacts.

Accelerometer derived data are provided on the tapes with a time interval of 0.0005 s. Photographic derived variables are related to the time-base by a separate time-channel (time interval ≈ 0.002 s).

2.4 Testconditions of 30 selected tests

Datatapes containing the results of 85 human volunteer tests with subject H00083 and H00093 were obtained from NBDL. The number of frontal, lateral and oblique tests in this database is 14, 30 and 41 respectively. Out of these tests a subset of 30 of the most severe experiments is selected to be used for the analysis presented in this report. Table 3 summarizes these tests and the most important test characteristics. The selection of this subset was based on the following criteria:

- no large data gaps or data shifts in the photographic derived variables
- omission of test with a low impact level (i.e. low sled velocities and/or low sled accelerations)
- no large forward or lateral bending of the head and neck in the initial position.

Table 3 - Test characteristics of 30 selected runs with 2 human volunteers (H00083 and H00093).

Subject	Test number	Sled velocity change (m/s)	Peak sled ₂ acc. (m/s ²)	Rate ₃ of onset* (m/s ³)
<u>FRONTAL</u>				
H00083	LX3530	7.5	49	982
H00083	LX3536	10.5	73	1613
H00083	LX3544	12.4	92	2205
H00093	LX3531	7.6	51	1050
H00093	LX3537	10.1	71	1585
H00093	LX3548	12.2	90	2142
H00093	LX3550	13.3	98	2498
H00093	LX3558	14.3	110	2903
H00093	LX3578	16.0	132	3898
H00093	LX3583	16.7	142	4269
H00093	LX3616	17.2	150	4873
<u>LATERAL</u>				
H00083	LX1831	6.5	49	3229
H00083	LX2013	6.3	49	1079
H00083	LX2124	3.1	89	9435
H00083	LX2302	6.4	69	1497
H00093	LX2151	3.3	100	11075
H00093	LX2326	6.5	60	5764
H00093	LX2355	6.5	50	4961
<u>OBLIQUE</u>				
H00083	LX2786	7.5	50	7061
H00083	LX2872	9.0	61	8642
H00083	LX3093	10.3	71	1595
H00083	LX3102	9.0	60	1337
H00083	LX3133	8.8	79	1839
H00083	LX3153	8.8	80	8461
H00093	LX2784	7.5	50	6802
H00093	LX2843	3.0	89	1302
H00093	LX3122	8.9	79	1857
H00093	LX3148	8.9	97	2573
H00093	LX3158	8.8	78	8669
H00093	LX3417	8.8	59	3404

* Slope of the best least square line fit of the rising portion of the sled acceleration profile between 20% and 50% of the peak sled acceleration.

The resulting subset contains 11 frontal, 7 lateral and 12 oblique impacts. Sled acceleration time histories (ACXXOS) for the tests in this database are incorporated in Annex A. Fig. 5 presents a comparison of the sled accelerations in the most severe frontal, lateral and oblique test (i.e. LX3616, LX2302 and LX3148, respectively). The oblique test appears to be more severe than the lateral one, while the frontal test is more severe than the oblique one.

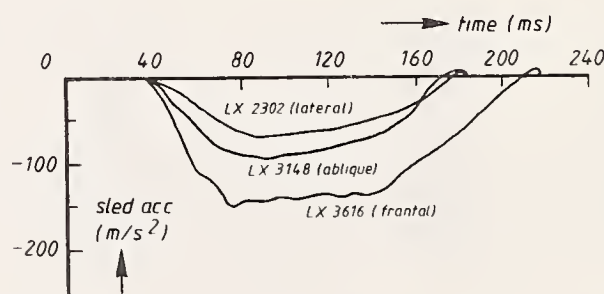


Fig. 5 Comparison of sled accelerations in the most severe frontal, lateral and oblique test.

CHAPTER 3

COORDINATE SYSTEMS AND HUMAN SUBJECT ANTHROPOMETRY

3.1 Introduction

Definitions taken for the coordinate systems are identical to those used by NBDL (7,10,17). Section 3.2 will discuss the head and T1 anatomical coordinate systems and section 3.3 the laboratory and sled coordinate systems. In addition instrumentation and camera coordinate systems are also defined by NBDL but these systems are not necessary to understand the results presented in this report.

In order to calculate neck loads, estimations have to be made for the head mass distribution and the location of the occipital condyles. Partly, these estimations will be based on available anthropometric data for each subject (section 3.4). Section 3.5 will present estimations for the head mass and moments of inertia while section 3.6 discusses the location of the occipital condyles and the center of gravity.

3.2 Head and T1 anatomical coordinate systems

The head and T1 anatomical coordinate systems defined by NBDL are orthogonal and right-handed (Fig. 6). For the head, the anatomical origin is at the midpoint of the line connecting the superior edges of the auditory meati. The positive x-axis is the axis from the origin through the midpoint of the line connecting the infraorbital notches. The positive z-axis is perpendicular to the x-axis in superior direction in such a way that the xz-plane is the midsagittal plane. The positive y-axis is perpendicular to the xz-plane toward the left ear. In this way the xy-plane is approximately the Frankfort plane.

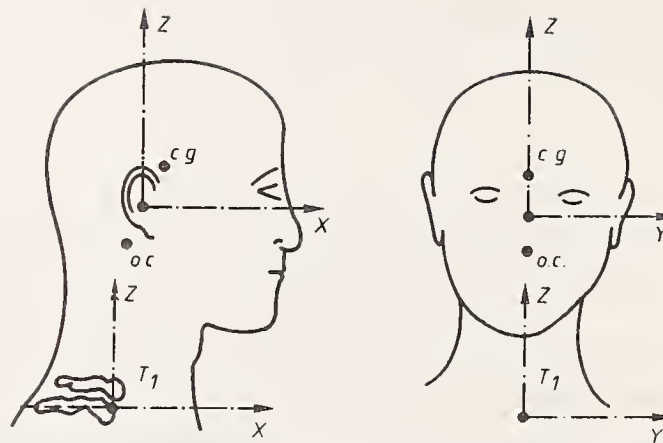


Fig. 6 Location of head and T1 anatomical coordinate systems
(o.c. = occipital condyles, c.g. = center of gravity).

The origin of the spine (T1) anatomical coordinate system is at the anterior superior corner of the first thoracic vertebral body (T1). The positive x-axis is directed from the most posterior point of the spinous process of T1 to the origin. the positive z-axis is perpendicular to the x-axis in superior direction and the positive y-axis is toward the left, perpendicular to the xz-plane.

Three-dimensional X-ray techniques were used to specify these anatomical coordinate systems relative to the anatomical landmarks, where for the identification of the landmarks in the head small lead markers were located near the auditory meati and the infraorbital notches. The location of the instrumentation packages with respect to the anatomical coordinate systems were determined using the same X-ray measurements.

3.3 Laboratory and sled coordinate systems

The basic reference frame in the NBDL tests is the laboratory coordinate system, which is a right-handed orthogonal coordinate system fixed in the laboratory (Fig. 7). The positive x-axis of this system is defined parallel but in opposite direction to the thrust vector of the accelerator. The positive z-axis is opposite in direction to gravity. To the sled, a sled coordinate system is connected with the same orientation as the laboratory coordinate system.

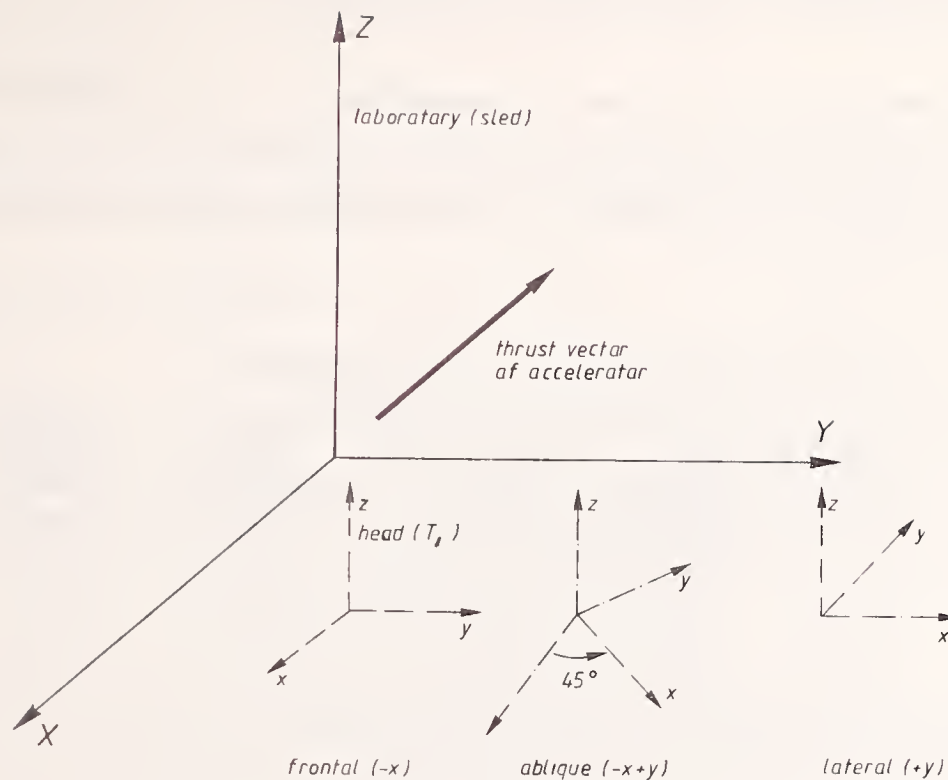


Fig. 7 Rough orientation of head and T1 anatomical coordinate systems relative to laboratory and sled coordinate system in case of frontal, oblique and lateral impacts.

The initial nominal orientation (i.e. before moving of the sled) of the head and T1 anatomical coordinate systems relative to the laboratory and the sled coordinate system for the 3 impact directions, is roughly indicated in Fig. 7. It follows that the nominal value of the third euler angle (i.e. rotation about head or T1 z-axis as specified in section 2.3) is 0 degrees in frontal, 45 degrees in oblique and close to 90 degrees in case of lateral impacts.

Later on in chapter 3 and 4 information on the actual initial orientation of T1 and head anatomical coordinate systems will be provided. It will be shown that the initial orientation of the T1 anatomical coordinate system varies considerably in different tests for the same subject, which is explained by errors in the specification of this coordinate system (chapter 4).

3.4 Human subject anthropometric measurements

At NBDL detailed anthropometric measurements are conducted for each subject as part of the test protocol. Table 4 summarizes the most significant data in this respect. Definitions for these antropometric variables can be found in ref. (7).

Table 4 - Selected Human Subject Anthropometry

Subject Number	Standing Height (cm)	Weight (kg)	Sitting Height (cm)	Head Circumference (cm)	Head Breadth (cm)	Head Length (cm)
H00083	180.0	75.7	92.4	54.7	15.5	18.3
H00093	173.0	72.5	93.5	52.1	14.4	17.8

3.5 Head mass and moments of inertia

Estimations for the subjects head mass and the moments of inertia about the principal axes will be based on regression equations proposed by McConville et al. (24). Separate equations were given for estimations based on stature and weight and based on head circumference, head breadth and head length. Since estimations using head anthropometry data are more reliable, these equations will be applied here. The following set of regression equations was used in our study:

$$M = d(C_1 \times HC - C_2 \times HL - C_3) \quad (2)$$

$$I_{xx} = C_1 \times HC + C_2 \times HB - C_3 \quad (3)$$

$$I_{yy} = C_1 \times HC - C_3 \quad (4)$$

$$I_{zz} = C_1 \times HC - C_2 \times HL - C_3 \quad (5)$$

where:

M = the head mass (kg)

I_{xx} = moment of inertia about principal x-axis (kgm^2)

I_{yy} = moment of inertia about principal y-axis (kgm^2)

I_{zz} = moment of inertia about principal z-axis (kgm^2)

d = density (kg/dm^3)

HC = head circumference (m)

HB = head breadth (m)

HL = head length (m)

The values for the constants C_1 , C_2 and C_3 are summarized in Table 5.

Table 5 - Coefficients in regression eqs. (2-5).

eq.(2) : C_1	= 21.618	C_2	= 12.184	C_3	= 5.5936
eq.(3) : C_1	= 0.11639	C_2	= 0.10605	C_3	= 0.0625049
eq.(4) : C_1	= 0.17924			C_3	= 0.0794181
eq.(5) : C_1	= 0.11857	C_2	= 0.07320	C_3	= 0.0382935

The density will be taken 1 here based on recommendations made by McConville et al. (24). This value is slightly smaller than values obtained from cadaver segment measurements, to account for reported overestimations by these regression equations (24).

Table 6 summarizes the masses and moments of inertia for each subject resulting from these regression equations. These values have to be corrected for the effect of the head instrumentation. Based on data presented by Ewing and Thomas (16) the correction for the head mass is + 0.53 kg and for the moment of inertia about the principal y-axis: + 0.0075 kgm². A similar correction is made for the moment of inertia about the principal x-axis, while the correction for the moment of inertia about the principal z-axis is estimated to be very small: + 0.0005 kgm². The resulting masses and moments of inertia are incorporated in Table 6.

Table 6 - Estimations for Masses and Moments of Inertia

Subject	M (kg)	I_{xx_2} (kgm ²)	I_{yy_2} (kgm ²)	I_{zz_2} (kgm ²)
<u>Without Instrumentation</u>				
H00083	4.00	0.0176	0.0186	0.0132
H00093	3.50	0.0134	0.0140	0.0105
<u>Corrected for Instrumentation</u>				
H00083	4.53	0.0251	0.0261	0.0137
H00093	4.03	0.0209	0.0215	0.011

The location of the principal inertia axes will also be based on calculations of McConville et al. (24): the principal y-axis is taken parallel to the anatomical y-axis and the angle between principal z-axis and head anatomical z-axis is taken: -36° (principal z-axis is rotated backwards). These values are close to data reported by Beier (25). The orientation of the principal axis is assumed here not to be affected by the head instrumentation packages.

3.6 Location of center of gravity and occipital condyles

No regression equations are available to estimate the location of the center of gravity and the location of the occipital condyles as a function of anthropometric data. The location of the center of gravity will be based here on average values reported by Beier (25) resulting from measurements on 21 fresh cadaver heads (Table 7). These values have been corrected for the head instrumentation based on data by Ewing and Thomas (16). The resulting c.g. location is incorporated in table 7.

The location of the occipital condyles will be based on average values reported by Ewing and Thomas (16) resulting from measurements on 12 human subjects (Table 7). The occipital condylar point is defined by Ewing and Thomas as the point most representative of the center of the condyles as seen on lateral X-ray and projected onto the midsagittal plane of the head.

The approximate location of the center of gravity (c.g.) and the occipital condylar point (o.c.) is indicated in Fig. 6.

Table 7 - Location of center of gravity and occipital condyles with respect to head anatomical coordinate system

	x (cm)	y (cm)	z (cm)
<u>Center of gravity</u>			
Beier (25)	0.83	0	3.12
Shift due to instrumentation(16)	+0.35	0	-0.20
Resulting c.g. location	1.2	0	2.9
<u>Occipital condylar point</u>	-1.1	0	-2.6

CHAPTER 4

ANALYSIS OF T1 MOTION AND CORRECTION OF T1 COORDINATE SYSTEM

4.1 Introduction

In order to visualize volunteer test results, a computer program was developed which generates a graphic representation of the three-dimensional head and spine displacements, based on photographic derived data on the NBDL tapes. This program generates two types of plots: The first plot contains displacements in a vertical plane with the same orientation as the laboratory (x,z)-plane. Since this plane is parallel to the thrust vector of the accelerator, it will be called plane of impact. The second plot contains displacements in a vertical plane perpendicular to the plane of impact and with the same orientation as the laboratory (y,z)-plane.

For the vertebra T1, the trajectory of the T1 anatomical origin relative to the sled is generated, together with the T1 anatomical z-axis at specified time frames. Section 4.2 will present resulting plots (in the impact plane) for the 30 tests in the selected subset.

Section 4.3 evaluates the initial neck length which is defined as the distance between head and T1 anatomical origin. This quantity shows large variations in different tests with the same subject which will be explained by errors in the specification of the T1 coordinate system. In section 4.4 a corrected T1 coordinate system will be proposed.

4.2 T1 motion in the plane of impact and T1 initial orientation

T1 motions in the plane of impact are presented in Fig. 8. For all three impact directions, trajectories of the T1 anatomical origin relative to the sled and the corresponding position of the T1 anatomical z-axis at various time frames, are shown. The relative T1 origin displacements in horizontal direction appear to vary from 0.04 m for the less severe up to 0.075 m for the more severe impacts.

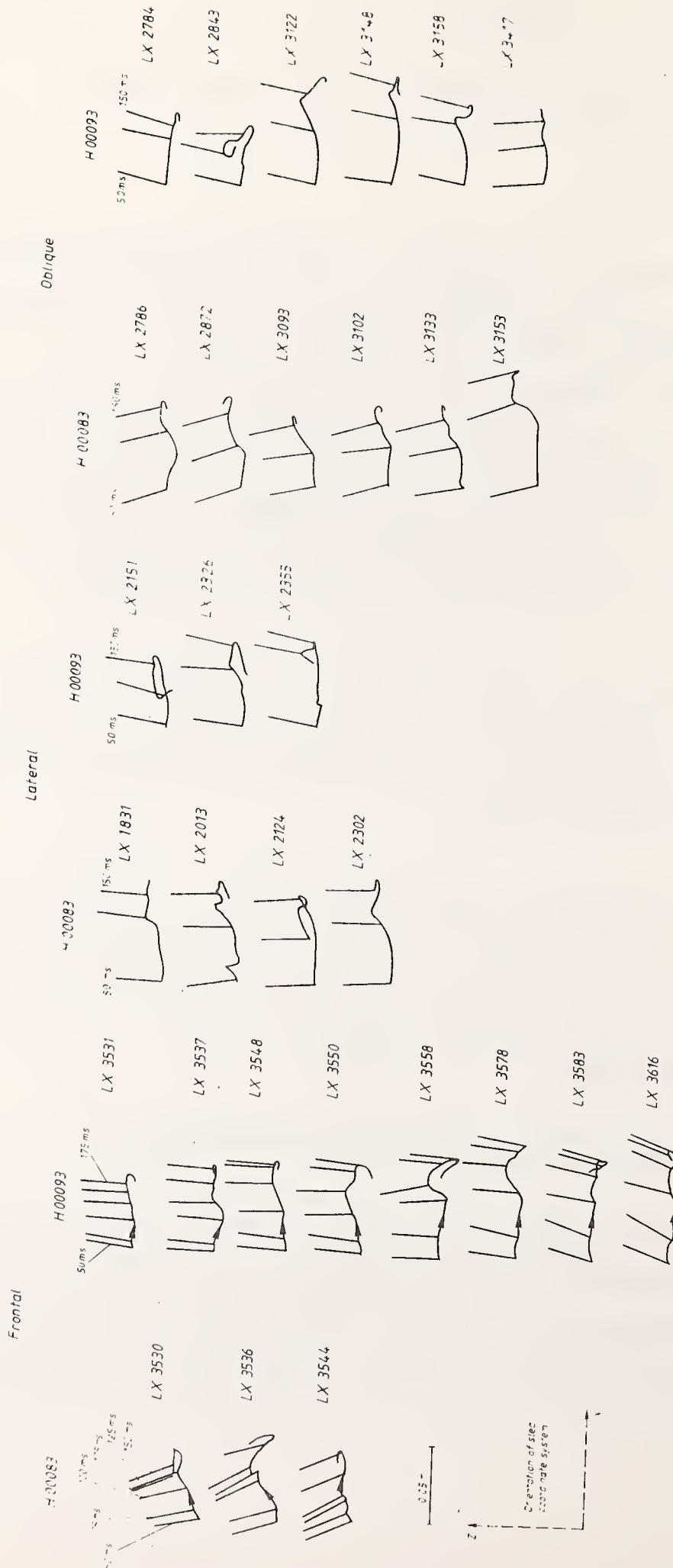


Fig. 8 Displacement of T1 anatomical origin relative to sled in plane of impact. Vertical line segments indicate position of T1 z-axis at different time frames.

Fig. 8 indicates small vertical translations and small rotations of the T1 vertebra in response to the impact. These displacements are considered small enough to justify neglecting them further in our analysis. The same holds for the out of impact plane displacements which also are found to be very small. Consequently the only significant displacement of T1 is a horizontal translation in the impact direction. Corresponding T1 accelerations as function of time together with the sled deceleration are presented in Fig. 9 for three impact directions. For each impact direction results of one typical severe test are shown. Annex A presents this type of data for all 30 selected tests.

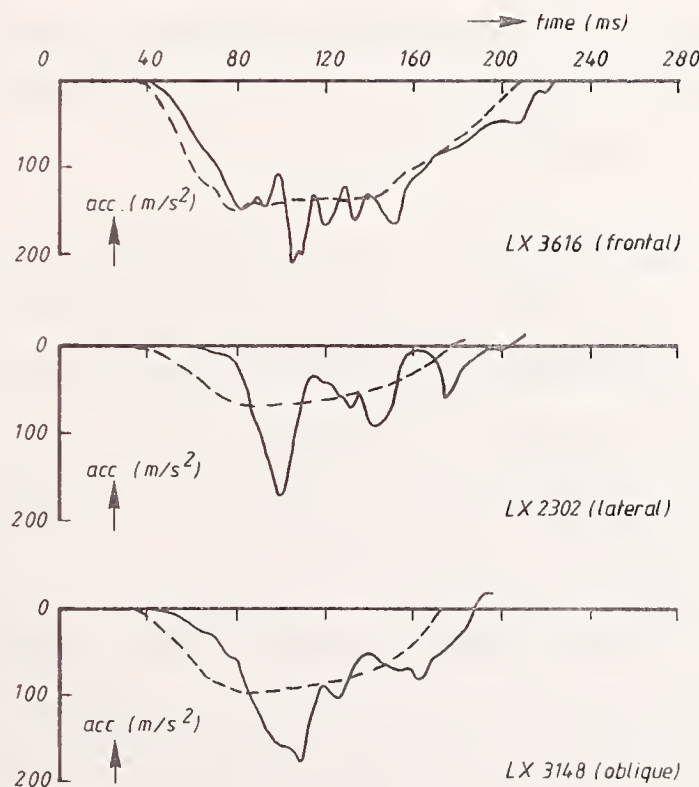


Fig. 9 Typical examples of horizontal T1 and sled acceleration as function of time in three different impact directions.
 — = T1; ---- = sled.

In frontal impacts this T1 acceleration curve, except for some small oscillations and a phase shift, appears to be close to the sled acceleration curve. In lateral and oblique impacts, however, a much larger deviation between both curves can be observed, indicating the different nature of the interaction between the restraint system and torso or shoulder in these type of tests. A comparison of the initial orientation of the T1 anatomical coordinate system in different tests for the same subject shows in a number of cases considerable variations. This is clearly illustrated for instance

for tests LX3558 and LX3616 with subject H00093 in frontal flexion (see Fig. 8). Such deviations which cannot be fully explained from variations in the initial torso orientation, are most likely caused by errors in the specification of the T1 coordinate system. Section 4.4 will present a corrected T1 coordinate system of which the initial orientation is identical to the orientation of the sled (laboratory) coordinate system.

4.3 The initial neck length

The initial neck length will be defined here as the distance between T1 and head anatomical origin at time = 0 (i.e. before moving of the sled). Fig. 10 presents a comparison of this parameter for all tests obtained from NBDL (i.e. 85 experiments). For the same subject, variations up to 0.07 m in this quantity can be observed.

The most likely reason for such large differences seems to be inaccurate positioning of the T1 and/or head anatomical coordinate systems. In order to analyse this, the vertical positions of head and T1 anatomical origins in the sled coordinate system are presented in Fig. 11 as a function of the initial neck length. These figures clearly show that the neck length is strongly related to the vertical position of the T1 anatomical origin: increase in the height of the T1 anatomical coordinate origin causes a similar decrease in neck length. In other words, the difference in neck length seems to be mainly due to errors in vertical location of the T1 anatomical origin. In the next section a method will be proposed to correct for this error.

4.4 Correction of T1 coordinate system

The preceding sections showed errors in the vertical position of the T1 coordinate system and the initial T1 orientation. The following method is proposed in order to correct for these errors:

- From all tests with the same subject a mean value for the initial neck length has been determined. This value is 0.111 m for subject H00083 and 0.154 m for subject H00093.

- The origin of the new T1 coordinate system is shifted vertically with respect to the laboratory in such a way that the initial neck length becomes identical to this mean value.
- The new T1 coordinate system is initially aligned with the sled (laboratory) coordinate system.

Note that the orientation of the T1 coordinate system relative to the T1 vertebra as defined in this way, is dependent on the impact direction. In lateral (oblique) direction it is rotated nominally 90 degrees (45 degrees) with respect to its orientation in frontal direction.

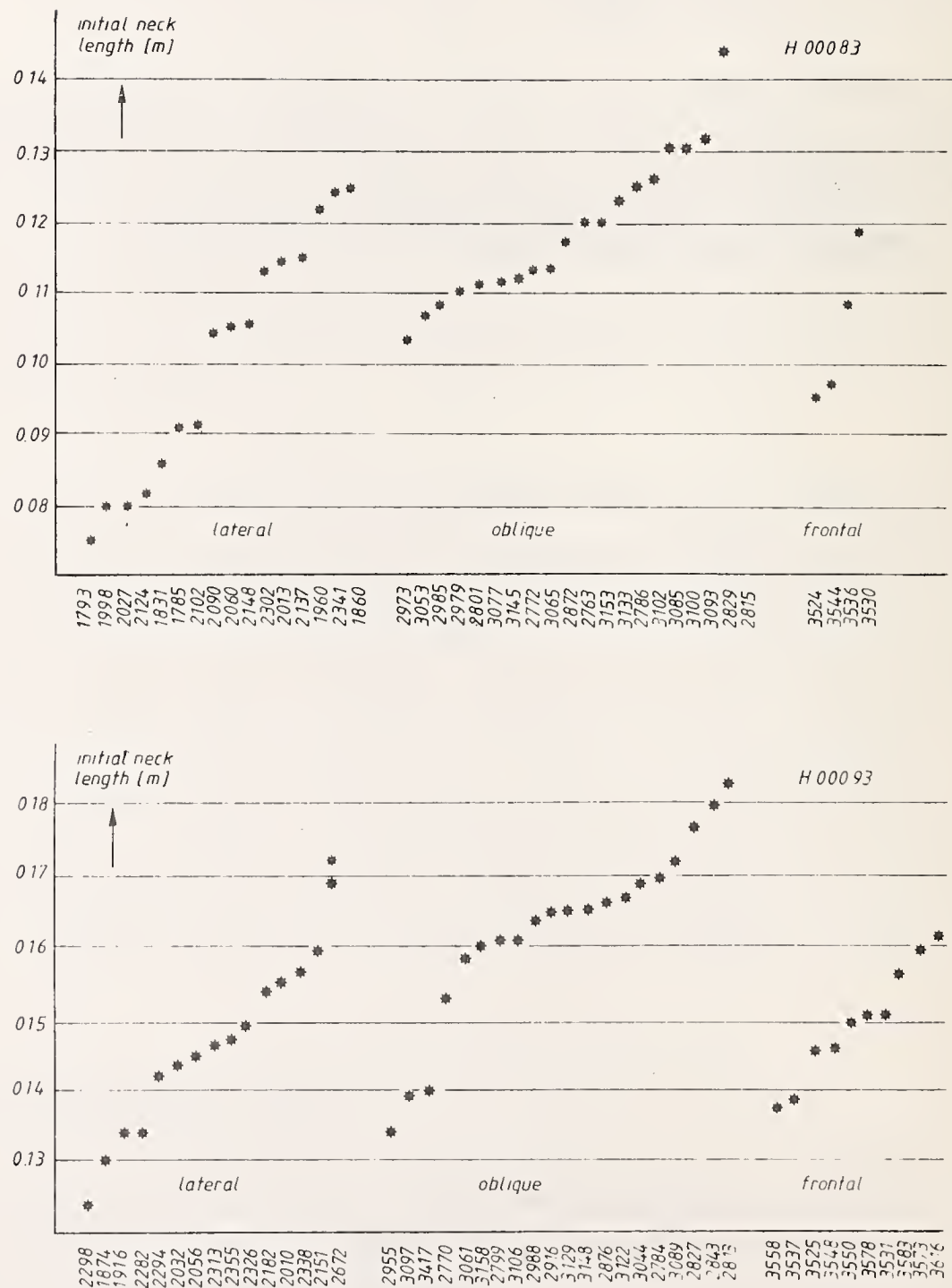


Fig. 10 Initial neck length (i.e. distance between head and T1 anatomical origin at time = 0) in 85 tests with subjects H00083 and H00093.

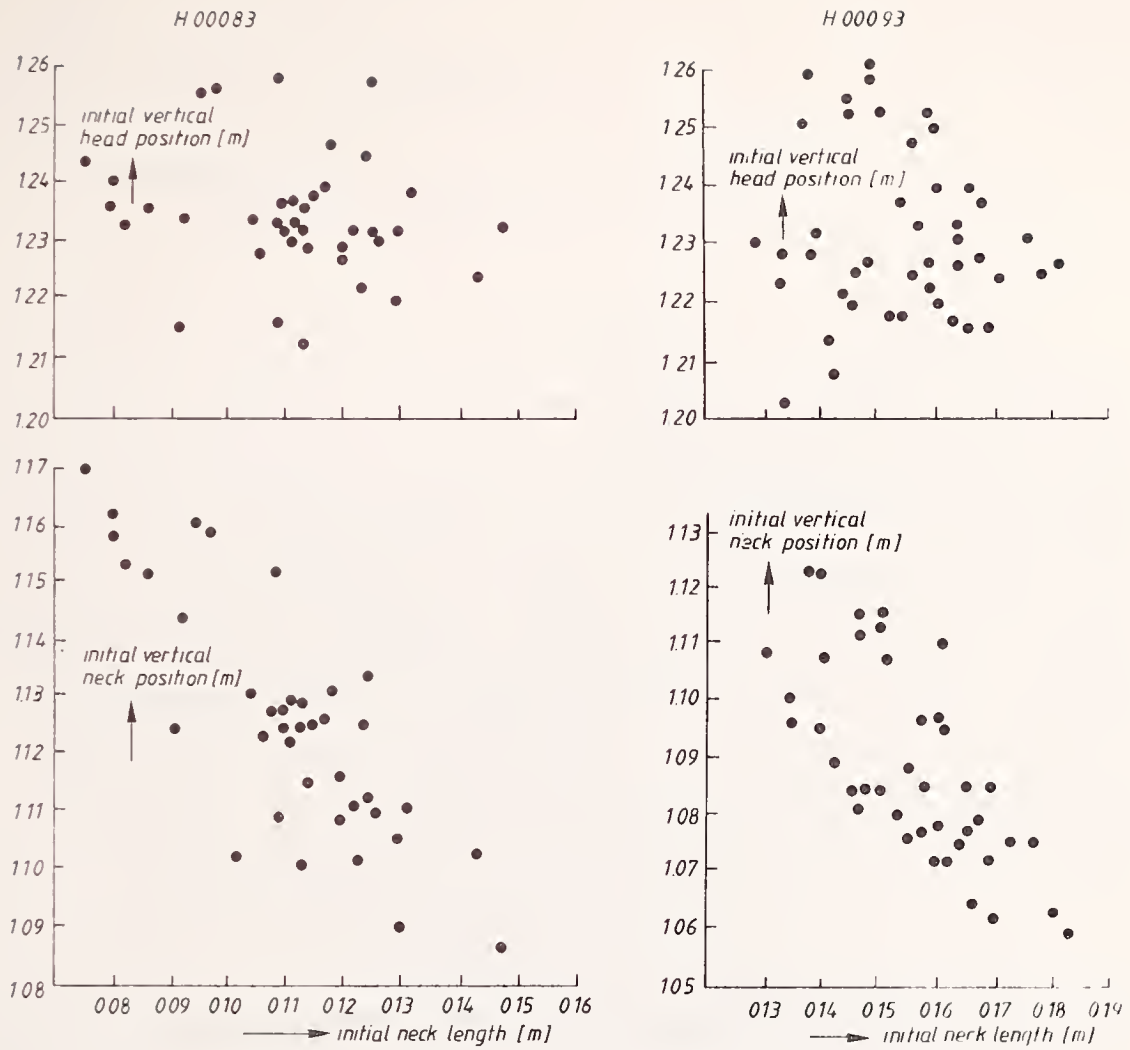


Fig. 11 Initial vertical position of the head and T1 anatomical origin relative to the sled coordinate system as a function of the initial neck length.



CHAPTER 5

ANALYSIS OF RELATIVE HEAD MOTION

5.1 General

The preceding chapter briefly mentioned the computer program which generates a graphical representation of the T1 displacements relative to the sled. For the head this program allows occipital condyles and anatomical origin trajectories to be presented relative to a coordinate system with the same orientation as the laboratory (sled) coordinate system and with its origin in the origin of the T1 anatomical coordinate system. In addition to these trajectories, also a trajectory of a point near the 'top' of the head and the position of the head anatomical z-axis at different time frames follows from this program. Head twist is visualized by means of small triangles connected to the z-axis.

Annex B presents for the 30 selected tests the resulting plots. Only displacements in the plane of impact are presented here since displacement out of this plane were found to be small. For instance for the occipital condyles and anatomical origin trajectories these out of plane displacements in general were smaller than 0.02 m.

In section 5.2 an analysis will be presented of these relative head motions. For each impact direction, results of different tests with the same subject will be summarized in one figure. The resulting plots show that these impact plane motions can be approximated quite well by means of a linkage mechanism with 2 pivots. Details of this mechanism will be discussed in section 5.3.

The motion of this linkage mechanism in the impact plane is characterized by two degrees of freedom: the neck link rotation θ and the head flexion ϕ . Section 5.4 will present this neck link rotation as function of the head rotation. In addition to these impact plane rotations, in lateral and

oblique impacts, a third significant rotation can be observed namely the head torsion or twist, defined as a rotation about the head anatomical z-axis. Section 5.4 will present this rotation, which will be denoted by ψ , as function of the head flexion ϕ .

5.2 Head trajectories and displacements of the head anatomical z-axis in the impact plane

Fig. 12 presents for the loading phase of the motion, trajectories in the plane of impact of the head anatomical origin and the occipital condyles. The position of the head anatomical z-axis at three different time frames (i.e. 50, 100 and 150 ms) is also given. The displacements are presented relative to the corrected T1 coordinate system and for each subject and impact direction the results are summarized in a separate figure. The following observations can be made:

- Trajectories from different tests are quite close to each other in particular for the tests of subject H00093.
- For the same subject more severe impact levels in general cause larger head excursions.
- Maximum head excursions in frontal impacts are slightly larger than in oblique impacts and much larger than in lateral impacts.
- In the initial phase the head motion is more of a translational nature than in the remaining part of the motion.
- Both the anatomical and occipital condyles trajectories can be approximated quite well by a circular arc.

This last finding allows the relative head motions in the plane of impact to be approximated in a simple way by a 2-pivot linkage mechanism. Geometrical details of this mechanism are provided in the next section.

5.3 Geometrical properties of the linkage mechanism

The preceding results suggest that the relative head motions in the impact plane can be approximated quite well by a 2-pivot linkage mechanism (Fig. 13). The upper link of this mechanism represents the head, the middle link the neck and the lower link the torso.

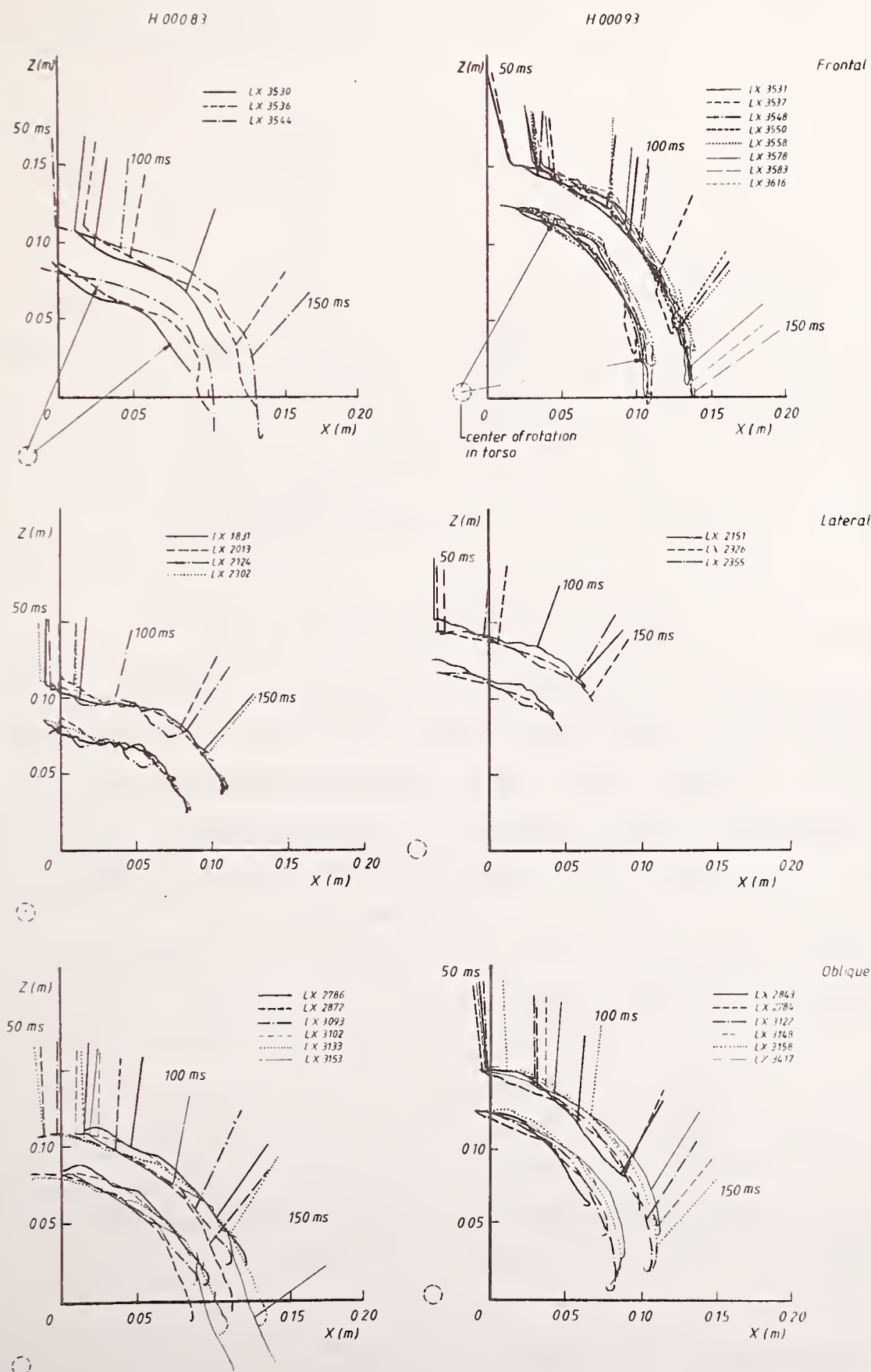


Fig. 12 Head displacements relative to corrected T1 coordinate system for three impact directions. Upper curves: head anatomical origin. Lower curves: occipital condyles. Stick figures: head z-axis at 50, 100 and 150 ms.

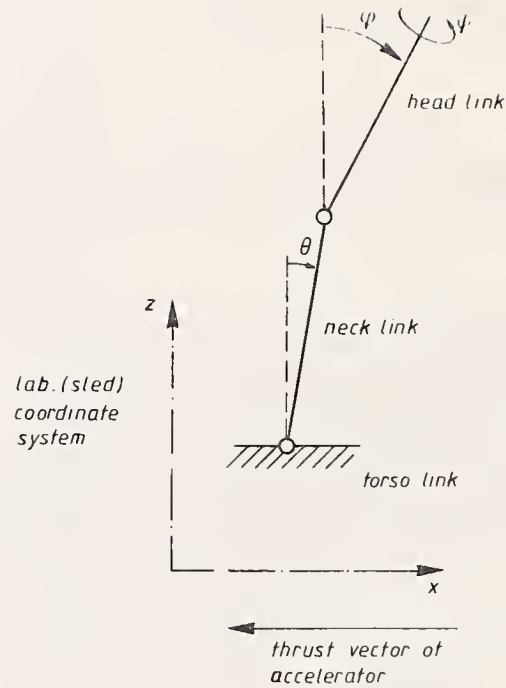


Fig. 13 Two-pivot linkage mechanism.

The upper pivot is a joint with two degrees of freedom (universal joint). The first degree of freedom of this joint allows the head link to rotate relative to the neck link in the plane of impact. This rotation angle will be denoted by ϕ and is defined here as the angle in the plane of impact between the z-axis of the head anatomical and the corrected T1 coordinate system (Fig. 13) (since T1 rotations are neglected in this study the z-axis of the T1 coordinate system is aligned with the laboratory z-axis). The mathematical expression for ϕ is:

$$\tan \phi = \frac{A_{13}}{A_{33}} \quad (6)$$

where A_{13} and A_{33} are components of the transformation matrix A of the head (see eq.(1)).

The second degree of freedom of this upper joint is the rotation ψ of the head about the head anatomical z-axis indicating the head torsion or twist. This angle will be derived here from the third euler angle specified by NBDL (see section 2.3). Due to definitions of the coordinate systems the

nominal initial value of the third euler angle is 0 degrees in frontal impacts, 45 degrees in oblique and 90 degrees in lateral impacts (see also Fig. 7). Consequently this rotation will be defined by:

$$\begin{aligned}\psi &= \text{PHC03P} && \text{in frontal impacts} \\ \psi &= \text{PHC03P}-0.785 && \text{in oblique impacts} \\ \psi &= \text{PHC03P}-1.571 && \text{in lateral impacts}\end{aligned}\quad (7)$$

The upper pivot will be located in the occipital condylar point. Preliminary results of a numerical study to estimate optimal geometrical parameters of a 2-pivot linkage model for a set of 6 frontal, 6 lateral and 6 oblique tests with subjects H00083 and H00093, show that also other locations in the head can be chosen for this pivot (27). However, this study did not show a significant improvement of the goodness of fit, if another pivot location was selected.

The lower pivot is a pin joint i.e. a joint with one degree of freedom. The axis of the pin joint is perpendicular to the plane of impact. This joint allows the neck link to rotate relative to the torso link. The corresponding rotation angle will be denoted by θ and is defined as the angle in the plane of impact between the neck link and the z-axis of the corrected T1 coordinate system (i.e. laboratory z-axis).

Graphically it can be shown that the circular arc for approximation of the occipital condyle trajectories varies in radius from 0.11 m to 0.14 m. Here a radius of 0.125 m will be used for approximation of the occipital condyle trajectories in all the tests. Consequently the neck link length, i.e. distance between upper and lower pivot will be 0.125 m. The corresponding location of the lower pivot which has been determined graphically per subject and per impact direction is incorporated in Fig. 12. Its coordinates relative to the corrected T1 coordinate system are summarized in Table 8.

Table 8 - Location of lower pivot relative to corrected T1 ^{*}
coordinate systems for a neck link length of 0.125 m

Impact direction	H00083		H00093	
	x (m)	z (m)	x (m)	z (m)
frontal	-0.02	-0.04	-0.015	0.00
lateral	-0.02	-0.04	-0.045	0.00
oblique	-0.025	-0.04	-0.035	0.00

* accuracy ± 0.005 m.

The rotations θ and ϕ are calculated with the computer program ANGLE from the data provided on the NBDL tapes. Eqs. (6) and (7) show that ϕ and ψ are independent of the geometrical parameters of the linkage mechanism. This is not the case, however, for the neck link rotation θ . Consequently a change in pivot location and/or neck length will effect the θ value ^{*}. The accuracy for the graphical determination of the torso pivot location is estimated to be ± 0.005 m. The effect of this on the accuracy of the θ values is $\pm 2-3$ degrees. Numerical techniques are being developed that will allow a more accurate specification of link length and pivot location (26,27).

In the next section initial and maximum values for the 3 rotations θ , ϕ and ψ will be given for the 30 selected tests. In addition head torsion and neck link rotation in these tests will be presented as function of the head flexion.

5.4 Head torsion and neck link rotation as function of head flexion

Values for the angles ϕ , ψ and θ in the initial position (time = 0) will be denoted by ϕ_0 , ψ_0 and θ_0 , respectively. Table 9 summarizes these initial values for the 30 selected tests. The following observations can be made:

* In earlier interim reports and in ref. (28) and (29) for some of the tests slightly different values for the torso pivot location were selected, which might result in small differences in the θ values in this report.

- The initial head torsion (ψ_0) is close to zero.
- The initial head flexion in the plane of impact (ϕ_0) which is close to zero in lateral impacts shows larger variations in the other impact directions, particularly in frontal direction.
- The initial neck link rotation in the plane of impact (θ_0) shows a significant positive value, particularly in frontal and oblique direction.

The neck link rotation ($\theta - \theta_0$) is presented in Fig. 14 as function of the head flexion ($\phi - \phi_0$). For each subject and impact direction these curves are summarized in a separate figure. In the initial phase of the motion the head flexion is smaller than the neck link rotation for all runs illustrating the presence of a response which is frequently perceived as a translation of the head. As soon as the relative rotation $(\theta - \theta_0) - (\phi - \phi_0)$ is 15-30 degrees in frontal or oblique impacts, changes in head and neck angle, become almost identical. In other words, the head and neck link are more or less locked. A similar behaviour can be observed for the lateral impact response. However here the maximum angle between head and neck link is smaller, namely between 5 and 15 degrees, while in addition this relative angle appears to become smaller in the final part of the loading phase.

Table 9 summarizes extreme values for the head and neck link rotations in the plane of impact, denoted by ϕ_{\max} and θ_{\max} , respectively. Based on a comparison of $(\theta_{\max} - \theta_0)$ and $(\phi_{\max} - \phi_0)$ it can be seen that:

- For the most severe tests in the three impact directions head and neck link rotations in frontal flexion are slightly larger than in oblique impacts and much larger than in lateral impacts. Partly this can be explained by the different impact severities in the three impact directions.
- For similar test conditions maximum head and neck link rotations for subject H00093 are significantly less than for subject H00083. This difference may be partly due to the lower head mass and moment of inertia

of subject H00093: head breadth, head length and head circumference presented in table 4, are much smaller for this subject. Of course muscle strength and the acquired ability to reduce the impact shock after repeated tests may also contribute to this difference.

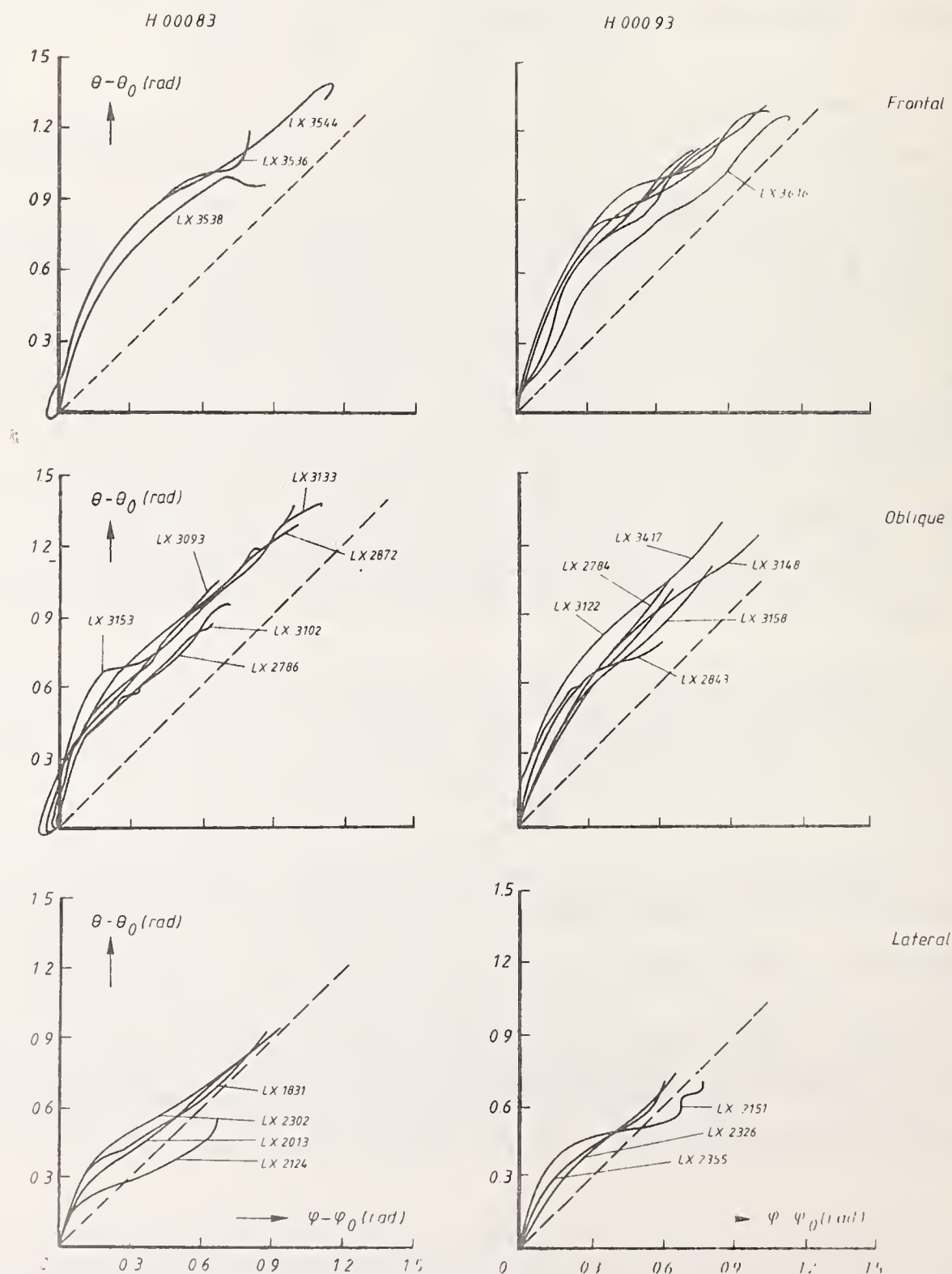


Fig. 14 Neck link rotation ($\theta - \theta_0$) as function of head flexion ($\phi - \phi_0$) in 30 tests with 2 subjects.

Table 9 - Initial and maximum values in degrees for head flexion ϕ , head torsion ψ and neck link rotation θ .

Subject (test number)	V Sled (m/s)	Peak Sled Acc. (m/s ²)	ϕ_0	ϕ_{\max}	(ϕ_{\max} $-\phi_0$)	ψ_0	ψ_{\max}	(ψ_{\max} $-\psi_0$)	θ_0	θ_{\max}	(θ_{\max} $-\theta_0$)
<u>FRONTAL</u>											
H00083											
LX3530	7.5	49	6	55	49	-	-	-	9	66	57
LX3536	10.5	73	9	55	46	-	-	-	9	79	70
LX3544	12.4	92	1	67	66	-	-	-	6	86	80
H00093											
LX3531	7.6	51	-14	24	38	-	-	-	11	68	57
LX3537	10.1	71	-10	40	50	-	-	-	9	76	67
LX3548	12.2	90	1	46	45	-	-	-	17	80	63
LX3550	13.3	98	-5	40	45	-	-	-	17	82	65
LX3558	14.3	110	-6	46	52	-	-	-	16	82	66
LX3578	16.0	132	-7	55	62	-	-	-	16	91	75
LX3583	16.7	142	-6	57	63	-	-	-	21	93	72
LX3616	17.2	150	-12	55	67	-	-	-	20	92	72
<u>LATERAL</u>											
H00083											
LX1831	6.5	49	1	51	50	-2	-46	-44	4	57	53
LX2013	6.3	49	0	40	40	-1	-36	-35	9	51	42
LX2124	3.1	89	-2	35	37	-3	-29	-26	6	39	33
LX2302	6.4	69	-3	50	53	2	-43	-45	3	58	55
H00093											
LX2151	3.3	100	0	44	44	-2	-44	-42	3	44	41
LX2326	6.5	60	-3	35	38	-3	-43	-40	3	48	45
LX2355	6.5	50	0	32	32	-5	-39	-34	6	44	38
<u>OBLIQUE</u>											
H00083											
LX2786	7.5	50	5	48	43	0	-14	-14	13	66	53
LX2872	9.0	61	-1	59	60	3	-17	-20	2	77	75
LX3093	10.3	71	1	40	39	0	-12	-12	6	66	60
LX3102	9.0	60	2	39	37	1	-11	-12	11	62	51
LX3133	8.8	79	-5	58	63	3	-21	-24	3	83	80
LX3153	8.8	80	5	62	57	-3	-31	-28	14	93	79
H00093											
LX2784	7.5	50	-8	38	38	3	-21	-24	10	68	58
LX2843	3	89	-5	29	34	-4	-25	-21	10	57	47
LX3122	8.9	79	-4	46	50	-1	-29	-28	11	85	74
LX3148	8.9	97	-7	50	57	-4	-31	-27	12	83	71
LX3158	8.8	78	-3	44	47	-4	-29	-25	17	80	63
LX3417	8.8	59	-3	37	40	-4	-26	-22	10	75	65

Fig. 15 presents the head torsion (twist) ($\psi - \psi_0$) as a function of the head flexion ($\phi - \phi_0$) for both lateral and oblique impacts. No data for frontal impacts are incorporated here since head torsion was found to be negligible in this impact direction.

For lateral impacts an almost linear relationship can be observed between head torsion and head flexion while the order of magnitude of both rotations appears to be almost identical, particularly for subject H00093.

For oblique impacts the relation between head torsion and head flexion appears to be quite different from lateral flexion. Peak head torsion values, which are incorporated in Table 9, are significantly less in oblique than in lateral impacts.

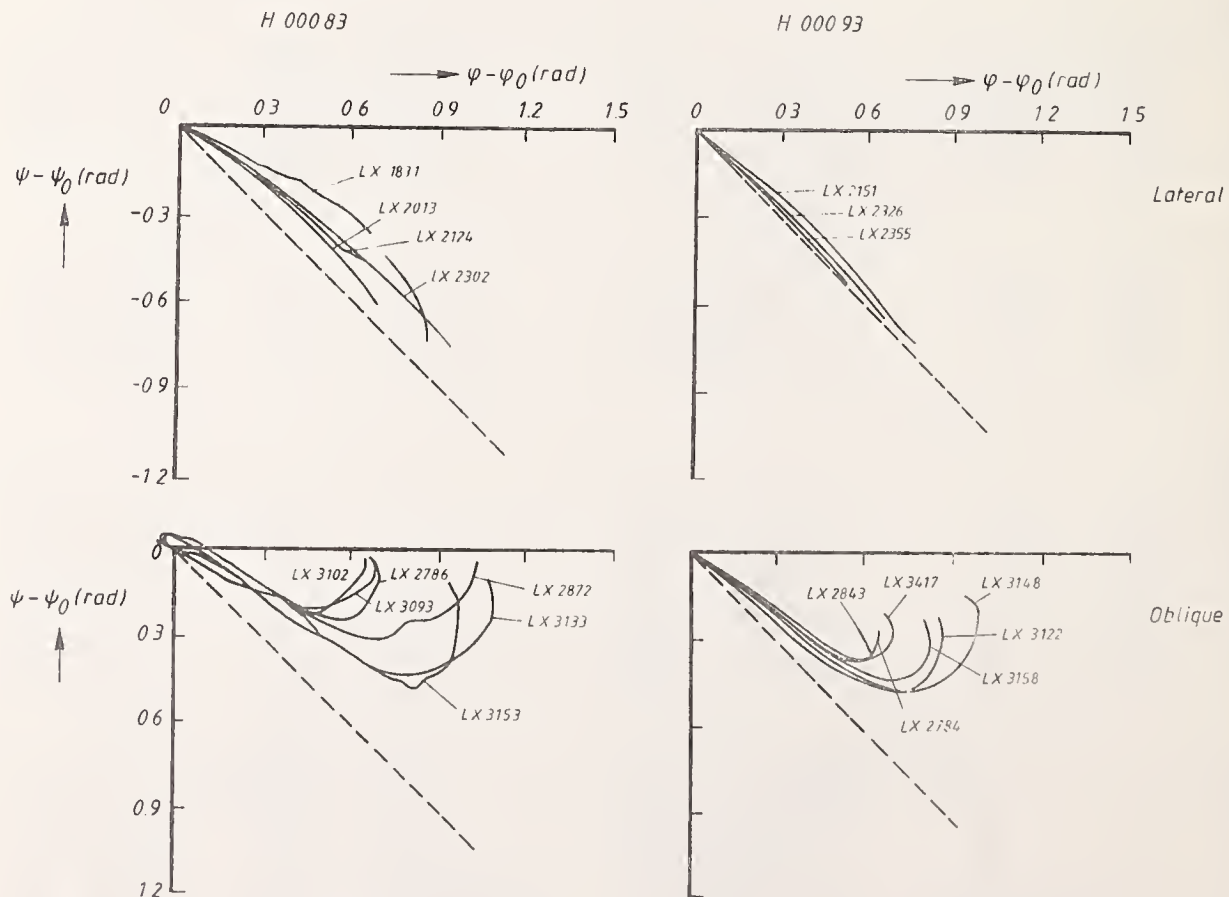


Fig. 15 Head torsion ($\psi - \psi_0$) as function of head flexion ($\phi - \phi_0$) in 19 tests with 2 subjects.

CHAPTER 6

LOAD CALCULATIONS

6.1 Introduction

The loads applied by the neck to the head near the occipital condyles can be calculated by using measurements of head acceleration and angular velocity, if the head is regarded as rigid body and does not come into contact with any other object or body part. Reasons to perform these calculations are, among otherthings:

- they offer an excellent insight in the system's behaviour for instance with respect to the role of the muscle activity
- load-displacement relations can be used to formulate dummy performance requirements and dummy design specifications
- determination of dynamic properties in a mathematical analog
- it is generally assumed that neck loads correlate quite well with neck injuries.

The vector equations for the force and the torque at the occipital condyles are obtained by applying Newton's laws:

$$\bar{F} = m_h(\bar{a}_g - \bar{g}) \quad (8)$$

$$\bar{M} = I \cdot \bar{\alpha} + \bar{\omega} \times (I \cdot \bar{\omega}) + m_h(\bar{r}_{go} \times (\bar{a}_g - \bar{g})) \quad (9)$$

where:

\bar{F} , \bar{M} are the force and torque, respectively applied by the neck to the head

m_h is the mass of the head

I is the moment of inertia tensor of the head (about c.g.)

\bar{r}_{go} is the position of the head c.g. with respect to the occipital condyles

\bar{g} is the acceleration of gravity

\bar{a}_g is the linear acceleration of the head c.g.

$\bar{\alpha}$, $\bar{\omega}$ are the angular acceleration and angular velocity, respectively, of the head

The linear acceleration at the head c.g. follows from:

$$\bar{a}_g = \bar{a}_a + \bar{\omega} \times (\bar{\omega} \times \bar{r}_{ga}) + \bar{\alpha} \times \bar{r}_{ga} \quad (10)$$

where \bar{a}_a is the linear acceleration of the head anatomical origin and \bar{r}_{ga} the position of the head c.g. with respect to this origin.

These equations and additional relations for transformations between coordinate systems have been programmed at TSC in Cambridge, using as input accelerations and velocities derived from accelerometer data and quaternions based on photographic data. The program allows expressing the components of the calculated force and torque with respect to various coordinate systems. Due to its three-dimensional set-up, this program can be used to evaluate neck loads in all impact directions. More details on this program can be found in ref. (30).

Results for the occipital condyle torques are presented in section 6.2. This program was also used to estimate the load at the center of the corrected T1 origin. Errors made in these calculations by neglecting the inertia effects of the neck are expected to be small.

6.2 Occipital condyle and T1 torques

Fig. 16, 17 and 18 present torques applied to the head near the occipital condyles. Fig. 16 shows the component M_ϕ of this torque about an axis perpendicular to the plane at impact as function of the head flexion $\phi - \phi_0$. For each subject and impact direction these characteristics are summarized in a separate figure. The same torques are presented in Fig. 17, however, now as function of the relative angle $(\theta - \theta_0) - (\phi - \phi_0)$ between head and neck link. The component M_ψ of the occipital condyle torque about the head anatomical z-axis as function of the head torsion $(\phi - \phi_0)$ is shown in fig. 18. Results presented here only relate to oblique and lateral impacts since for frontal flexion no significant rotations about the head anatomical z-axis were observed.

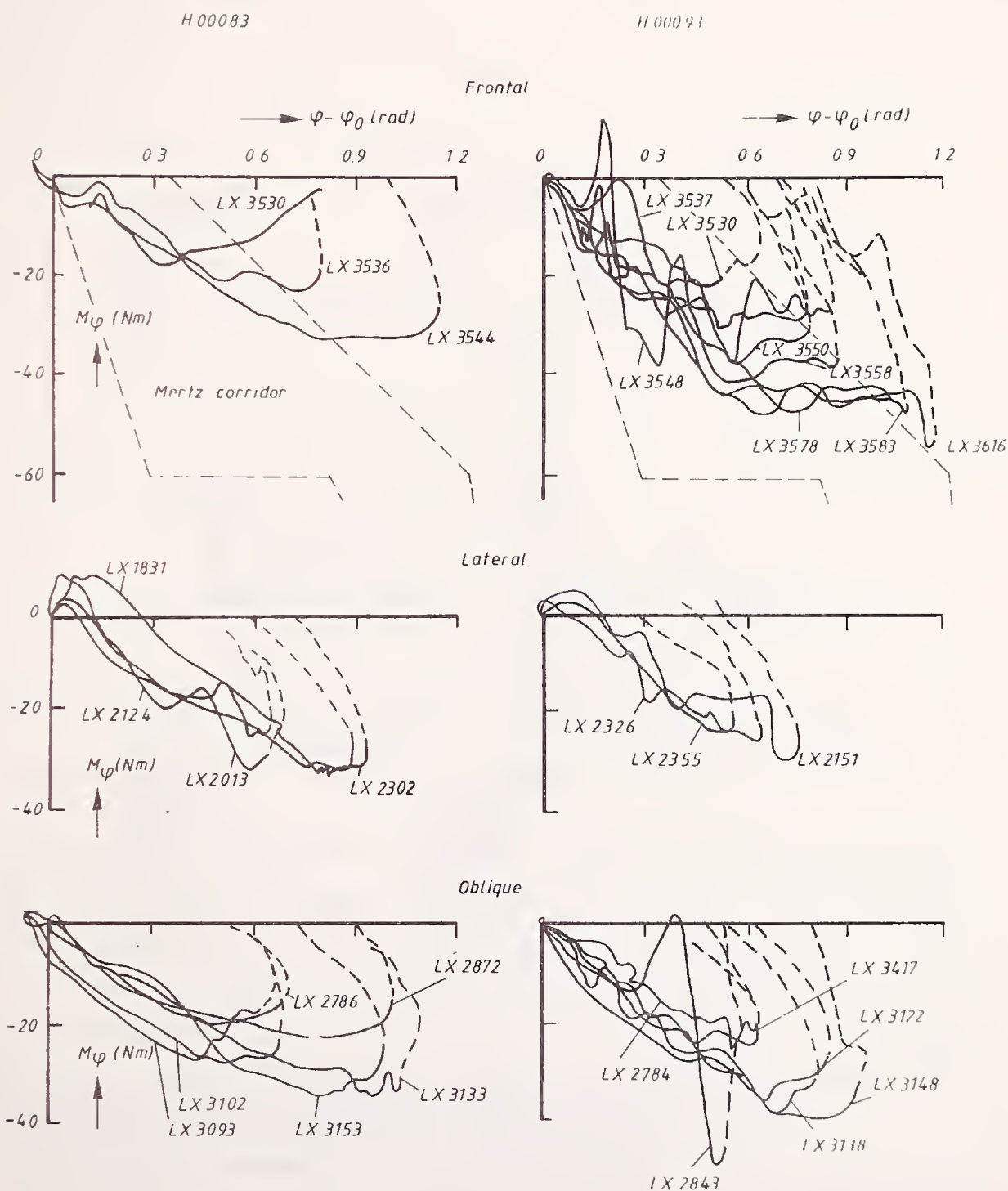


Fig. 16 Torque M_{φ} near occipital condyles about an axis perpendicular to the plane of impact as function of head flexion $(\varphi - \varphi_0)$.

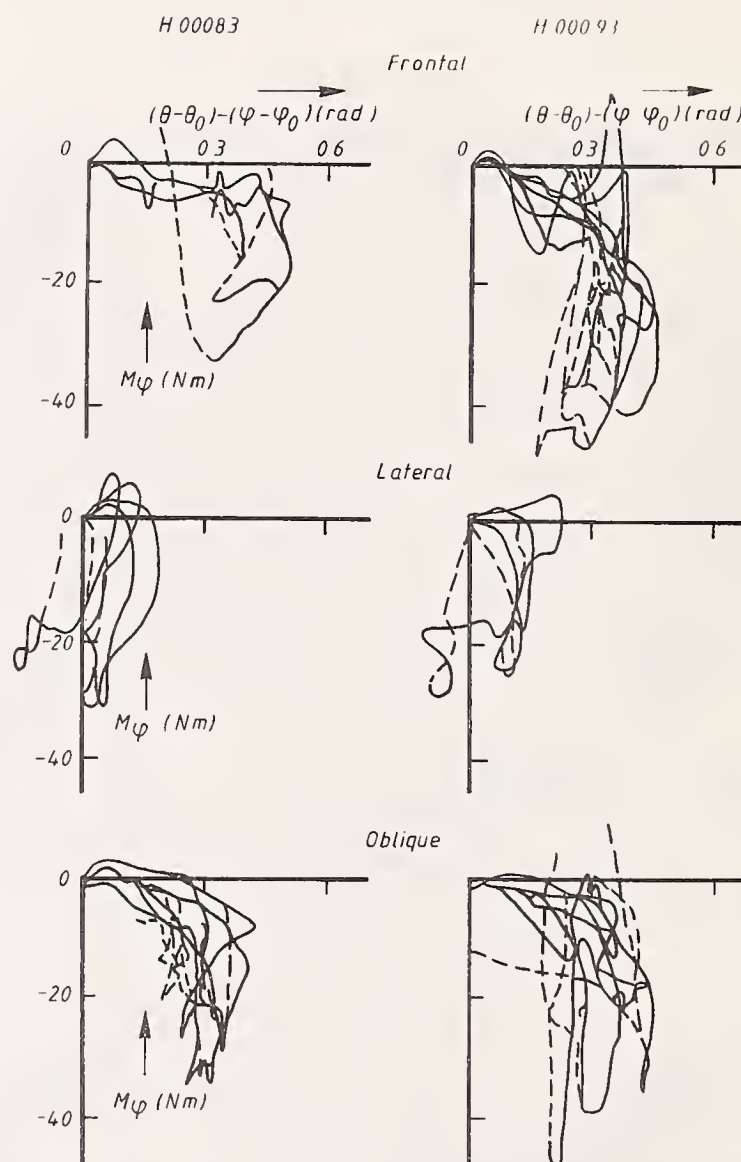


Fig. 17 Torque M_ϕ near occipital condyles about an axis perpendicular to the plane of impact as function of the relative angle between head and neck link $(\theta - \theta_0) - (\phi - \phi_0)$.

H 00083

H 00094

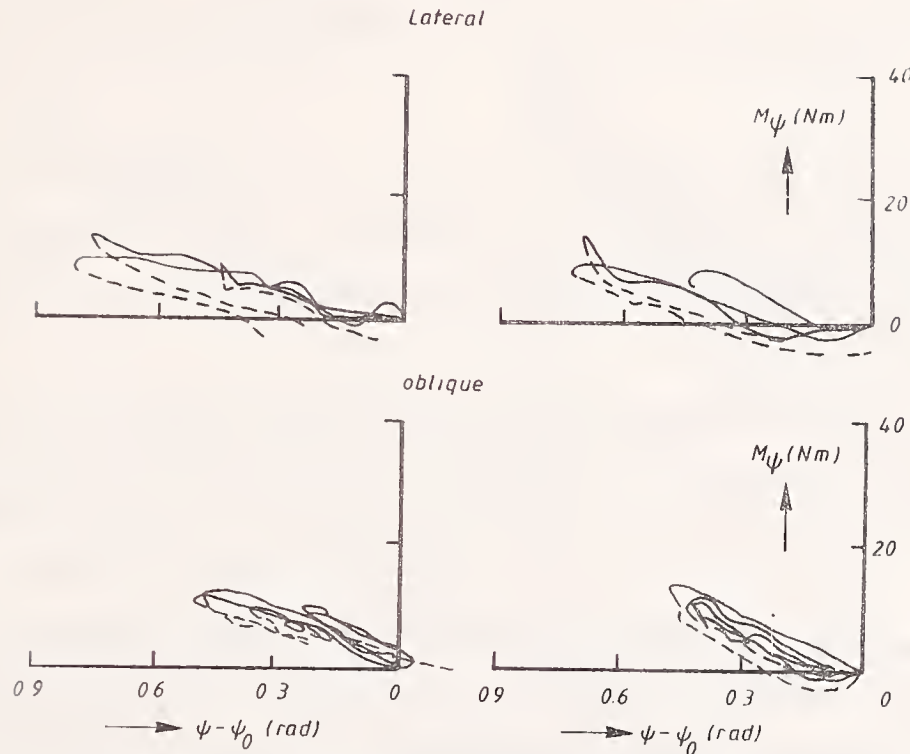


Fig. 18 Torque M_ψ near occipital condyles about the head anatomical z -axis as function of head torsion $(\psi - \psi_0)$.

For frontal impacts the characteristics in fig. 16 are presented along with the corridor for loading proposed by Mertz et al. (2). The calculated torque-head flexion characteristics appear to lie within or close to this corridor. Our calculations seem to suggest that this Mertz corridor is too wide. Largest torque values (i.e. 45-55 Nm) can be observed in the frontal tests with subject H00093. These tests appear to be the most severe tests in terms of sled deceleration and sled velocity.

In lateral impact tests initially a small positive torque M_ϕ can be observed which is almost completely absent in the other impact directions. An explanation for this might be the limited flexibility in the upper part of the neck in lateral direction compared to the flexibility in the other directions.

The occipital condyle torques presented in fig. 17 as function of the relative angle between head and neck link confirm the findings in section

5.4 for the relative motion in the upper pivot of the linkage. Dependent on the impact direction a certain free range of motion exists where the occipital condyle torque is relatively small. As soon as this angle is exceeded the upper pivot more or less gets locked and the occipital condyle torque increases.

Fig. 18 shows that the peak value of the component M_ψ of the occipital condyle torque about the head anatomical z-axis is much smaller than the component of this torque about an axis perpendicular to the impact plane.

Fig. 19 shows an estimation for the torque applied to the head near the (corrected) T1 origin as function of the neck link rotation $(\theta - \theta_0)$. Presented is the component of this torque about an axis perpendicular to the plane of impact. As for the occipital condyle torques, largest torque values appear in the most severe frontal impact tests with subject H00093. Peak torque values are lower in the tests with subject H00083 than with H00093, which can be partly explained from the smaller initial neck length in subject H00083 (resulting in a smaller value for the radius \bar{r}_{go} in eq. (9)).

Fig. 16-19 include data for loading as well as unloading. The ratio of the area between loading and unloading curve and the area between loading curve and the abscissa varies between 0.6 and 0.9 for the occipital condyles and T1 torques along an axis perpendicular to the impact plane as function of ϕ and θ , respectively. For the component of the occipital condyle torque about the head anatomical z-axis as function of the head torsion ψ_0 a much lower hysteresis is observed.

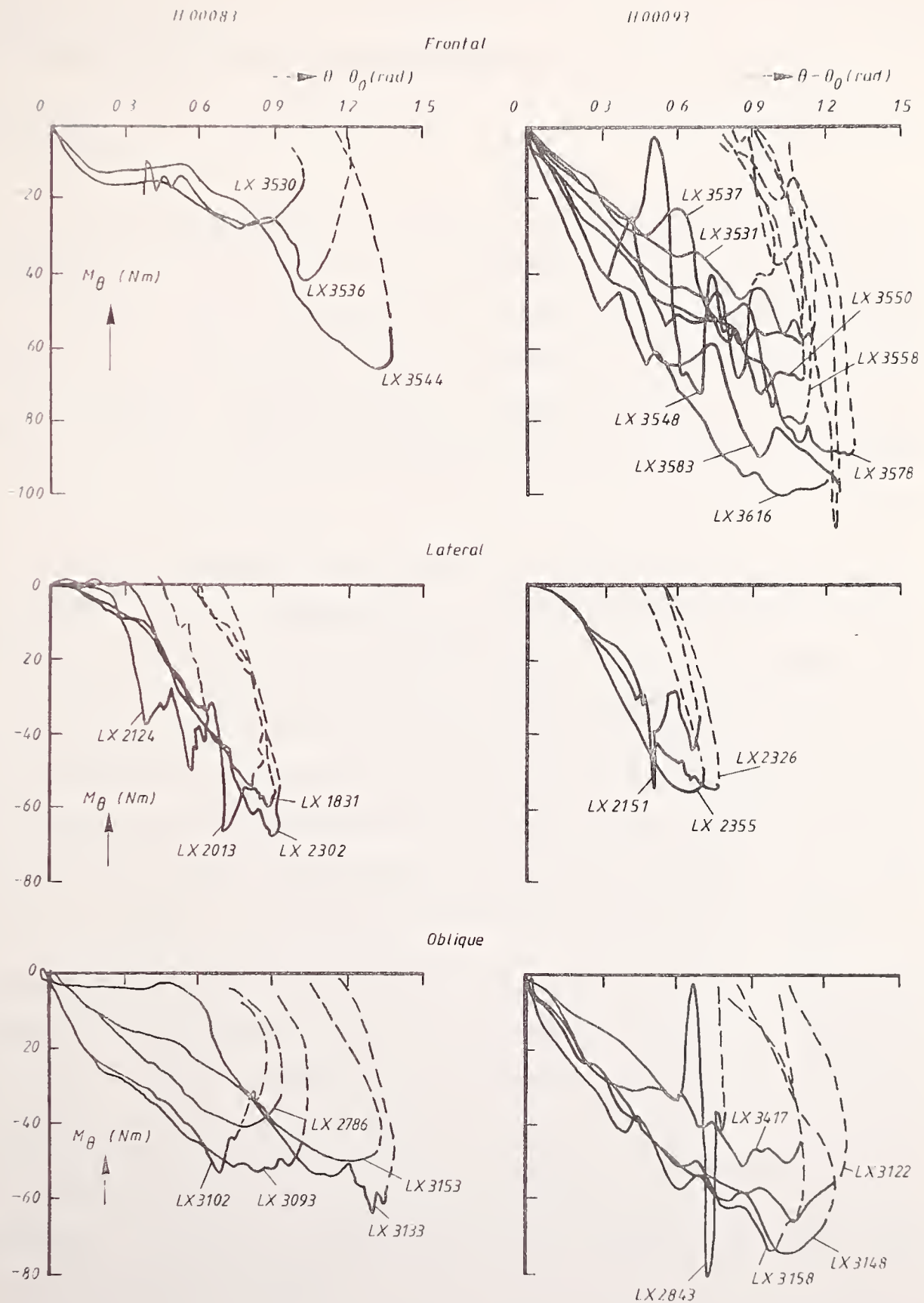


Fig. 19 Torque M_θ near the corrected T1 origin about an axis perpendicular to the plane of impact as function of neck rotation $(\theta - \theta_0)$.

CHAPTER 7

PERFORMANCE REQUIREMENTS BASED ON NBDL TESTS WITH TWO SUBJECTS

7.1 Introduction

In section 1.2 it was shown that performance requirements for mechanical necks presented in literature on this subject are limited mainly to the response in frontal flexion. Requirements for this impact direction which were developed in the early seventies, considered the relation between the torque of the occipital condyles and the angular position of the head. This, however, is not a sufficient condition to ensure a humanlike response.

One method to define necessary and sufficient conditions is specification of an analog system with a dynamical behaviour similar to that of the real head-neck system. If such an approach is selected, the analog should be as simple as possible in order to limit the set of parameters required to describe the analog. The mechanical analog to be defined herein, is only expected to reproduce the motions of the head relative to the torso (T1) in an impact situation. No realistic simulation of the neck behaviour itself is required. In fact, since measurements have been conducted only at the head and at T1, no actual information on this neck behaviour is available.

From the analysis presented in chapter 5 it follows that a relatively simple 2-pivot linkage mechanism can be used to reproduce the kinematic behaviour of the head with respect to T1. Section 7.2 deals with a brief literature review of this type of analog systems for the simulation of head-neck behaviour. In section 7.3 joint properties will be defined for the 2-pivot linkage on the basis of the load calculations presented in the preceding chapter. In this way together with mass distribution data, the mechanical analog is fully defined.

A second method to define performance requirements is by means of a set of kinematic requirements like displacements and accelerations derived from the measured test data. Such a formulation is useful for instance to verify

the response of a mathematical or mechanical substitute at a specific impact level. An example of this type of requirement will be given in Vol. II of this report where the response of the analog systems proposed in section 7.3, will be compared with the human subject response using mathematical simulations .

7.2 Literature review linkage mechanisms for head-neck motion

Analog systems for the head-neck response under impact conditions can be subdivided into three categories:

- linkage systems with a limited amount of degrees of freedom
- mechanical neck system as used in various crash dummy designs
- complicated mathematical (32,33,34) or mechanical (35) models in which the anatomical structure of the neck (vertebra and ligaments) is represented in detail (structure models).

This section deals with simple linkage systems, while a review of mechanical neck systems in crash dummy designs is presented in ref. (31). Structure models are too complex and too detailed due to the large number of system parameters involved, to be used here for the specification of performance requirements. This type of model is particularly useful for the study of injury mechanisms.

Most linkage systems proposed in literature for the head-neck behaviour in frontal flexion, have two degree of freedom (e.g. 36,37,38), although also a one degree (39) and a seven degrees (40) system have been proposed. The one degree of freedom system, contained one pin joint near the base of the neck and was based on tests with human cadavers. In the seven degrees of freedom system seven pin joints were specified distributed along the neck structure. The pivot locations were based on the analysis of X-ray's of voluntary flexion-extension motions in human subjects (40).

The two-pivot joint linkages for frontal flexion reported by Becker (36), Schneider and Bowman (37) and Frisch and Cooper (38) all resulted from the analysis of NBDL human volunteer tests. The lower pivot in these studies was located in the T1 origin, which is different from the approach in our

study where the lower pivot is located in the center of a circle arc approximating the occipital condyle trajectories. For the upper pivot various locations were proposed including the occipital condylar point (38) and a point 0.04 m above the head center of gravity (36). The linkage by Schneider and Bowman allows extension of the neck. Dynamical properties for the pin joints in these analog systems were based on a trial and error parameter fitting process with a mathematical simulation model until adequate replication of human response data was obtained.

For head-neck motions in lateral impacts, Ewing et al. (20,21) indicate that this type of motion can be approximated quite well by a single rotation about a fixed axis in the laboratory. This axis is located in the mid-sagittal plane perpendicular to the line connecting the origins of the T1 and head anatomical coordinate system.

A first promising attempt to identify a linkage mechanism suitable for simulation of frontal, lateral as well as oblique impacts is presented by Becker (41,42). This linkage contains four degrees of freedom and is illustrated in fig. 20. Eight geometrical parameters specify this mechanism: 4 parameters that characterize the position of head and T1 with respect to the linkage system and four parameter that specify the linkage geometry itself. Using a numerical iterative method these linkage parameters were calculated in such a way that the linkage approximates photographic data from a selected set of tests as close as possible. The method was applied to a small database consisting of a voluntary pitch motion and 2 lateral and 2 oblique impact tests with a single volunteer (i.e. H00093). Dynamical elements were not specified for this linkage.

7.3 The analog system

The results presented in chapter 5 indicate that a simple 2-pivot linkage is suitable to reproduce the observed motions of the head relative to T1. For each impact direction a separate linkage was proposed. It was shown that the upper pivot location and the link length can be taken identical for the 3 impact directions. The upper pivot has one degree of freedom in frontal impacts (i.e. head flexion) and two degrees of freedom in oblique and lateral impacts (i.e. head flexion and head torsion). The lower pivot

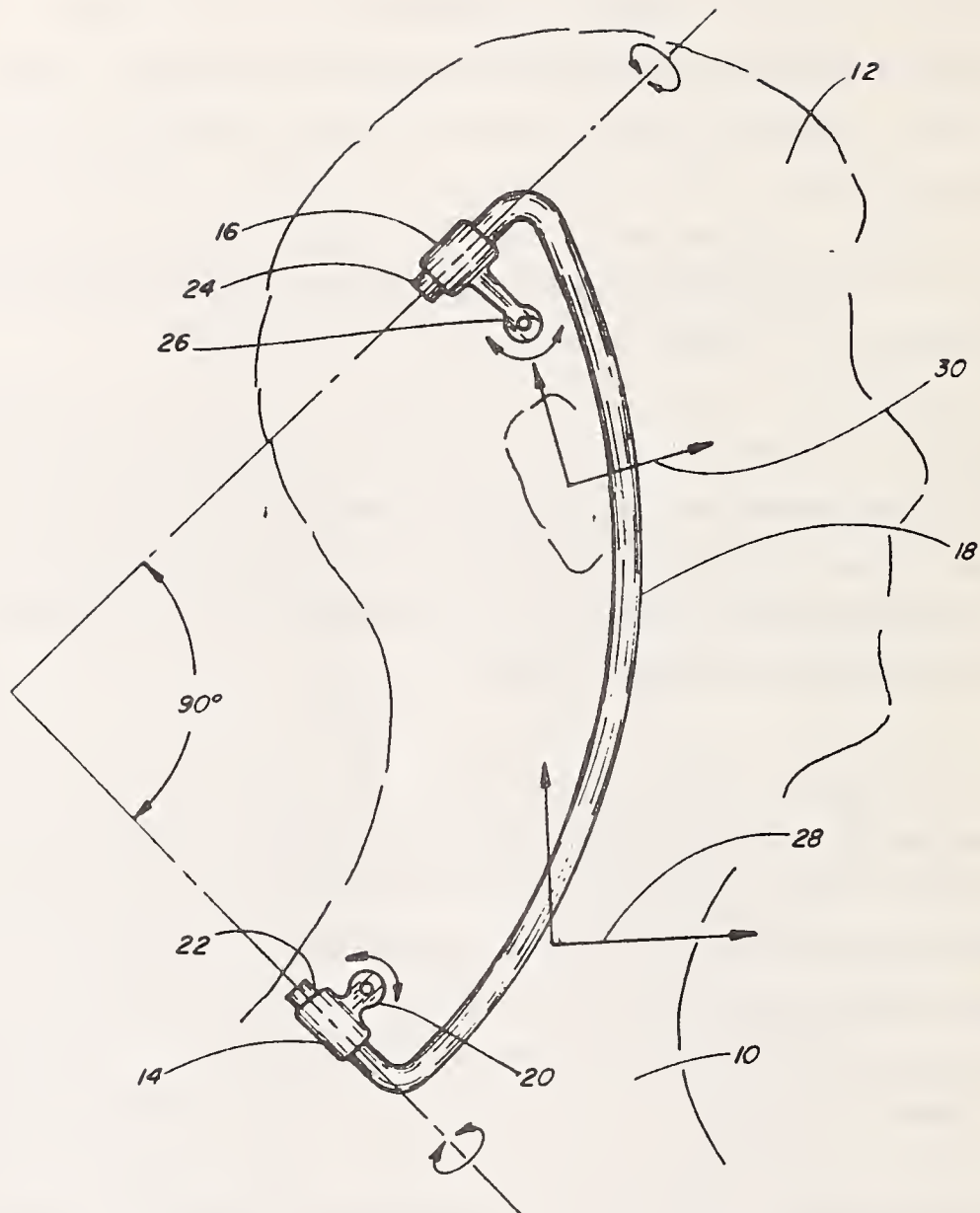


Fig. 20 Three-dimensional linkage according to Becker (41,42).

has one degree of freedom namely the neck link rotation about an axis perpendicular to the plane of impact.

The remaining linkage parameters to be defined here are the lower pivot location, the initial position of the linkage, dynamical properties of the pivots and the head mass distribution data. These linkage parameters will be determined for each impact direction separately on the basis of the results of the tests conducted in that impact direction.

Table 10 summarizes the proposed geometrical parameters and pivot characteristics. The following additional information can be given:

lower pivot location: Due to errors in the T1 specification it is not possible to specify this pivot uniquely with respect to T1 (or torso) anatomical landmarks. Pivot coordinates relative to the corrected T1 coordinate system, per subject, were provided in Table 8.

initial head link flexion and torsion: Although initial values for these angles are not completely zero in the tests, particularly with respect to the initial head flexion, the deviations from zero are not considered significant to be accounted for in the mechanical analog.

initial neck link rotation: In the tests significant positive values for this parameter were noted. The values proposed in Table 10 are mean values of the test data.

lower pivot linear stiffness: A linear torque - rotation characteristic is proposed here based on calculated torques near the T1 origin. For subject H00083 a correction has to be introduced in order to account for the difference between T1 origin and lower pivot location. Stiffness data in Table 10 are based on a graphical approximation of the torque - rotation characteristics (mean stiffness). The accuracy of this determination is estimated to be ± 0.25 Nm/deg. Stiffness in frontal and oblique direction are in the same order of magnitude, while in lateral direction as far as subject H00083 is concerned, a slightly larger linear stiffness value can be observed.

upper pivot linear torsion stiffness: These stiffness values appear to be relatively small and are, just as for the lower pivot stiffness based on a graphical estimation (accuracy = 0.1 Nm/deg.).

upper pivot free range of motion in the plane of impact: This parameter can be determined graphically from the torque-rotation characteristics provided in fig. 17. For frontal and oblique impacts the range of motion is of the same order of magnitude; for impacts in lateral direction a smaller value is found. Accuracy for this quantity is ± 3 degrees. No stiffness value for the joint stop (locking mechanism) can be specified here on the basis of the available data.

In addition to the preceding parameters the mass distribution of the head has to be defined. In this study this will be based on the mass distribu-

tion of subject H00083 and H00093 by defining average values from the mass distribution data provided in table 6. For the neck link the mass will be taken zero since the possible inertia effects of the neck were neglected in the T1 torque calculations.

Table 10 - Linkage parameters for the loading phase based on 30 impact tests with two subjects (H00083 and H00093)

Parameter	Frontal direction	Lateral direction	Oblique direction
<u>GEOMETRICAL PARAMETERS</u>			
upper pivot location	occipital condyles	occipital condyles	occipital condyles
link length	0.125 m	0.125 m	0.125 m
lower pivot location	see table 8	see table 8	see table 8
initial head link flex.	0	0	0
initial head link tors.	0	0	0
initial neck link rot.	14 deg.	5 deg.	10 deg.
<u>DYNAMICAL PARAMETERS</u>			
lower pivot linear stiffnes	1.25 Nm/deg.	1.5 Nm/deg.	1.25 Nm/deg.
upper pivot linear torsion stiffness	-	0.25 Nm/deg.	0.5 Nm/deg.
upper pivot free range of motion in the plane of impact	25 ^o	10 ^o	20 ^o

CHAPTER 8

ANALYSIS OF ADDITIONAL TESTS WITH OTHER SUBJECTS

8.1 Introduction

In addition to the tests with subject H00083 and H00093 discussed before, results will be presented here of a number of earlier frontal and lateral tests with other human subjects. The frontal tests were conducted in the period between 1967 and 1969 at Wayne State University and are reported by NBDL in reference (7,16). No experimental results on magnetic tape were available for these tests, therefore only a rough analysis of these tests could be made (see section 8.2).

The lateral tests to be considered here were reported by NBDL in reference (10). In contrast to the frontal tests, for this lateral test series, data tapes with experimental results were available. An analysis of these tests was presented at the 27th Stapp Conference (28) together with the lateral impact tests with subject H00083 and H00093. Section 8.3 gives a brief summary of the findings of this analysis.

8.2 Frontal impact tests

A detailed description including test method, subject anthropometry and test results of the additional frontal tests to be considered here, is given by Ewing and Thomas (7,16). These tests were conducted at Wayne State University. Test conditions were slightly different from those of the tests with subjects H00083 and H00093. For instance, the sled acceleration - time history was triangular rather than trapezoidal (see Fig. 21). Results of the most severe tests with 10 subjects are used here. Table 11 summarizes the most significant test conditions.

Table 12 summarizes the type of information available in reference (7) which was used for our analysis. From this data it was possible to reconstruct the location of the occipital condyles at certain points in time

relative to the sled coordinate system. The shape of the center of gravity trajectories was found to be circular and from the graphical reconstructed occipital condyles it followed that for most of the subjects a 2 pivot linkage system with a link length of 0.125 m can be used to approximate the observed motions.

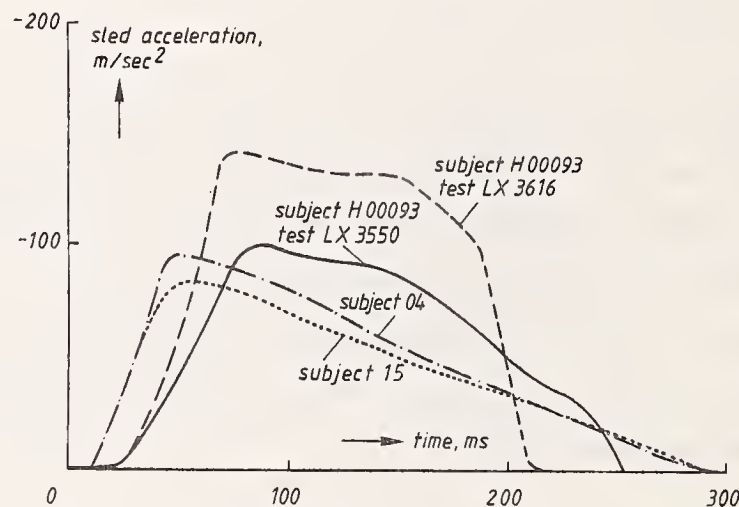


Fig. 21 Comparison of sled accelerations.

Table 11 - Test characteristics of earlier tests with 10 different subjects in frontal impacts (7).

Subject	Sled velocity change (m/s)	Peak sled acc. ² (m/s ²)	Rate of onset (m/s ³)
003	13	95	3500
004	13	94	3300
007	14	96	6300
009	13	90	3300
010	13	89	3300
011	12.5	89	3800
012	13.5	98	5300
013	12.5	91	5300
015	14	99	4600
016	12	84	3400

Table 13 summarizes the initial and extreme values for the head flexion which could be determined simply from the information available for the angular displacements (PDH). Initial and maximum values for the link rotation were graphically estimated from the reconstructed occipital condyle locations.

Table 12 - Selection of test results provided in reference (7).

Type of Data	Description
Center of gravity trajectory	Coordinate of center of gravity (MCX and MCZ) relative to T1 coordinate system
T1 angular displacement	Angular displacement (NRN) of T1 coordinate system as function of time relative to laboratory coordinate system
Head angular displacement	Angular displacement (PDH and PHN, respectively) as function of time relative to laboratory and T1 coordinate system, respectively.
Center of gravity acceleration	Linear accelerations (4XM and 4ZM) as function of time relative to laboratory x and z axis
Head angular acceleration	Angular acceleration (RAH) as function of time

Table 13 - Initial and maximum values for the head rotation ϕ and the link rotation θ (in degrees).

Subject	ϕ_0	ϕ_{\max}	$(\phi_{\max} - \phi_0)$	θ_0	θ_{\max}	$(\theta_{\max} - \theta_0)$
003	3	81	78	36	90	54
004	- 7	80	87	34	98	64
007	- 3	90	93	10	110	100
009	- 6	71	77	27	102	75
010	-15	71	86	19	105	86
011	0	72	72	32	108	76
012	-13	72	85	9	112	103
013	0	76	76	28	100	72
015	3	80	77	28	104	76
016	3	71	68	34	103	69

The accuracy for these graphically determined neck link rotations is estimated to be ± 3 degrees. Just as for the tests with subject H00083 and H00093, a significant positive value for the initial neck link rotation can be observed. Maximum neck link rotations ($\theta_{\max} - \theta_0$) are of the same order of magnitude as for the test with subjects H00083 and H00093, while values for the head flexion ($\phi_{\max} - \phi_0$) appear to be larger for most of these tests.

Peak torque values near the occipital condyles for the 1973 database were reported by Ewing and Thomas (16) to vary from 30 Nm to 50 Nm, which is

close to the peak values in Fig. 16. In contrast to our findings, Ewing and Thomas data showed significant positive torque values in the initial phase of the motion. This difference can be partly explained by different values used by Ewing and Thomas for the center of gravity location. Our calculations were based on more recent cadaver data (25) which showed a larger distance of the head c.g. to the anatomical origin than in the data used by Ewing and Thomas. Moreover, larger initial angular accelerations were measured in the Ewing and Thomas tests. The reasons for these larger values are not fully clear yet, but the fact that in these earlier tests slightly different test conditions were used might contribute to these differences. A more detailed discussion on these aspects is given by Spenny and Wismans (43).

From the mass distribution data provided in ref. (16) and the linear and angular accelerations given in ref. (7) a rough estimate could be made for the maximum torque near the center of rotation in the torso. These torques were found to vary from 59 Nm to 114 Nm which is close to the peak values in fig 19.

8.3 Lateral impact tests

The lateral tests which will be considered here were conducted by NBDL for NHTSA under contract DOT-HS-4-0852. In total 34 runs with 6 human volunteers and 12 runs with 2 chimpanzees were conducted. Photographic data on tape for the chimpanzee tests were limited to a time frame before onset of the sled acceleration, so that no further analysis of these animal tests was made. Out of the 34 tests with 6 human subjects a subset was defined of 9 of the most severe tests with four different subjects. Table 14 summarizes these tests and the most important test conditions. The impact severity in this database is of the same order of magnitude as the impact severity in the H00083 and H00093 lateral flexion tests.

Table 14 - Test Characteristics of 16 selected runs with 6 human volunteers in lateral flexion

Subject	Run Number	Sled Velocity Change (m/s)	Peak Sled Acc. ² (m/s ²)	Rate of Onset* (m/s ³)
H00044	LX1504	6.6	60	1246
H00044	LX1512	6.2	69	1519
H00044	LX1528	6.3	74	1644
H00064	LX1507	6.5	59	1202
H00064	LX1513	6.2	69	1506
H00065	LX1505	6.6	61	1233
H00065	LX1510	6.2	69	1526
H00067	LX1509	6.2	68	1498
H00067	LX1525	6.2	74	1708

* Slope of the best least square line fit of the rising portion of the sled acceleration profile between 20% and 50% of the peak sled acceleration.

Table 15 - Initial and maximum head flexion ϕ and neck link rotation θ (in degrees) in lateral flexion

Subject nr. (test nr.)	ϕ_0	ϕ_{\max}	$\phi_{\max} - \phi_0$	θ_0	θ_{\max}	$\theta_{\max} - \theta_0$
H00044						
1504	-1	39	40	0	47	47
1512	6	53	47	5	57	52
1528	3	48	45	5	56	51
H00064						
1507	3	61	58	-4	61	65
1513	4	64	60	2	65	63
H00065						
1505	1	59	58	7	67	60
1510	6	63	60	7	67	60
H00067						
1509	4	59	55	-1	58	59
1525	6	60	64	4	62	58

Results of these tests were found to agree quite well with the test results obtained with subjects H00083 and H00093. A similar linkage as proposed in chapter 7 for the lateral impacts could be used to characterize the observed displacements, namely a 2-pivot linkage mechanism with the upper pivot located at the occipital condyles and a link length of 0.125 m. The lower pivot location in the torso as for subject H00083 and H00093 was found to

be different for each subject. A rough estimation for these locations resulted in a distance varying from 0 - 0.02 m to the mid-sagittal plane, in the direction of the thrust vector of the accelerator.

In order to illustrate the similarity in kinematics a comparison is presented in Fig. 22 for the head torsion ($\psi - \psi_0$) and neck link rotation ($\theta - \theta_0$) as function of head flexion ($\phi - \phi_0$)*. A summary of extreme value for the head flexion ϕ and the neck link rotation θ is given in table 15. Maximum rotations ($\phi - \phi_0$) and ($\theta - \theta_0$) appear to be slightly larger for some of the subjects in this database compared to the tests with subject H00083 and H00093.

For the loads at the occipital condyles and at the torso center of rotation the tests in both databases showed good agreement (28).

* θ values in this figure for subject H00083 and H00093 may slightly vary from data presented in chapter 5, due to the use of a different method used for T1 coordinate system correction and for specification of the lower pivot location. The torso pivot was taken identical for all 6 subjects based on an average value for all 6 subjects (i.e. 0.02 m from the mid-sagittal plane).

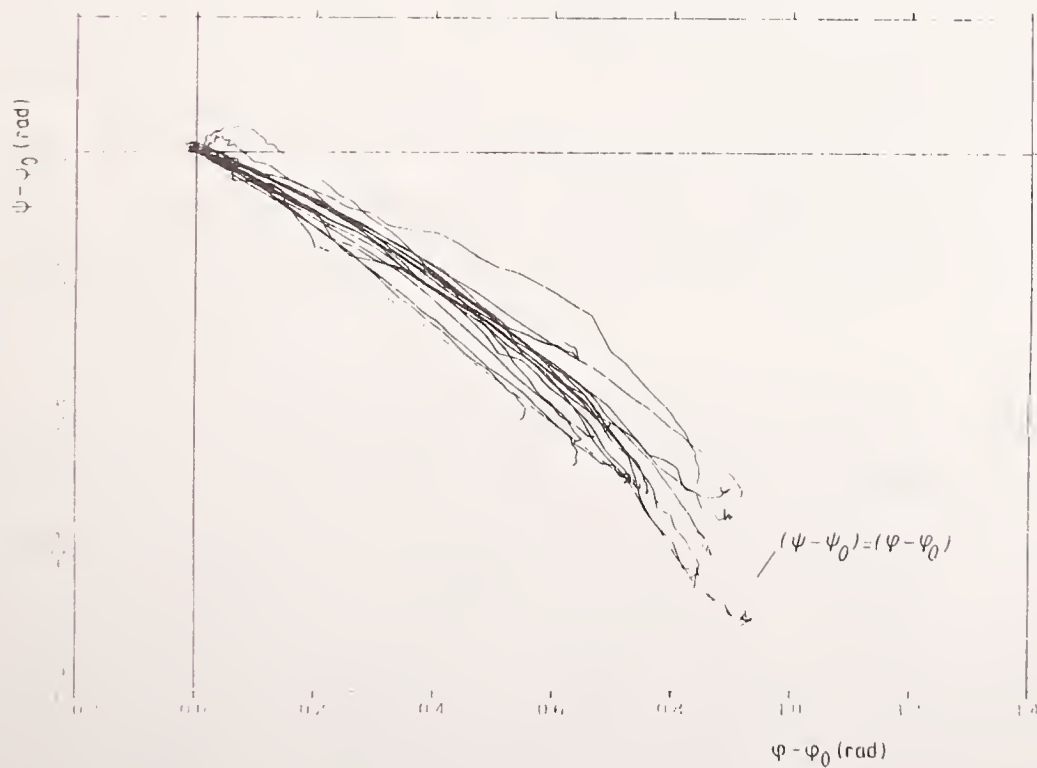
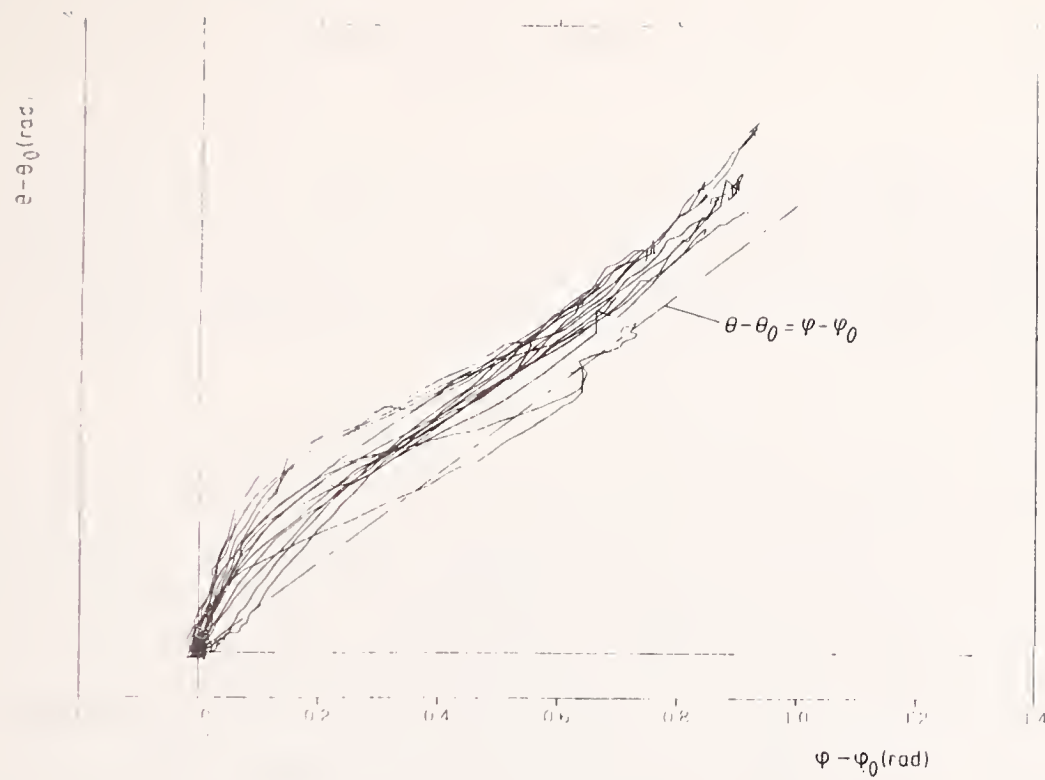


Fig. 22 Neck link flexion ($\theta - \theta_0$) and head link torsion ($\psi - \psi_0$) as function of head flexion ($\phi - \phi_0$) in 16 lateral impacts with subjects H00044, H00064, H00065, H00067, H00083 and H00093.

CHAPTER 9

DISCUSSION AND CONCLUSIONS

The study presented here is part of a research program to develop a mechanical neck with omnidirectional biofidelity. An analysis is presented of 30 tests with 2 human volunteers exposed to frontal, oblique and lateral impacts.

The most important finding of this study is that the observed human head-neck response can be represented adequately by a linkage system with 2-pivots. For the three impact directions a separate mechanical analog is proposed. For frontal impact this system has 2 and for lateral and oblique impacts 3 degrees of freedom. These degrees of freedom are a neck link rotation in the plane of impact, a head rotation in the plane of impact and a head torsion about the head anatomical z-axis respectively. This last degree of freedom is absent in frontal impacts. The neck link length and the upper pivot location roughly can be taken identical in all three impact directions. For some of the remaining parameters of the mechanical analog differences for the three impact directions can be observed (see 7.3). In Vol. II of this report the proposed mechanical analog systems will be simulated mathematically and the model response will be compared with the human volunteer behaviour.

In this study separate systems are proposed for the three impact directions. As an alternative, one single three dimensional linkage could also have been proposed to simulate all three impact directions. Such a mechanism would possess 5 degrees of freedom: 2 degrees of freedom in the lower pivot and three degrees of freedom in the upper pivot. In such a system the neck link rotation is not limited to a planar motion in the plane of impact. The major problem in defining such a system is the initial orientation of the neck link in lateral flexion. If this initial orientation (i.e. 5 degrees) can be neglected, formulation of such a 3-dimensional system is not expected to cause significant problems. Attractive aspects of such a three-dimensional system are, among other things, the possibility to pre

dict the head response in other directions than frontal, lateral or oblique directions and the possibility to determine out of impact plane motions which were neglected in the present analysis.

Geometrical linkage parameters in this study have been estimated using simple graphical techniques. In addition, numerical techniques were developed and applied to a limited set of tests which will allow a more accurate specification of these parameters (27). Especially for a database with a large number of human volunteer and cadaver tests a numerical approach is expected to be beneficial.

The head link rotation (flexion and torsion) can be determined directly from the test data provided by NBDL. However, this is not the case for the neck link rotation. A different correction method for the T1 coordinate system for instance and the limited accuracy of the graphical pivot specification will effect the θ values.

One of the most significant parameters in the mechanical analog is the lower pivot stiffness. This stiffness was estimated from torque data near T1, rather than based directly on torque calculations at the lower pivot location. It is strongly recommended in subsequent test series to calculate this torque at the location of the lower pivot in order to improve the accuracy of the lower pivot stiffness specification (see also Vol. II).

In this study pivot stiffness data are derived graphically from torque-rotation characteristics. The limited accuracy of this graphical approach should be improved by means of numerical (least squares) approximation techniques.

The findings in this study are primarily based on 30 tests with two subjects. These findings were roughly compared with some of the earlier tests by NBDL (see chapter 8) and in general good agreement could be observed. It is strongly recommended that additional tests with other human subjects are analysed to verify in more detail the findings presented here.

The NBDL tests were conducted with a variety of test conditions for relatively low g-levels. The severity of the most severe human volunteer test (i.e. 15.3 g, 17.2 m/s) is still less severe than the standard Part 572 neck pendulum calibration test, while on the other hand this calibration test is much less severe than for instance a 35 mph car crash test environment. Since the proposed analog is only valid for low severity impacts, i.e. the NBDL human volunteer test conditions, additional information should be obtained for higher exposure levels from human cadaver tests. If such data become available, adjustment of the proposed analog systems might be necessary. In conjunction with such tests mathematical simulation could be conducted in order to correct for the absence of muscle activity.

The mechanical analog systems, as defined herein, implicitly constitute a performance requirement. It is also possible to explicitly specify the necessary and sufficient conditions for achieving the major response by means of kinematic requirements (displacements, accelerations) for several impact levels. Such a formulation is desirable for establishing a standard to be used in the laboratory for verifying response of a dummy. In such a formulation the measured volunteer test data is the performance requirement, thereby eliminating the loss of rigor due to rigid body modelling assumptions and due to interpretation in formulating the mechanical substitute's characteristics from the test data. An example of this type of requirements is provided in Vol II of this final report where the response of an analog system which is simulated mathematically, will be compared directly with the human volunteer response.

ACKNOWLEDGEMENT

This study has been supported by the Department of Transportation/National Highway Traffic Safety Administration. All opinions given in this report are those of the authors, and not necessarily those of DOT/NHTSA.

The authors wish to express their gratitude to the staff of the Naval Biodynamics Laboratory in New Orleans in providing the human volunteer test data and the additional information necessary to perform this analysis; to J. Hofferberth and T. Hoyt of the Vehicle Research and Test Center, East Liberty (Ohio) and R. Eppinger and R. Morgan of the Office of Vehicle Research, Washington, DC for their guidance and valuable suggestions; to R. Stalnaker and D. Guenther of the Ohio State University, Columbus (Ohio) for their general support; to M. Cline of the Transportation Research Center, East Liberty, Ohio, D. Gordon of Systems Development Corporation in Cambridge and M. de Bruin and L. Wittebrood of the Research Institute for Road Vehicles TNO, Delft, The Netherlands for the processing of the test results; to C. Spenny of the Transportation Research Center in Cambridge who was responsible for the neck load calculations; to R. Saul of the Vehicle Research and Test Center, East-Liberty, Ohio who provided the dummy-neck test data; to M. Farris and J. Lyn of the Ohio State University Columbus, Ohio for their contribution in the MADYMO simulations.

REFERENCES

1. Mertz, H.J. and Patrick, L.M. (1971):
"Strength and Response of the Human Neck". In: Proceedings of the 15th Stapp Car Crash Conference, SAE Paper No. 710856.
2. Mertz, H.J., Neathery, R.F. and Culver, C.C. (1973):
"Performance Requirements and Characteristics of Mechanical Necks". In: Human Impact Response, Plenum Press, New York, London, pp. 263-288.
3. Melvin, J.W., Mc Elhaney, J.H. and Roberts, V.L. (1973):
"Evaluation of Dummy Neck Performance". In: Human Impact Response, Plenum Press, New-York, London, pp. 247-261.
4. Muzzy III, W.H. and Lustick, L. (1976):
"Comparison of Kinematic Parameters Between Hybrid II Head and Neck System with Human Volunteers for - Gx Acceleration Profiles". In: Proceedings of the 20th Stapp Car Crash Conference, SAE Paper No. 760801.
5. Patrick, L.M. and Chou, C.C. (1976):
"Response of the Human Neck in Flexion, Extension and Lateral Flexion". Final Report to the Society of Automotive Engineers. Vehicle Research Institute Report No. VRI-7.3.
6. Maltha, J. and Janssen, E.G. (1983):
"EEC Comparison Testing of Four Side Impact Dummies". In: Proceedings of the Seminar on the Biomechanics of Impacts in Road Accidents, Commission of the European Communities, Brussel 1983.
7. Ewing, C.L. and Thomas, D.J. (1973):
"Human Head and Neck Response to Impact Acceleration". NAMRL Monograph 21. Naval Aerospace Medical Research Laboratory, Pensacola, Florida, 32512.
8. Becker, E.B. (1975):
"A Photographic Data System for Determination of Three-dimensional Effects of Multiaxis Impact Acceleration on Living Humans". Proc. Soc. of Photo-Optical Instrumentation Engineers, Vol. 57. SPIE, Box 1146, Palos Verdes Estates, Ca. 90274.
9. Becker, E.B. and Willems, G. (1975):
"An experimentally Validated Three-dimensional Inertial Tracking Package for Application in Biodynamics Research". In: Proceedings of the 19th Stapp Car Crash Conference, SAE Paper no. 751173.
10. Ewing, C.L., Thomas, D.J., Lustick, L., Williams, G.G., Muzzy III, W.H., Becker, E.B. and Jessop, M.E. (1978):
"Dynamic Response of Human and Primate Head and Neck to + Gy Impact Acceleration". Report DOT HS-803 058.

11. Becker, E. (1977):
"Stereoradiographic Measurements for Anatomical Mounted Instruments".
Proceedings of the 21st Stapp Car Crash Conference.
12. Ewing, C.L., Thomas, D.J. and Lustick, L. (1978):
"Multiaxis dynamic response of the human head and neck to impact acceleration". Aerospace Medical Panel's Specialist's meeting. Paris, AGARD Conference Proceedings no 253. North Atlantic Treaty Organisation. Advisory Group for Aerospace research and Development.
13. Ewing, C.L., Thomas, D.J. and Beeler, G.W. (1968):
"Dynamic response of the head and neck of the living Human to - Gx Impact acceleration". Proc. of the 12th Stapp Car Crash Conference, P-26. Society of Automotive Engineers.
14. Ewing, C.L., Thomas, D.J., Patrick, L.M., Beeler, G.W. and Smith, M.J. (1969):
"Living human dynamic response to - Gx impact acceleration. II Accelerations measured on the head and neck". Proc. of the 13th Stapp Car Crash Conference, P-28. Society of Automotive Engineers.
15. Ewing, C.L. and Thomas, D.J. (1971):
"Human Impact Response to - Gx impact acceleration". AGARD - Conference proceedings, AGARD-CP-88-71, June 1971.
16. Ewing, C.L. and Thomas, D.J. (1973):
"Torque versus Angular Displacement Response of Human Head to - Gx Impact Acceleration". Proceedings of the 17th Stapp Car Crash Conference.
17. Ewing, C.L., Thomas, D.J., Lustick, L., Becker, E., Willems, G. and Muzzy III, W.H. (1975):
"The effect of the Initial Position of the Head and Neck on the Dynamic Response of the Human Head and Neck to - Gx impact acceleration". Proceedings of the 19th Stapp Car Crash Conference.
18. Ewing, C.L., Thomas, D.J., Lustick, L., Muzzy III, W.H. Willems, C. and Majewski, P.L. (1976):
" The Effect of Duration, Rate of Onset and Peak Sled Acceleration on the Dynamic Response of the Human Head and Neck". Proceedings of the 20th Stapp Car Crash Conference. SAE-paper 760800.
19. Ewing, C.L., Thomas, D.J., Majewski, P.L., Black, R. and Lustick, L. (1977):
"Measurement of head, T1 and Pelvic Response to - Gx Impact Acceleration". Proceedings of the 21st Stapp Conference.
20. Ewing, C.L., Thomas, D.J., Lustick, L., Muzzy III, W.H., Willems, G.C. and Majewski, P. (1977):
"Dynamic Response of the Human Head and Neck to + Gy Impact Acceleration". Proc. of the 21st Stapp Car Crash Conference.

21. Ewing, C.L., Thomas, D.J., Lustick, L., Muzzy III, W.H., Willems, G.C. and Majewski, P. (1978):
"Effect of Initial Position on the Human Head and Neck Response to + Y impact acceleration". Proc. of the 22nd Stapp Car Crash Conference.
22. Willems, G.C. and Becker, E.B. (1981):
"An algorithm for minimizing the effect of low frequency error in kinematic variables derived from cinematography". 2nd Int. Symp. of Biomechanics Cinematography and High Speed Photography. Proc. SPIE Vol 291.
23. Seeman, M.R. and Lustick, L.S. (1981):
"Combination of accelerometer and photographic derived kinematic variables defining three-dimensional rigid body motion". 2nd Int. Symp. of Biomechanics Cinematography and High Speed Photography. Proc. SPIE Vol 291.
24. McConville, J.T., Churchill, T.D., Kaleps, I., Clauser, C.E. and Cuzzi, J. (1980):
"Antropometric Relationships of Body and Body Segment Moments of Inertia". Report AFAMRL-TR-80-119. Air Force Aerospace Medical Research Lab. Wright Patterson Airforce Base, Ohio 45433.
25. Beier, G., Schuller, E., Schuck, M., Ewing, C.L., Becker, E.D. and Thomas, D.J. (1980):
"Center of Gravity and Moments of Inertia of Human Heads". Proc. 6th IRCOBI Conference, Birmingham, England, 1980, pp. 218-228.
26. Woltring, H.J. and Wismans, J. (1984):
"Parameter estimation for single- and dual-pivot, kinematical neck models in crash injury research". Fourth meeting of the European Society of Biomechanics, Davos, Switzerland.
27. Woltring, H.J. (1984):
"Parameter estimation for single- and dual-pivot kinematical neck models in crash injury research". Report prepared for the Ohio State University Research Foundation under contract no. RF OSU-82-0043-01.
28. Wismans, J. and Spenny, C.H. (1983):
"Performance requirements for mechanical necks in lateral flexion". In: Proceedings of the 27th Stapp Car Crash Conference. SAE, Paper No. 831613.
29. Wismans, J. and Spenny, C.H. (1984):
"Head neck response in frontal flexion". Proceedings of the 28th Stapp Car Crash Conference.
30. "Analysis of Head/Neck Response of Human Volunteers", NHTSA report prepared by the US DOT Transportation Systems Center, Cambridge, M.A. (in preparation).
31. Farris, M.V. (1983):
"Literature review: Mechanical Dummy Necks". Interim report SRL-59. Vehicle Research and Test Center, East Liberty, Ohio 43319.

32. Privitzer, E., Hosey, R.R. and Reyerson, J.E. (1982):
"Validation of a Biodynamic Injury Prediction model of the Head-Spine System". In: AGARD Conference Proceedings no. 322. Presented at the Aerospace Medical Specialists Meeting, Cologne, West-Germany, April 1982.
33. Merrill, T., Goldsmith, W. and Deng, Y.C. (1984):
"Three-dimensional response of a lumped parameter head-neck model due to impact and impulsive loading". J. Biomechanics, Vol. 17, no. 2, pp. 81-95.
34. Huston, R.L., Huston, J.C. and Harlow, M.W. (1978):
"Comprehensive, Three-Dimensional Head-neck model of impact and high acceleration studies". Aviation, Space and Environmental Medicine. Jan. 1978, pp 205-210.
35. Kabo, J.M. and Goldsmith, W. (1983):
"Response of a human head-neck model to transient sagittal plane loading". J. Biomechanics Vol 16 no. 5 pp 313-325.
36. Becker, E.B. (1973):
"Preliminary discussion of an approach to modeling living human head and neck to - Gx impact acceleration. In: Human Impact response. Plenum Press, New York-London pp 321-329.
37. Schneider, L.W. and Bowman, B.M. (1978):
"Prediction of head/neck dynamic response of selected military subjects to - Gx acceleration". Aviation, Space and Environmental Medicine, jan. 1978.
38. Frisch, G.D. and Cooper, C. (1978):
"Mathematical modeling of the head and neck response to - Gx impact acceleration (minimum articulation requirements)". Aviation Space and Environmental Medicine, jan. 1978.
39. Tarriere, C. and Sapin, C. (1969):
"Biokinetic study of the head to thorax linkage. Proc. of the 13th Stapp Car Crash Conference.
40. Moffatt, E.A. and Schulz, A.M. (1979):
"X-ray study of the human neck during voluntary motion". SAE Paper 790134.
41. Becker, E.B. (1983):
United States Patent 4395235. July 26, 1983.
42. Becker, E.B. (1980):
"Head and Neck Kinematics for frontal, oblique and lateral crash impact". Report NBDL-80R009. Naval Biodynamics Laboratory, New Orleans.
43. Spenny, C.H. and Wismans, J. (1983):
"Kinematic and dynamic analysis of head-neck motion". Proceedings of the Symposium of Mechanisms of Head and Spine Trauma (in press), 13th Annual Meeting of Neuroelectric Society, Marco Beach, Florida.

APPENDIX A

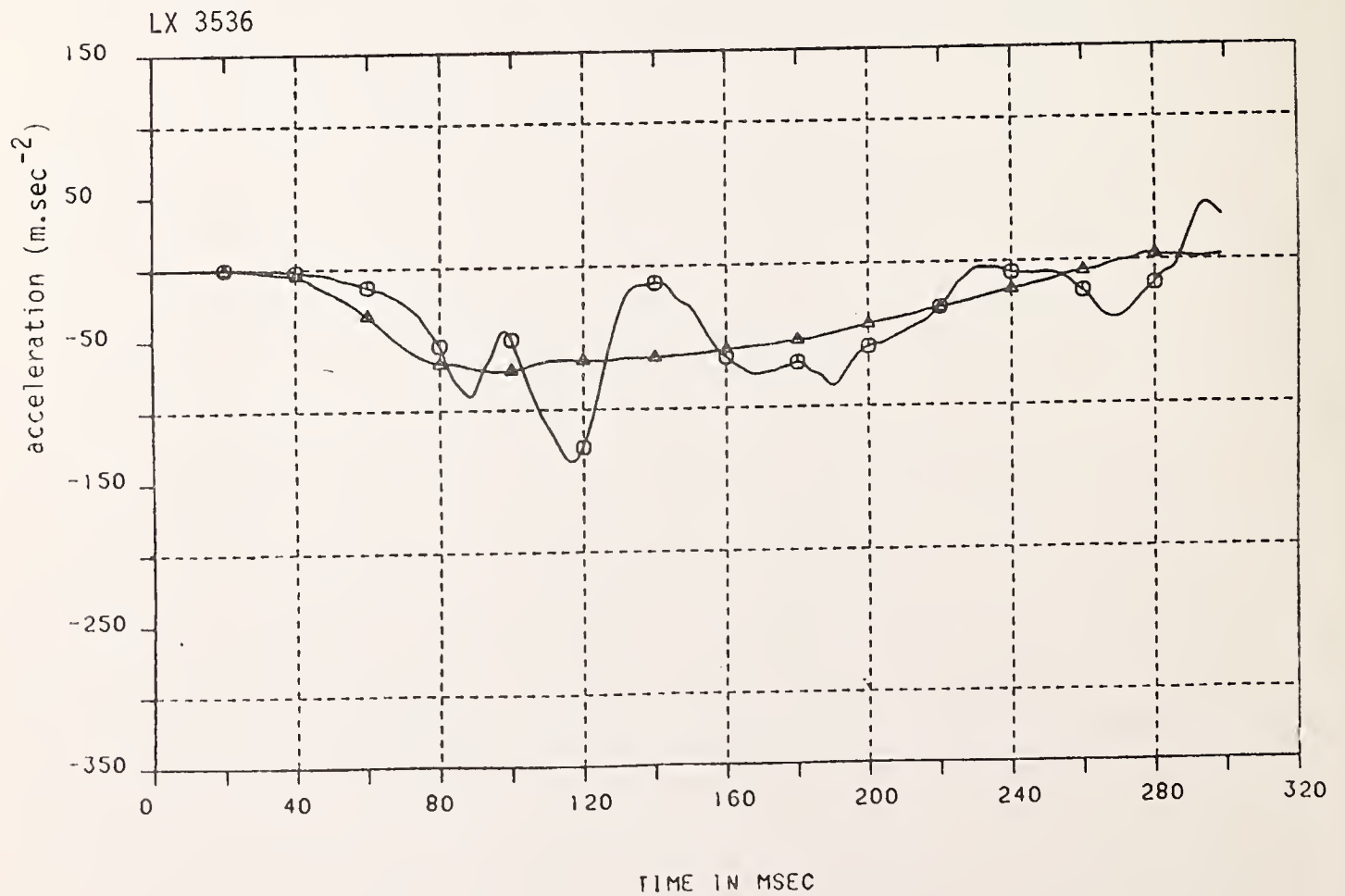
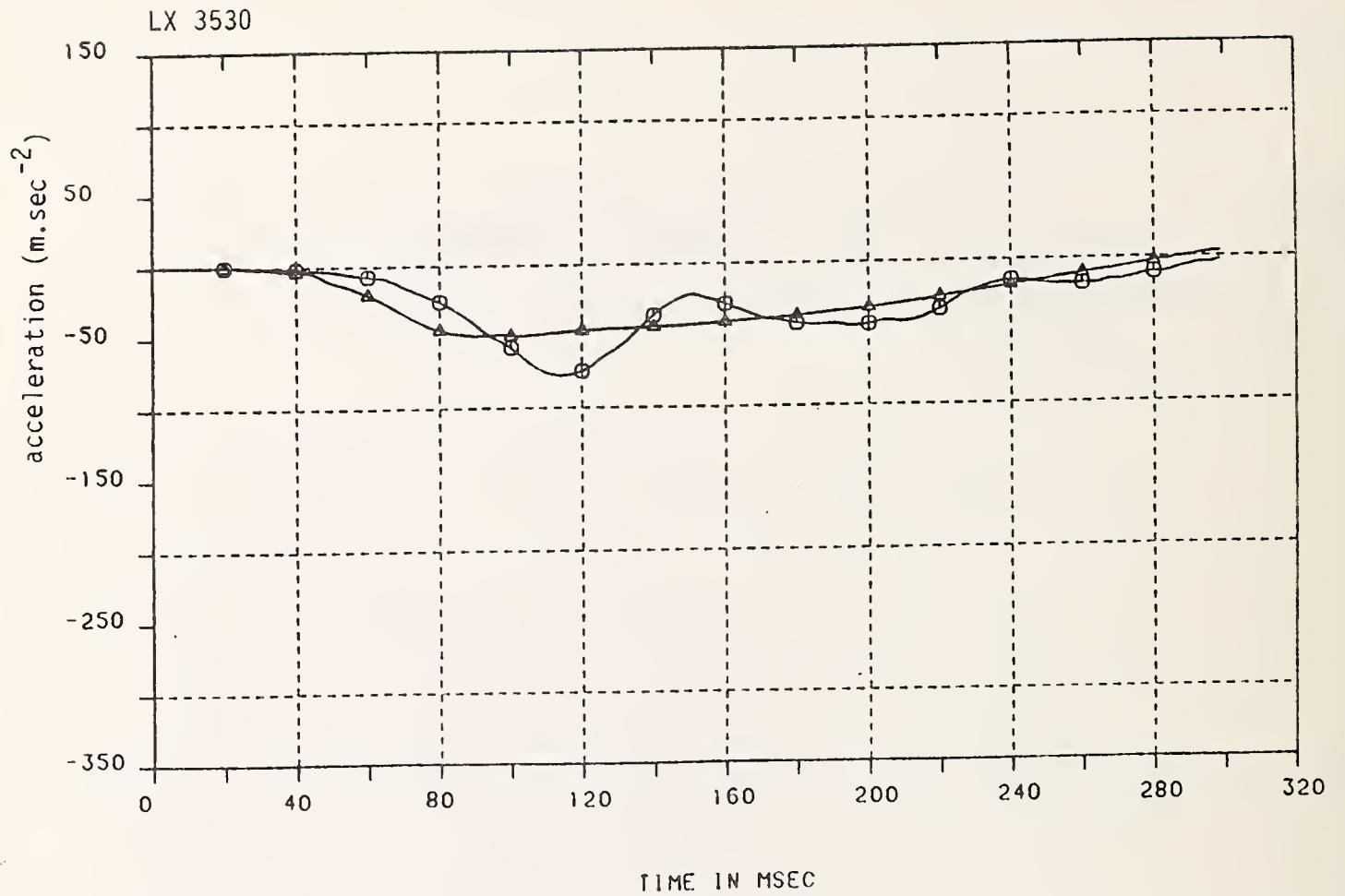
COMPARISON OF SLED ACCELERATION AND HORIZONTAL T1
ACCELERATION IN 30 SELECTED TESTS WITH SUBJECT
H00083 AND H00093.

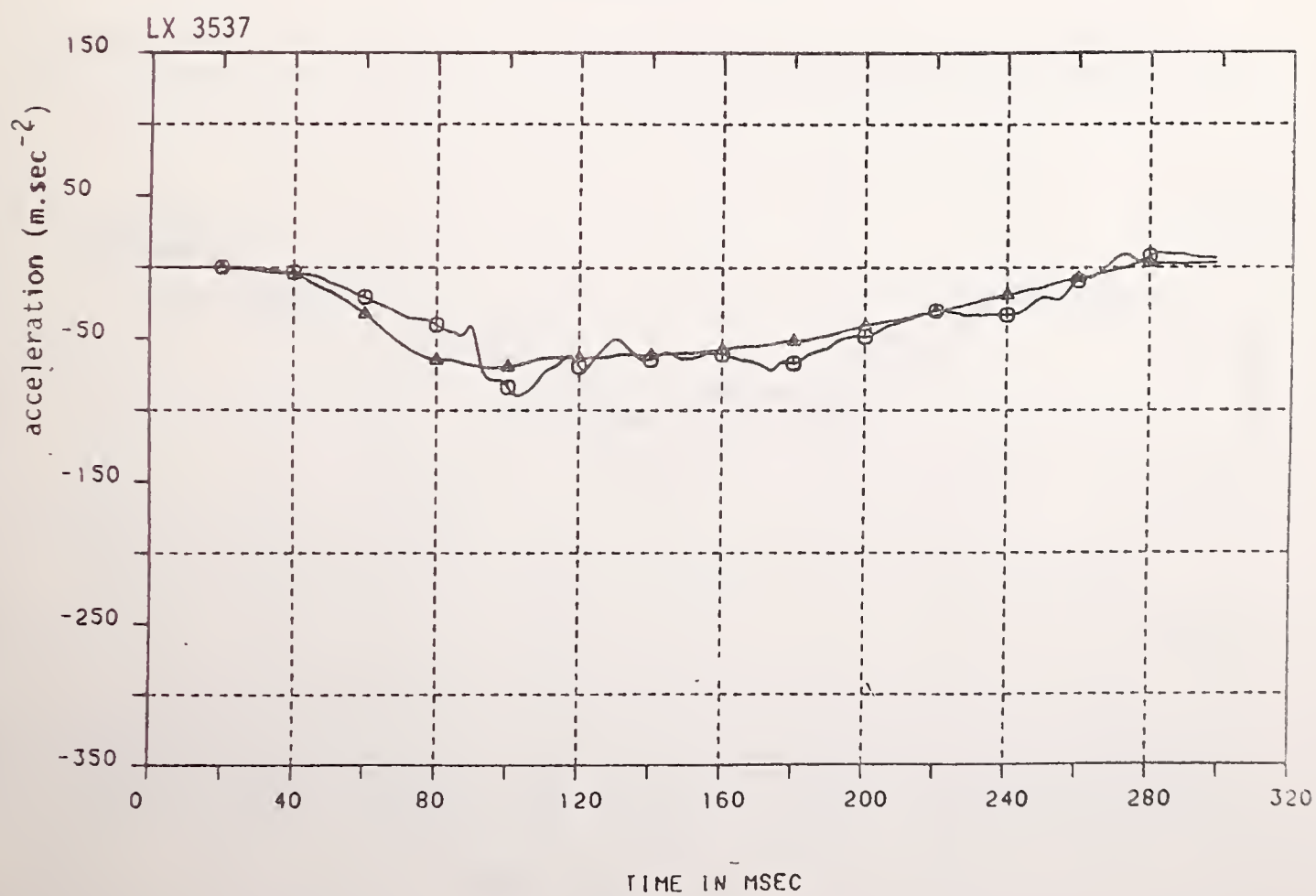
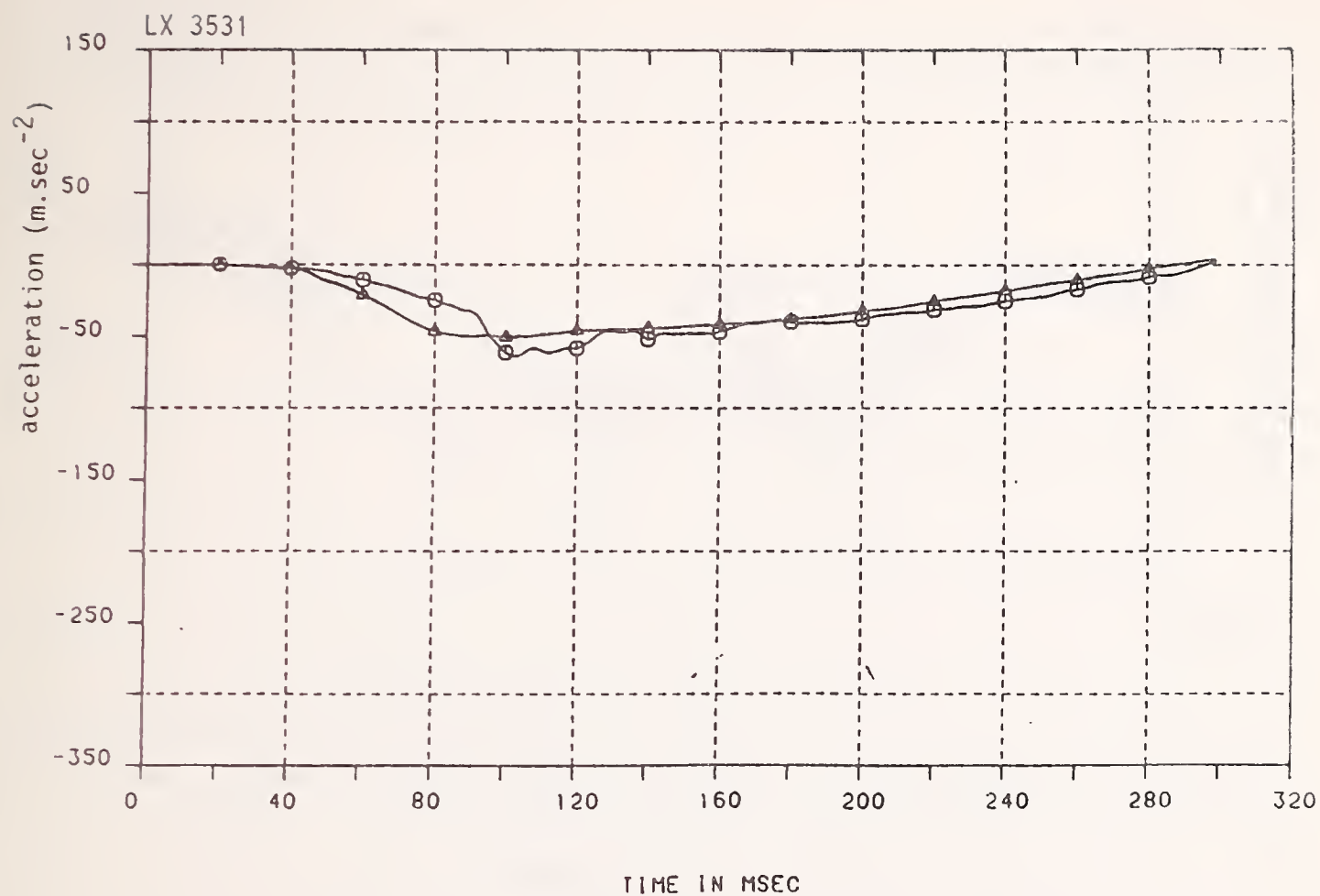
Annex A

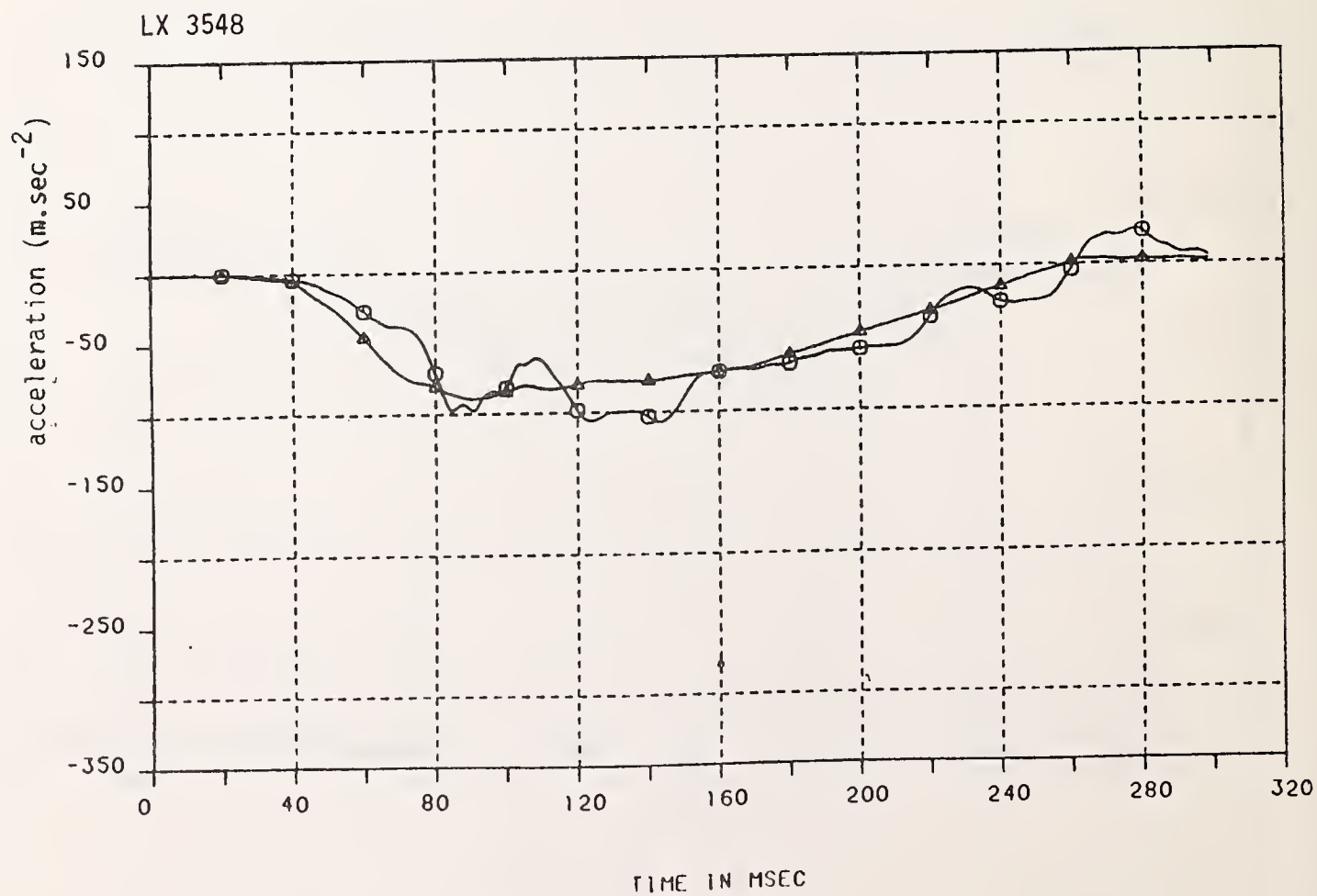
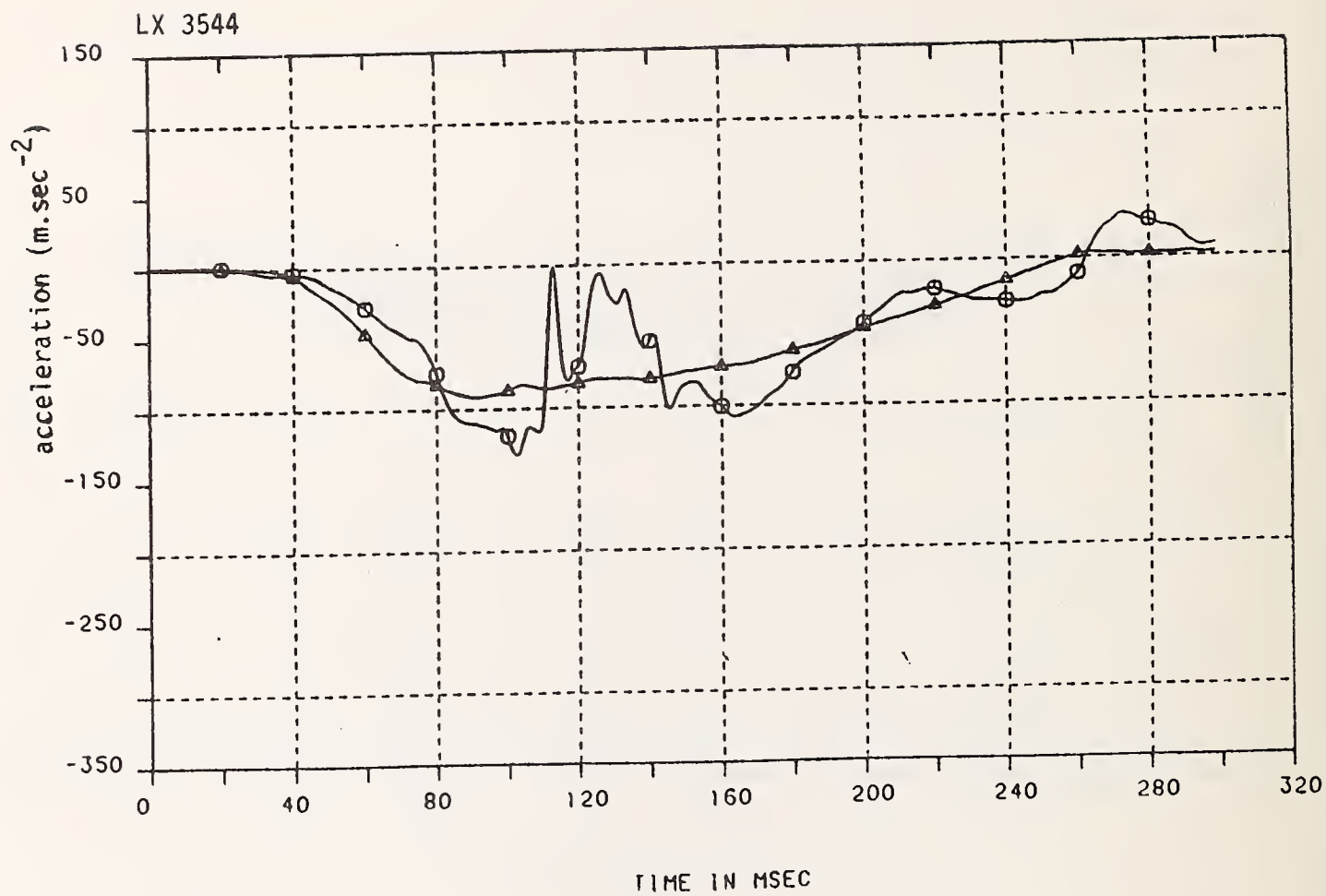
Comparison of sled acceleration and horizontal T1 acceleration in 30 selected tests with subject H00083 and H00093.

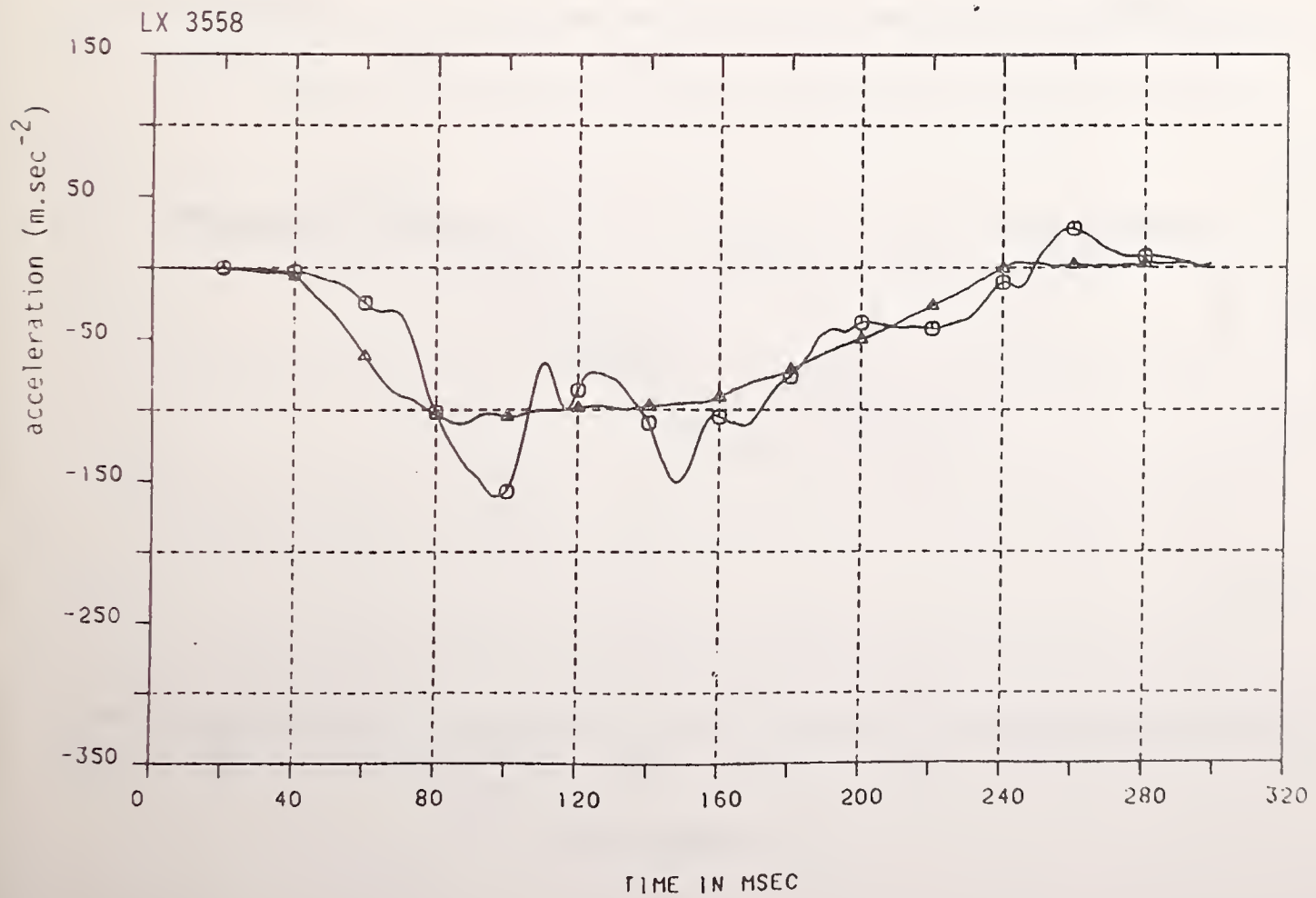
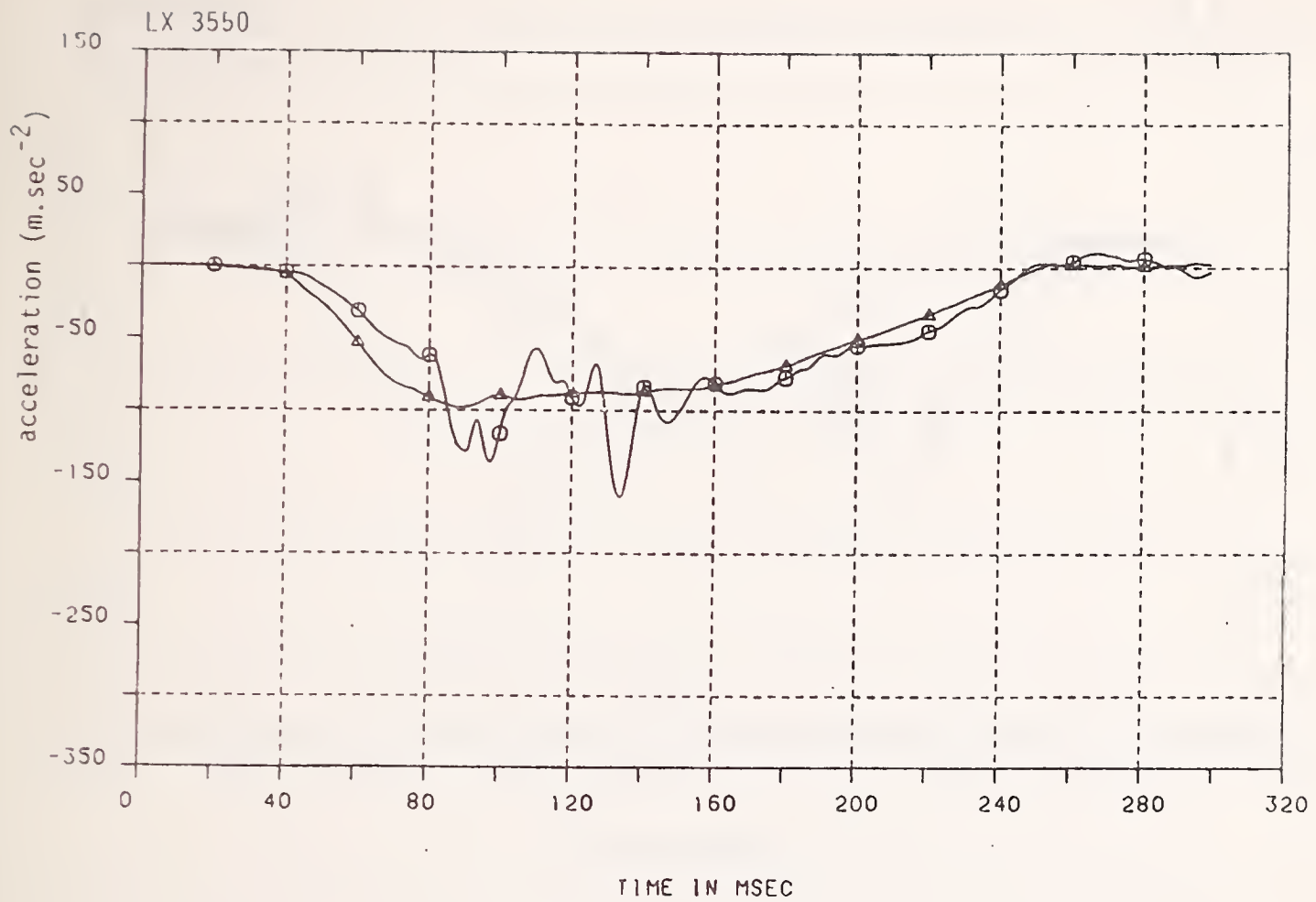
Δ — Δ sled acceleration

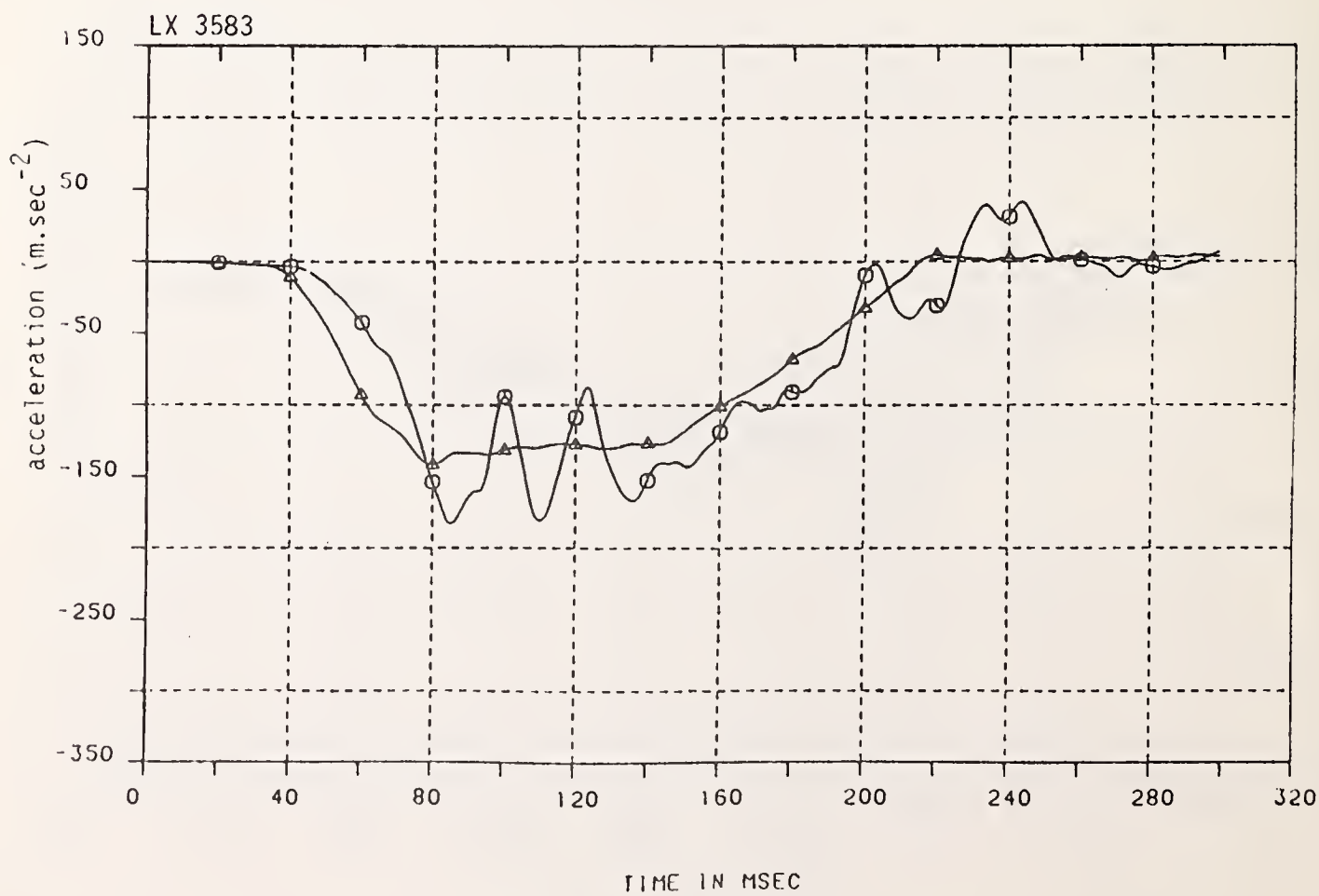
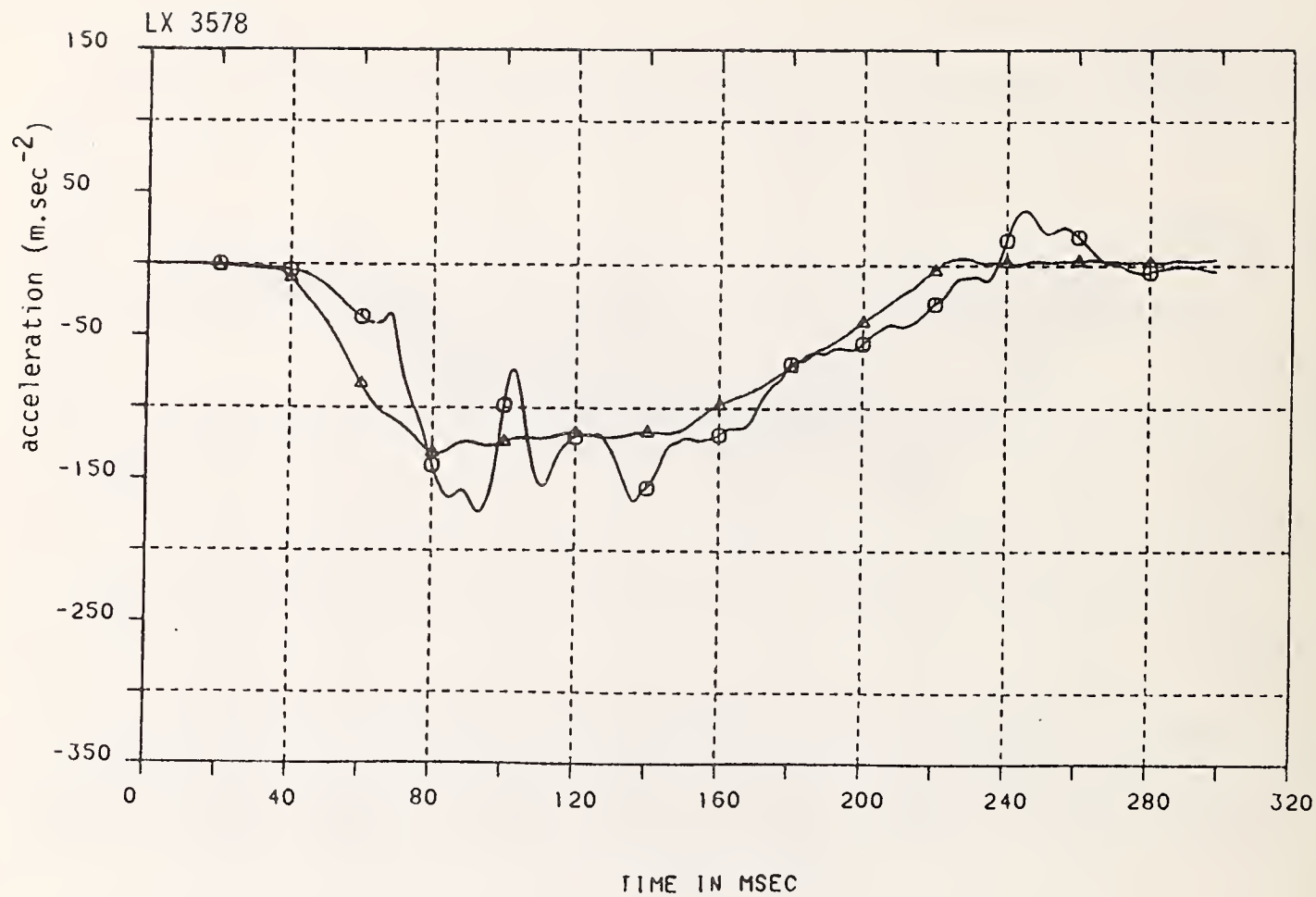
\circ — \circ T₁ acceleration

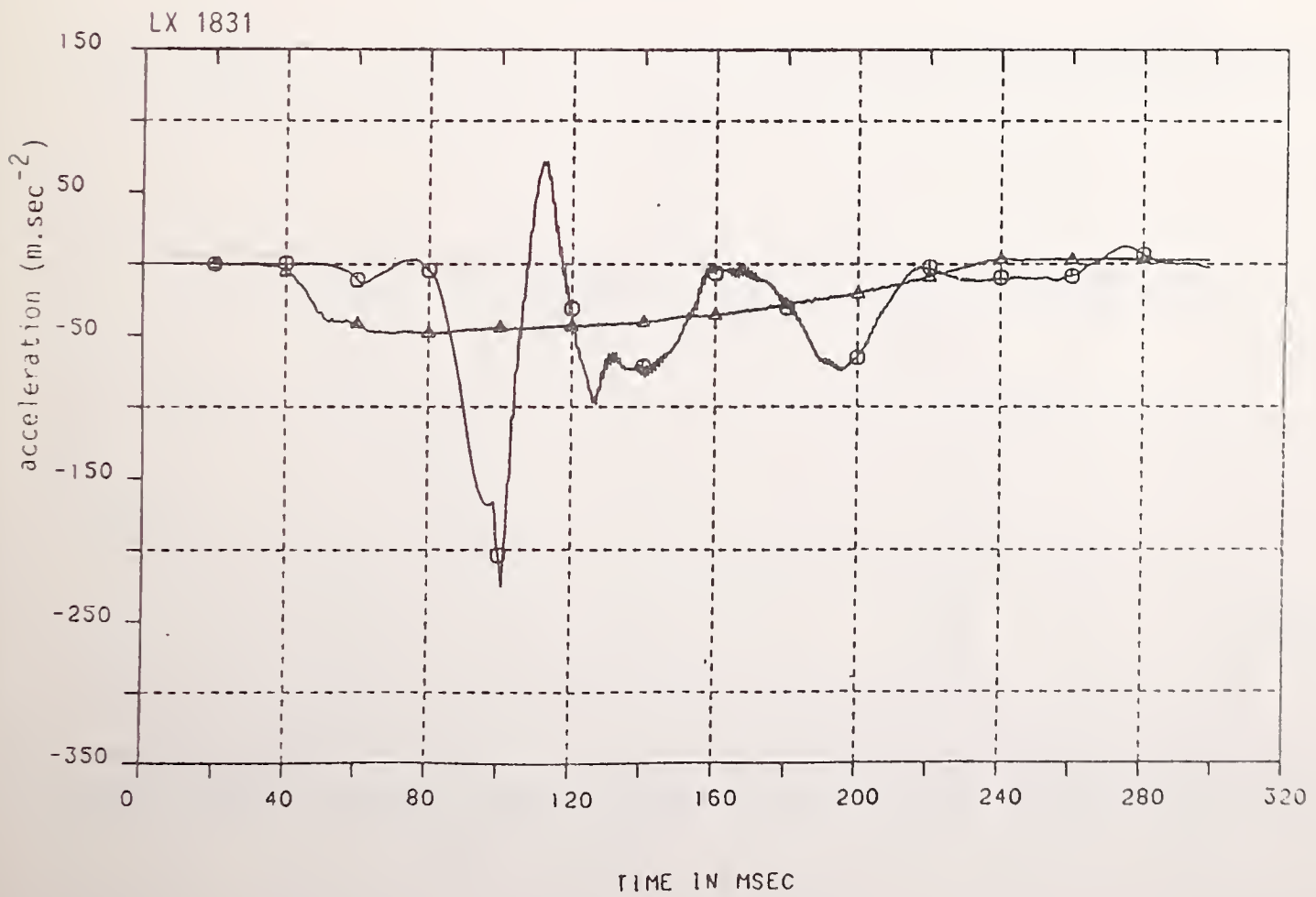
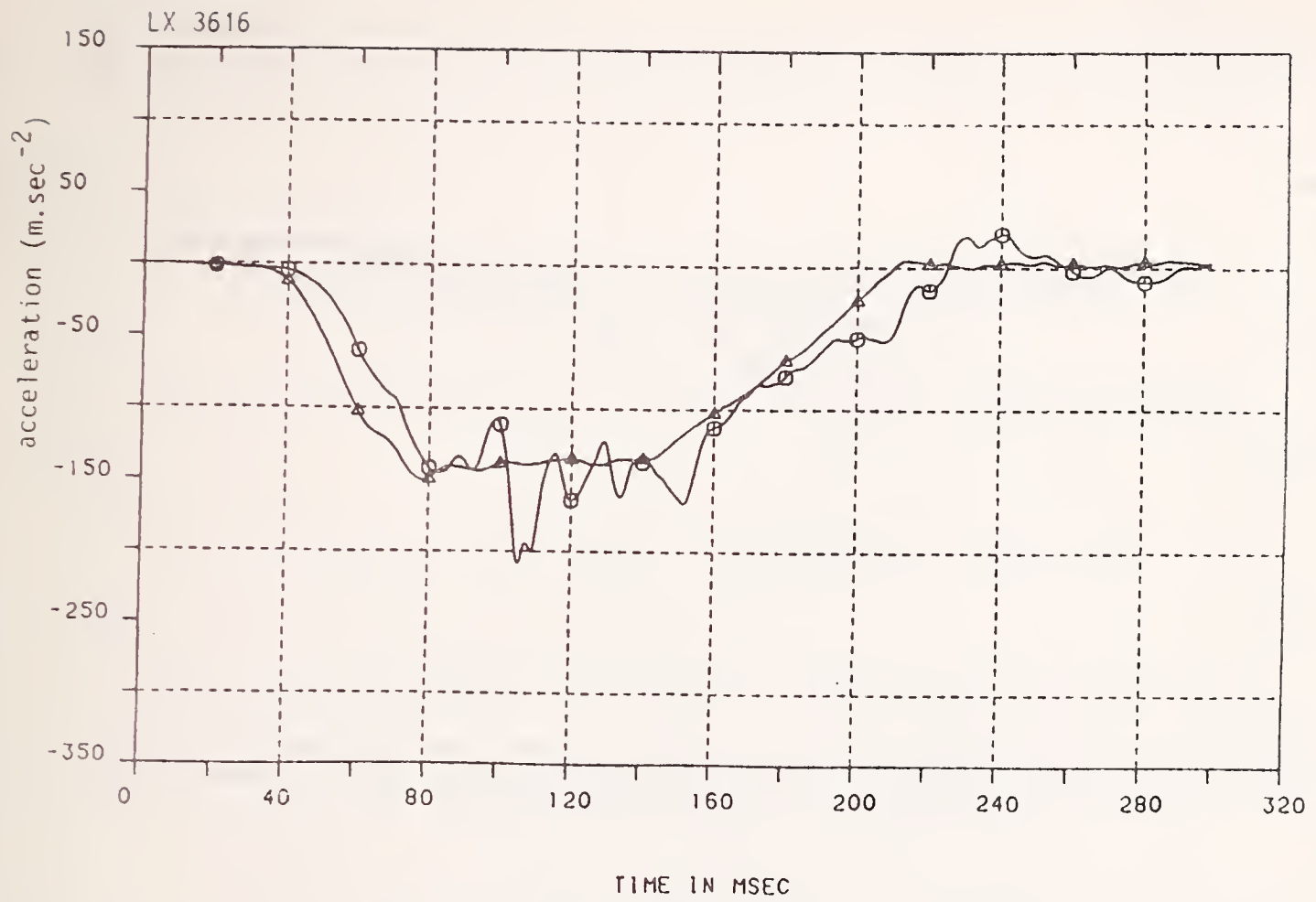


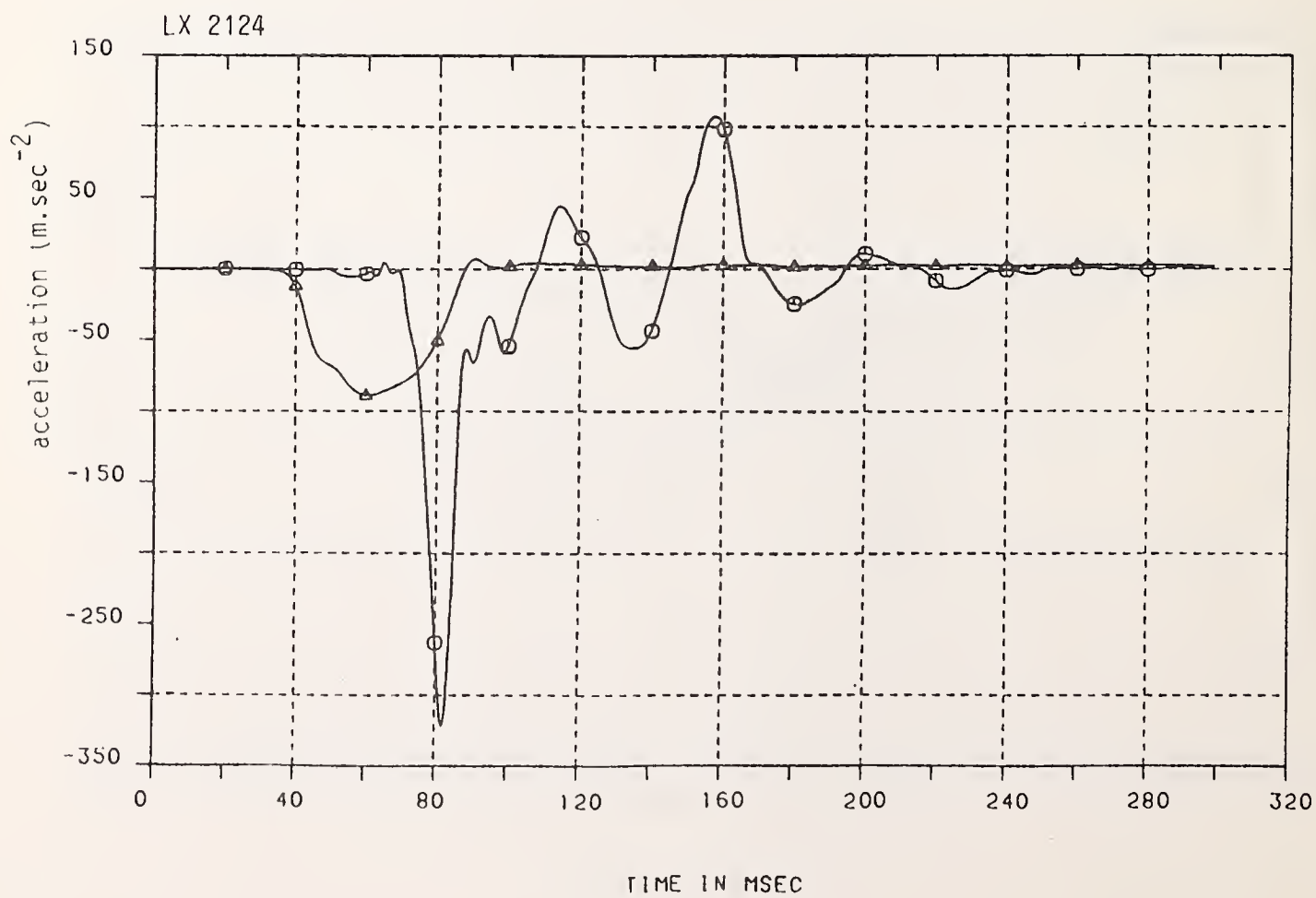
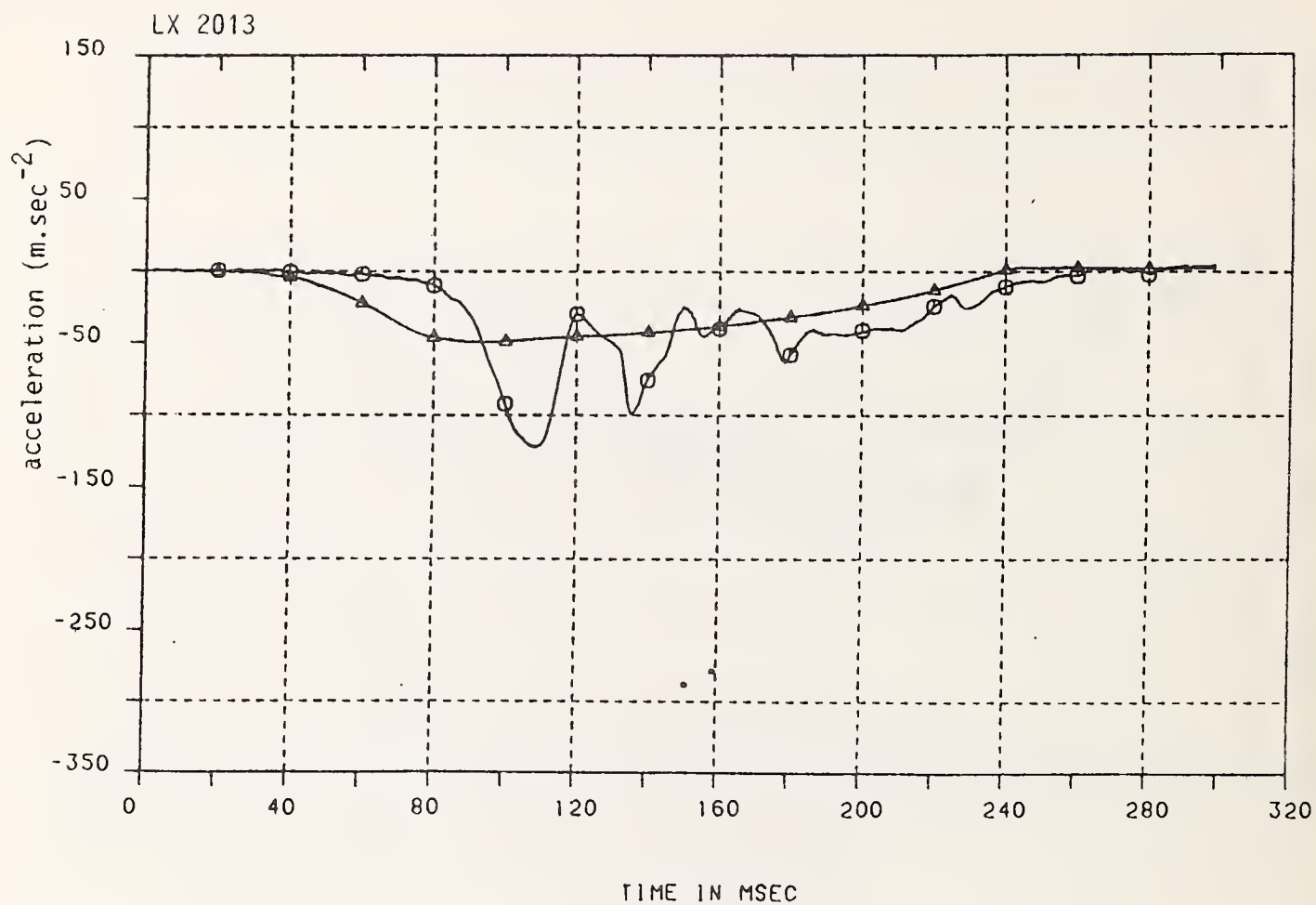


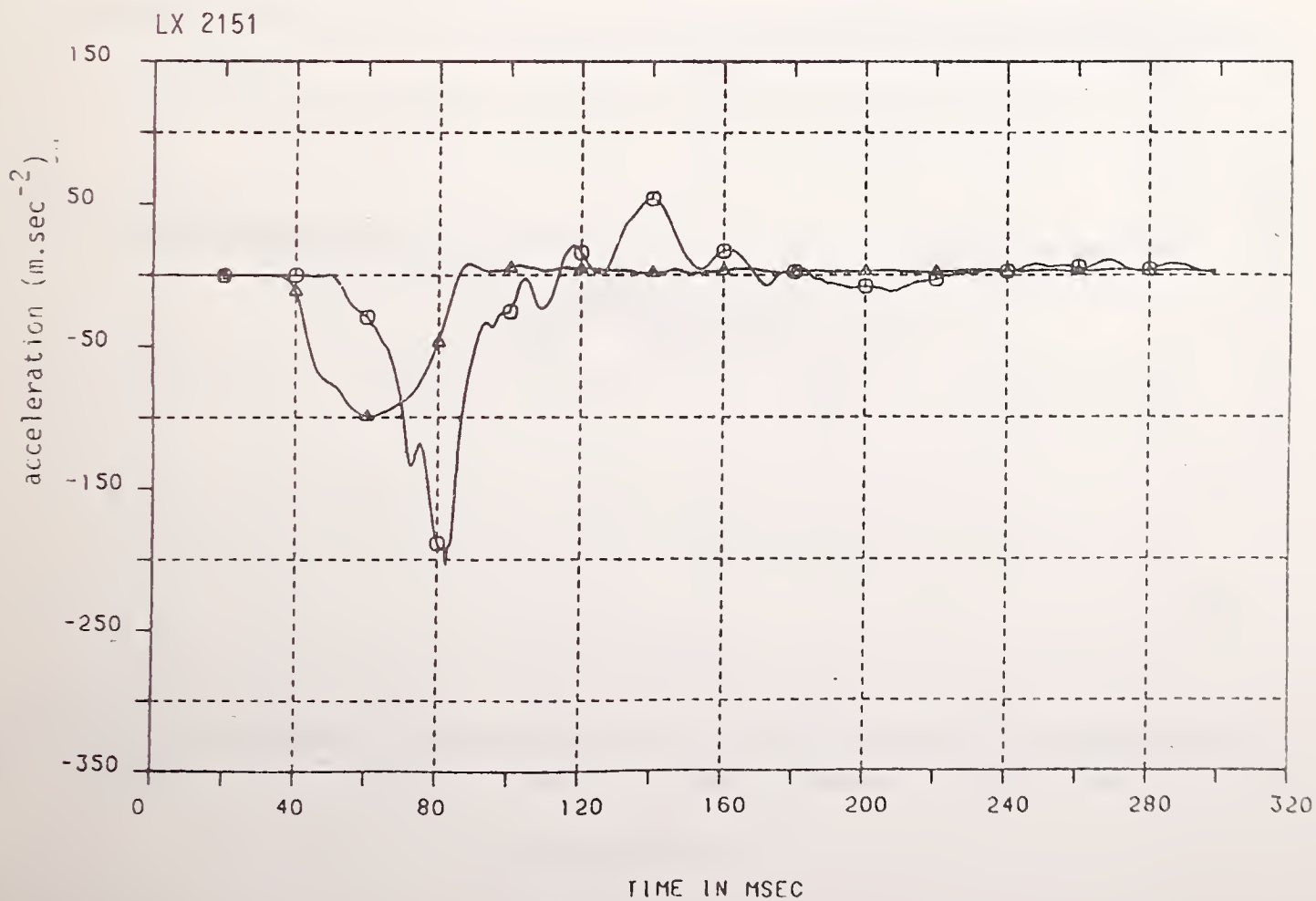
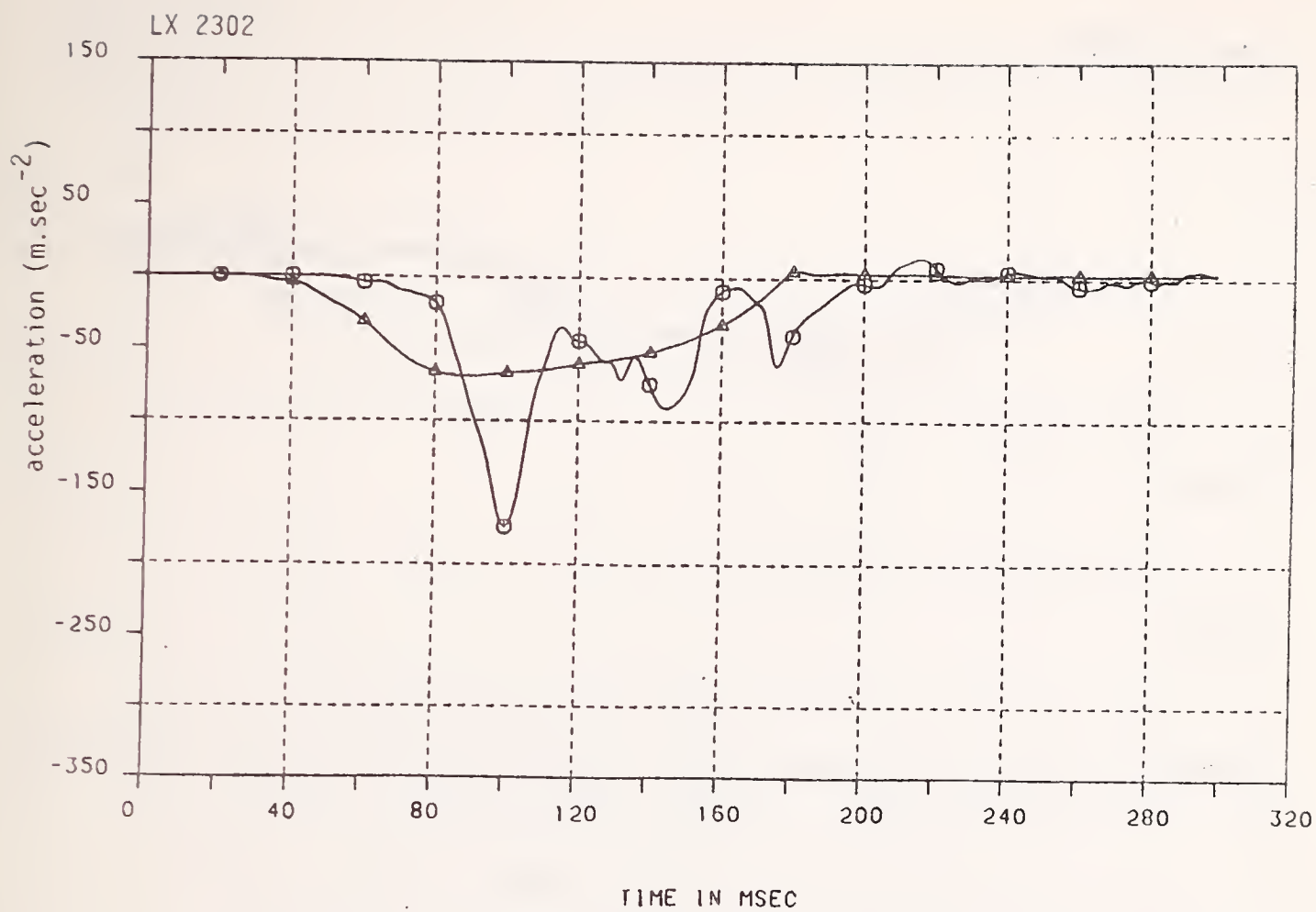


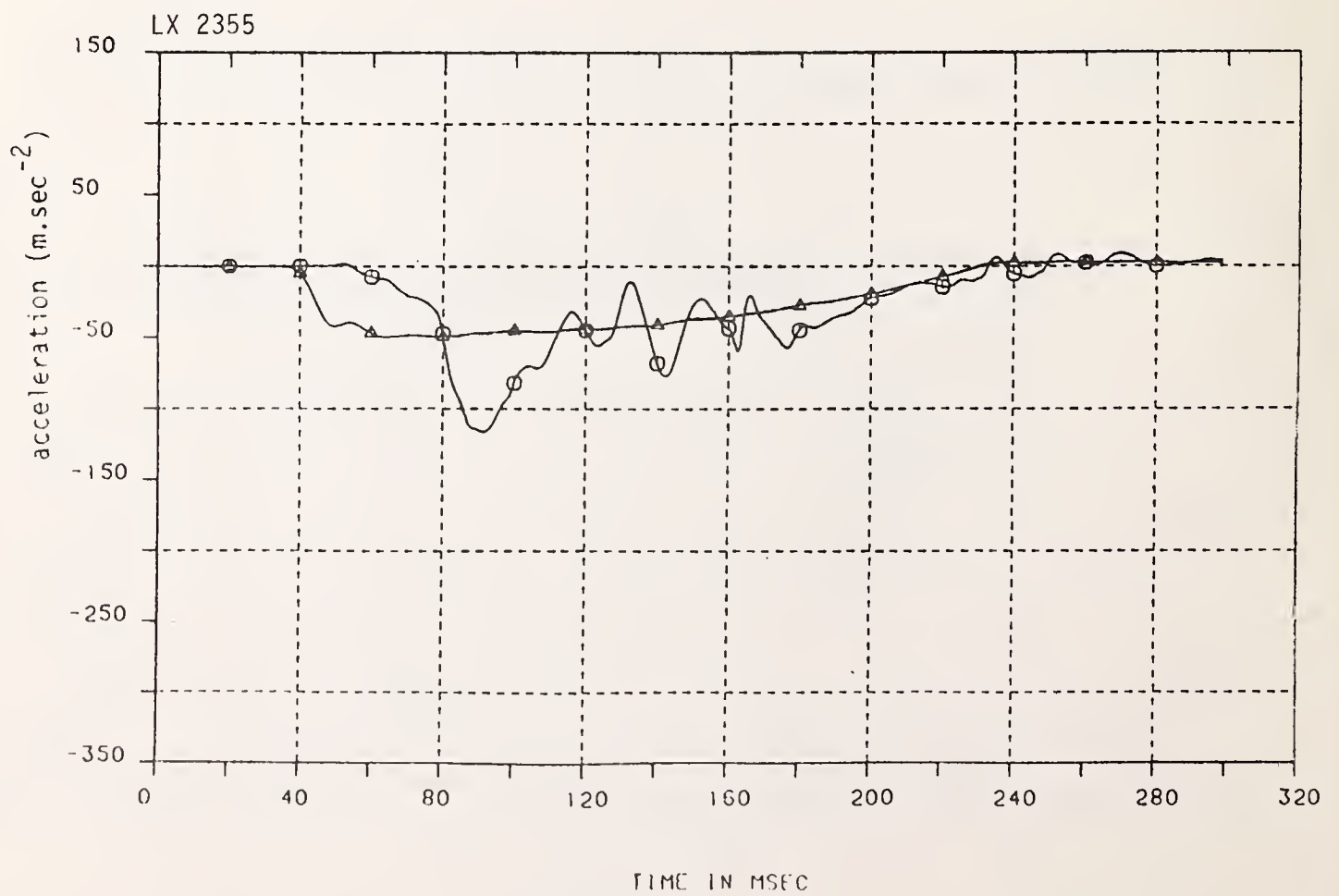
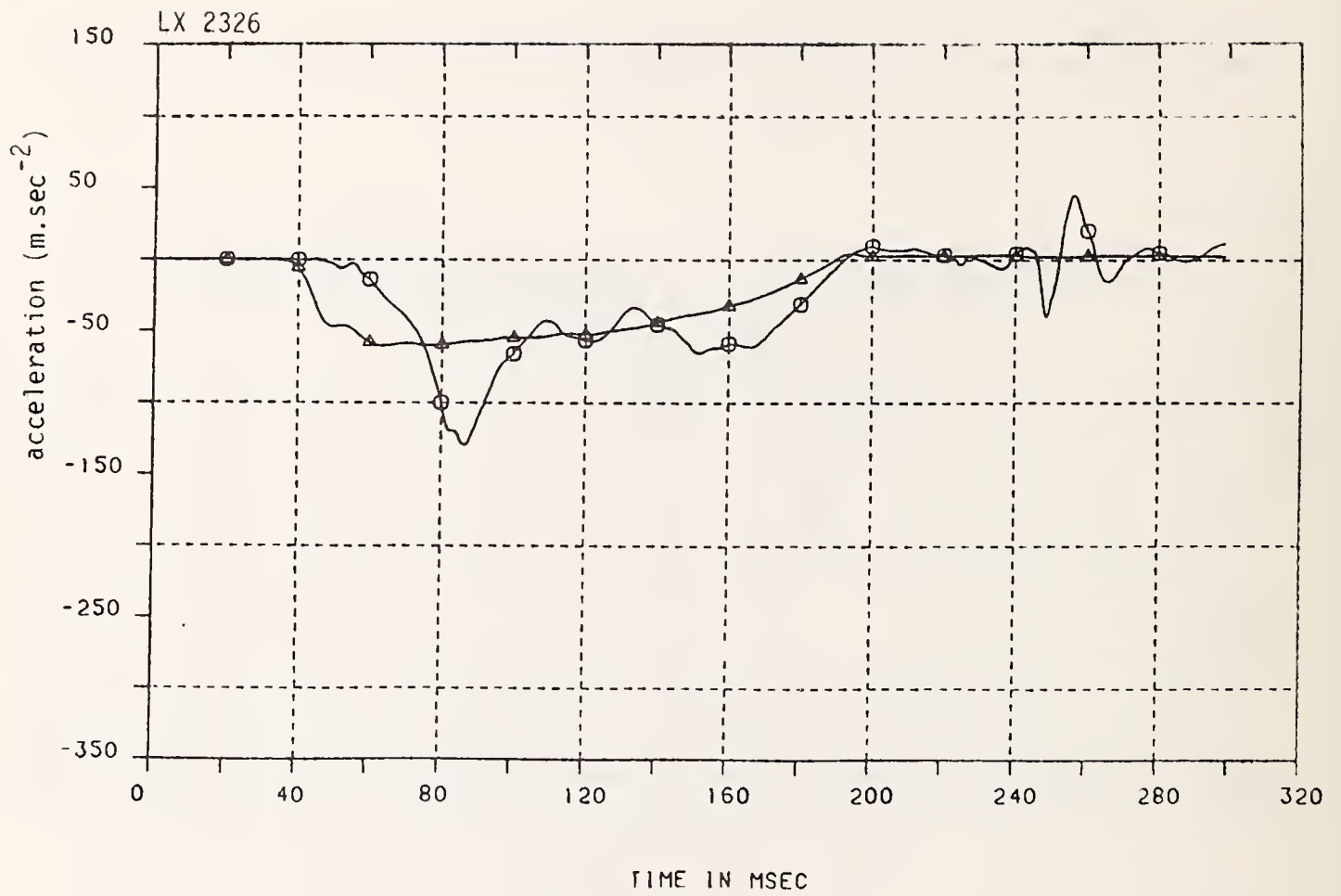


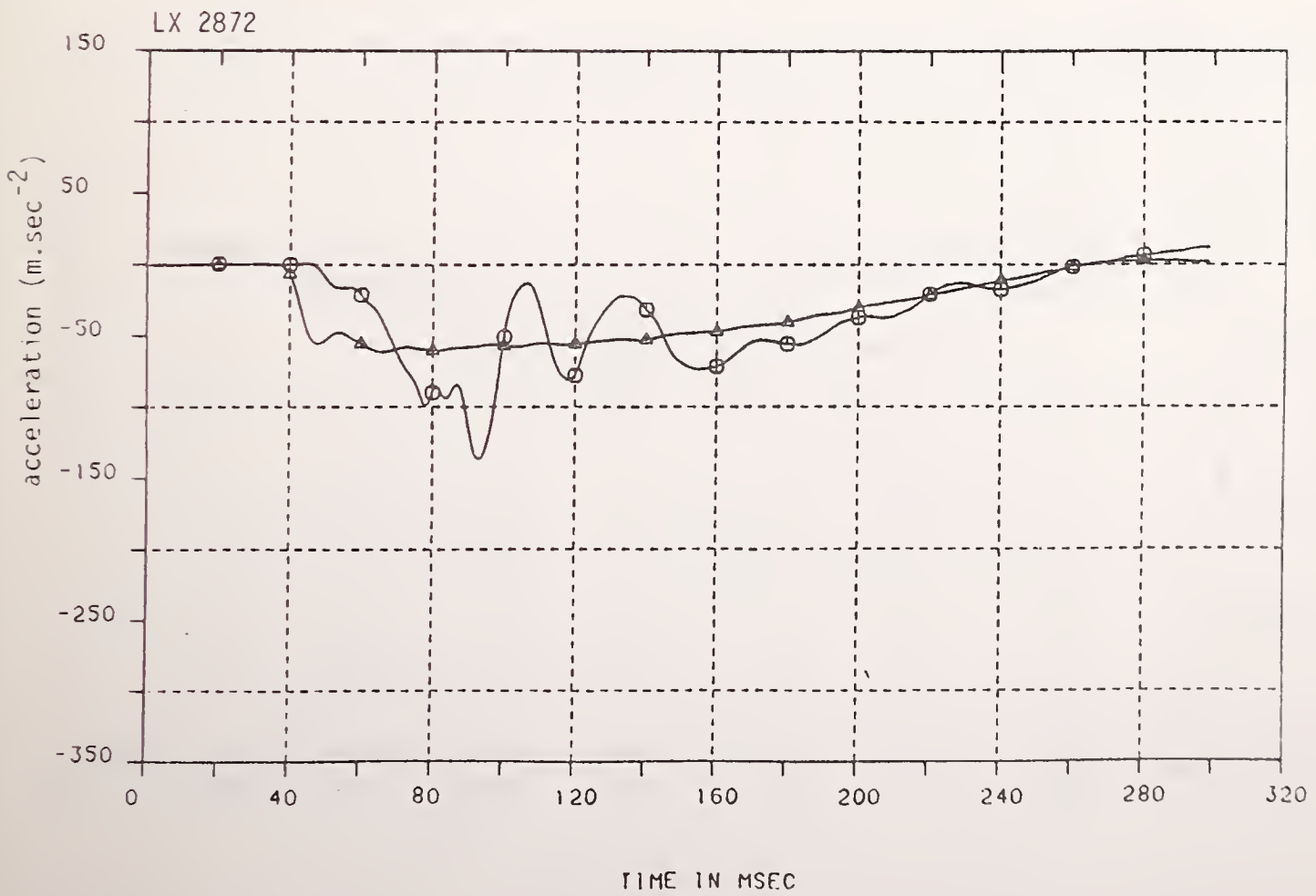
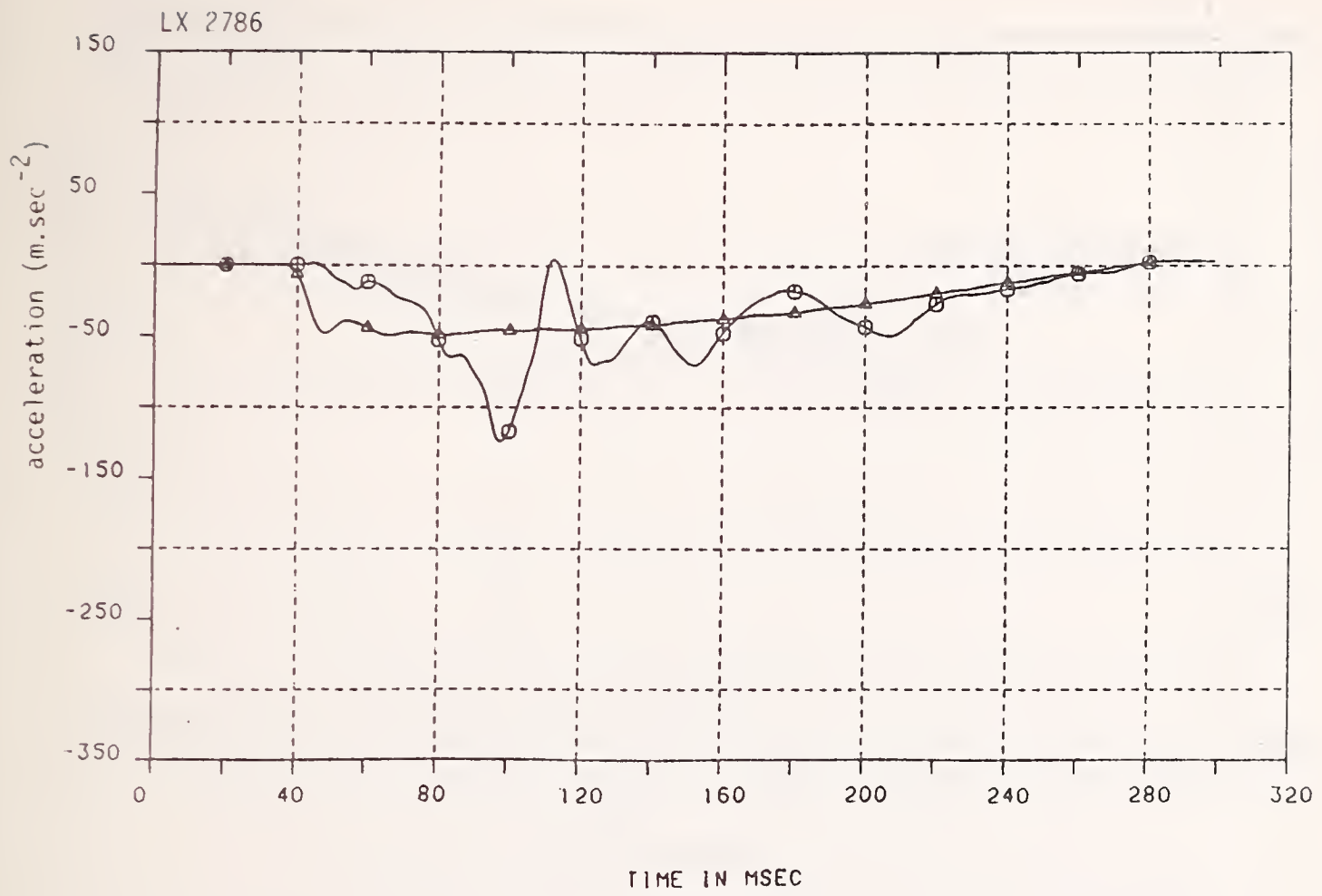


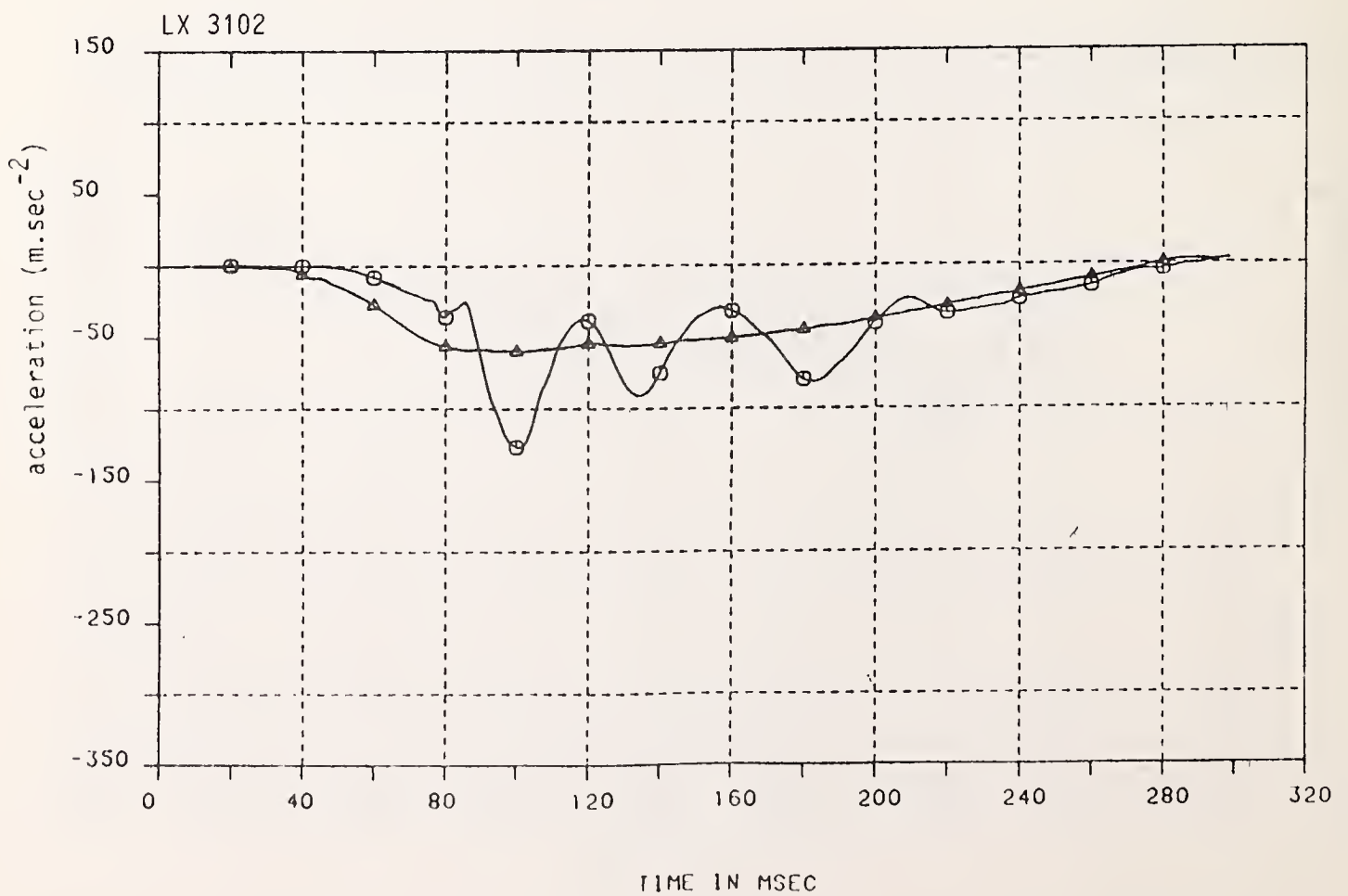
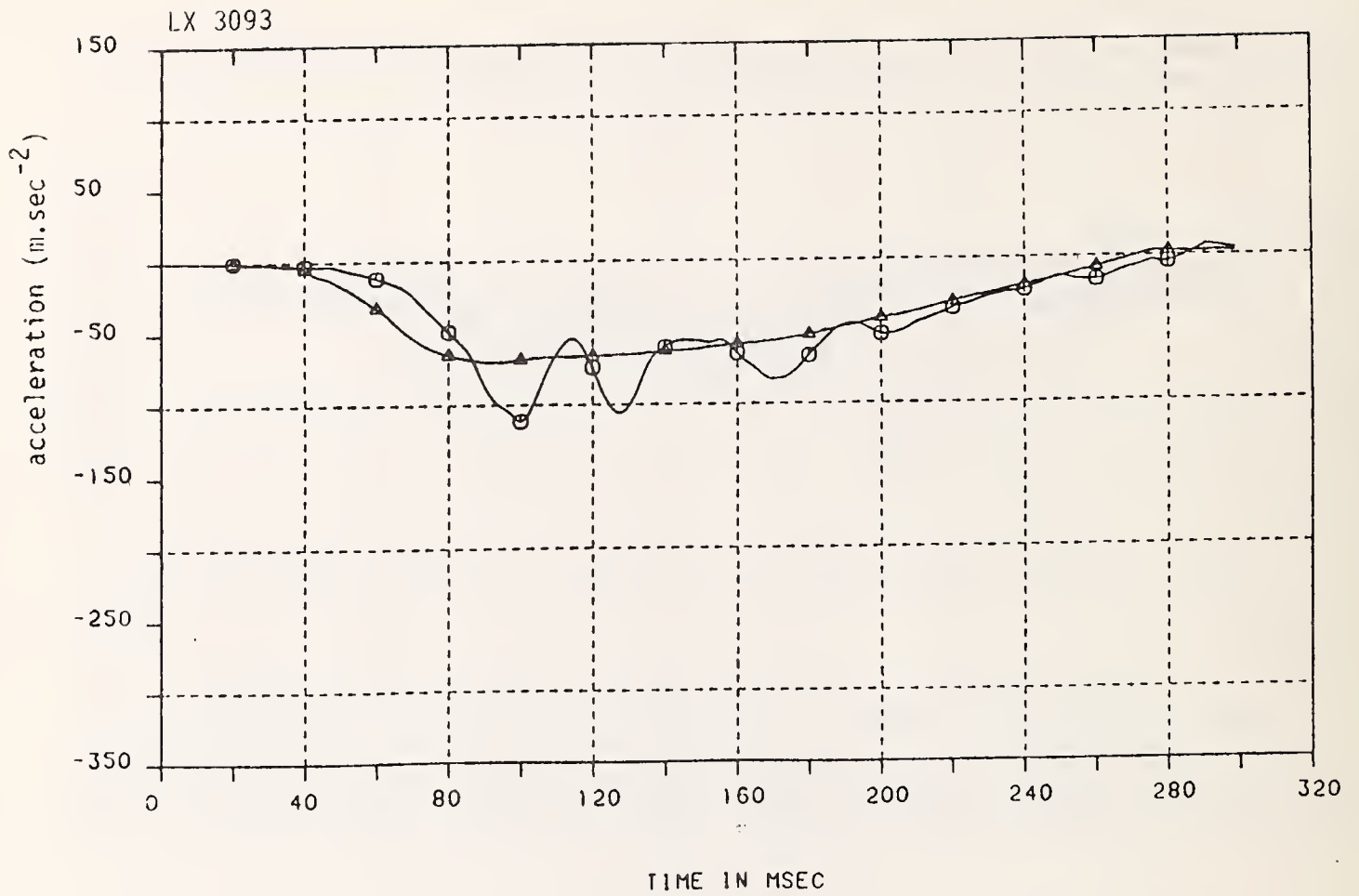


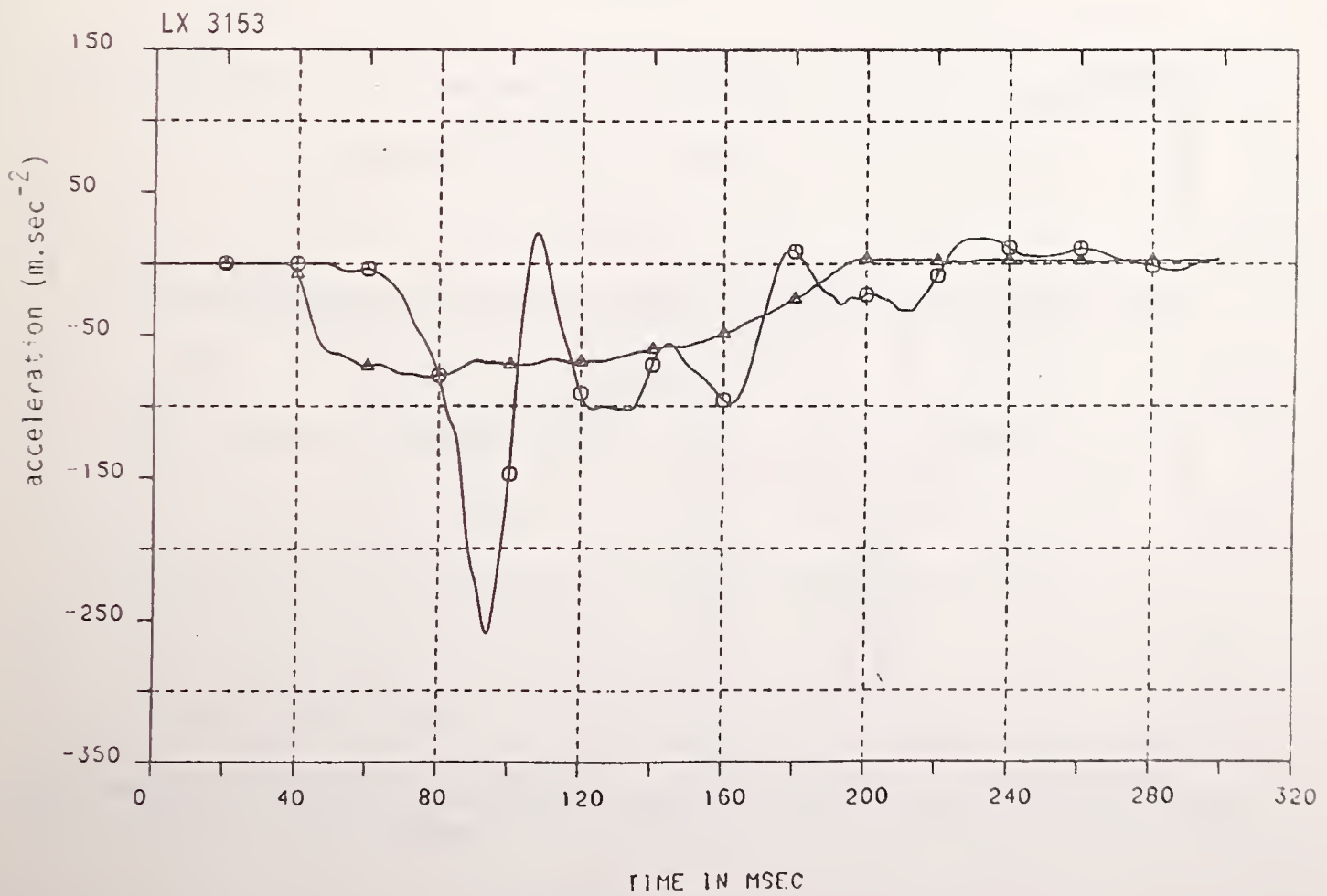
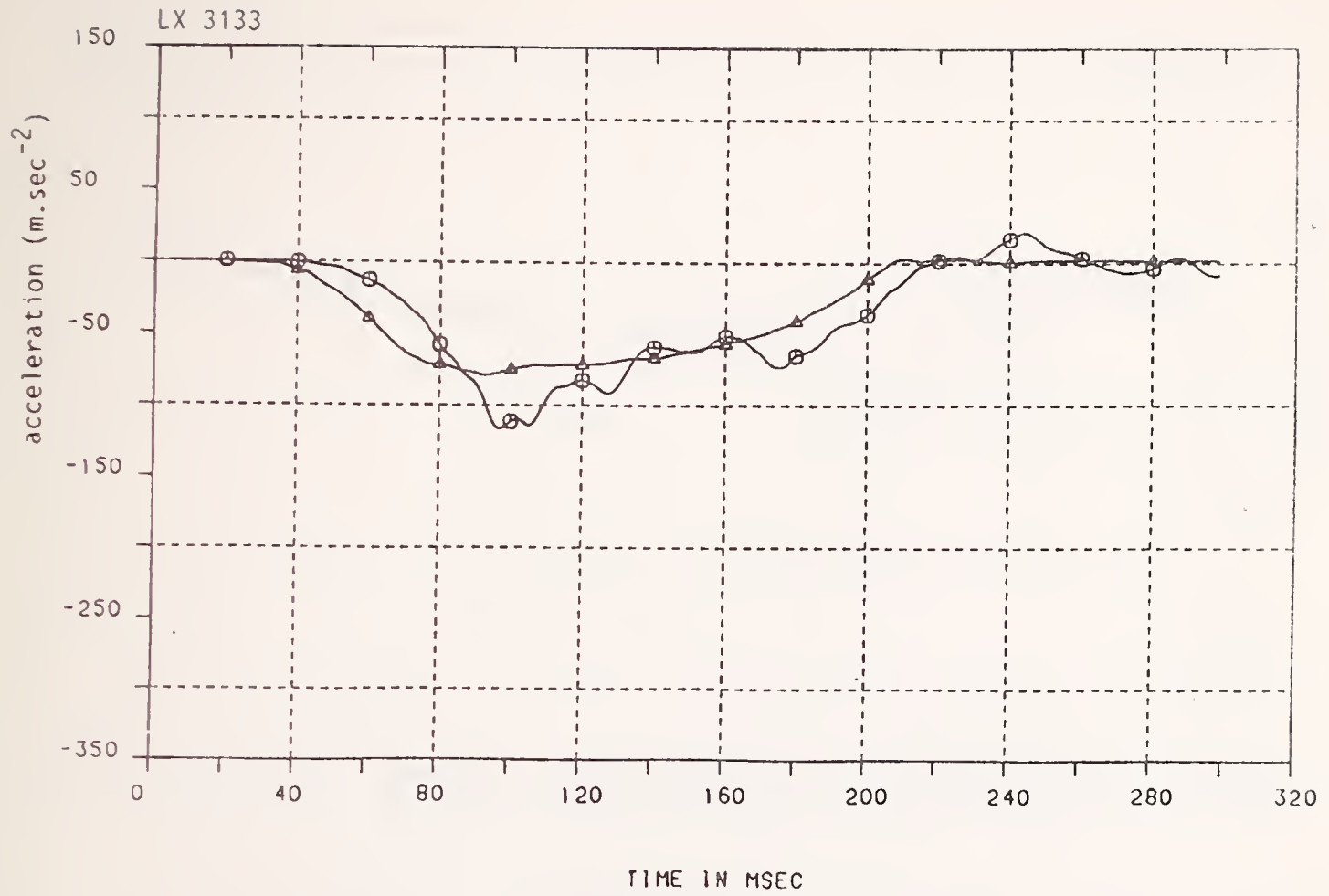


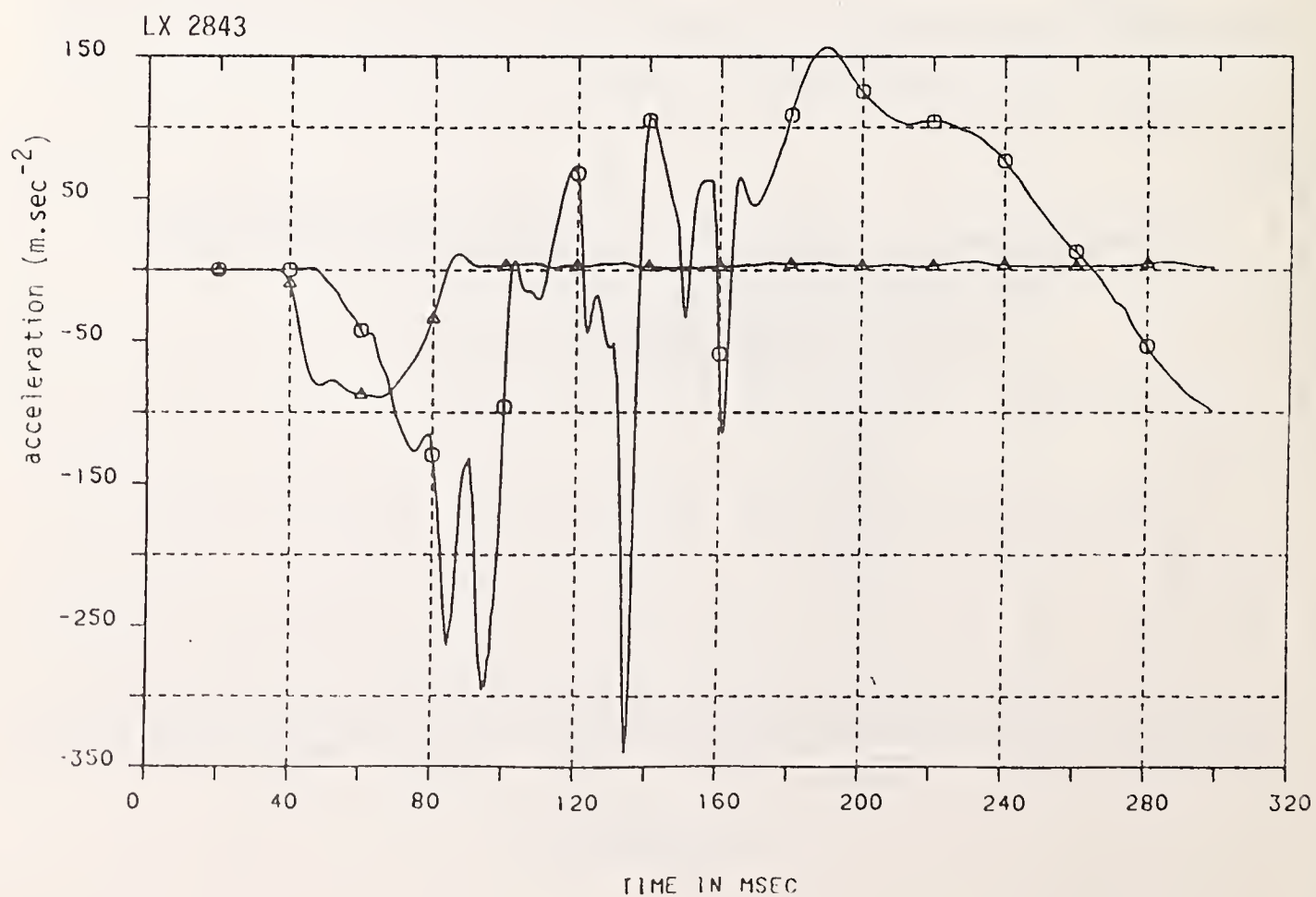
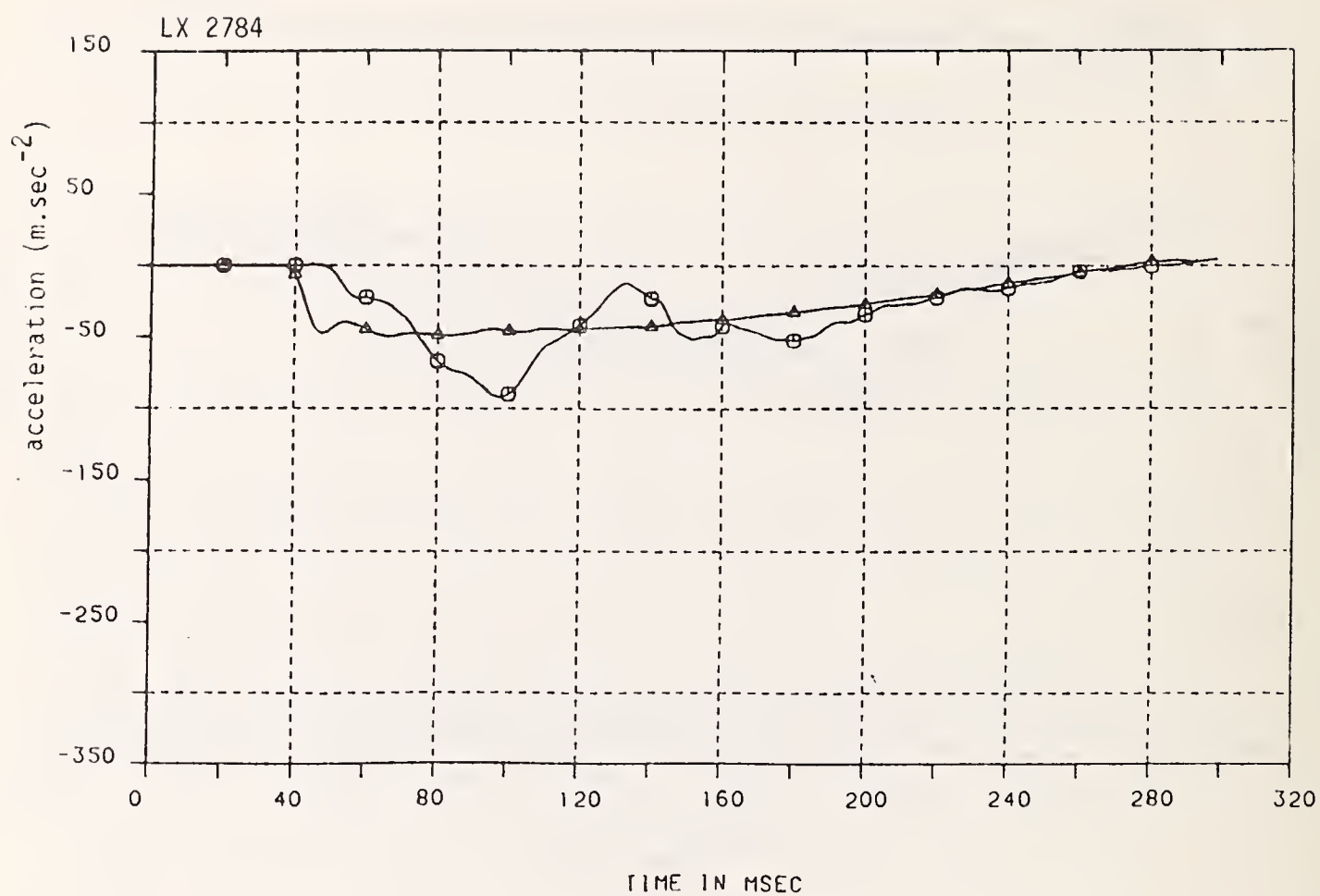


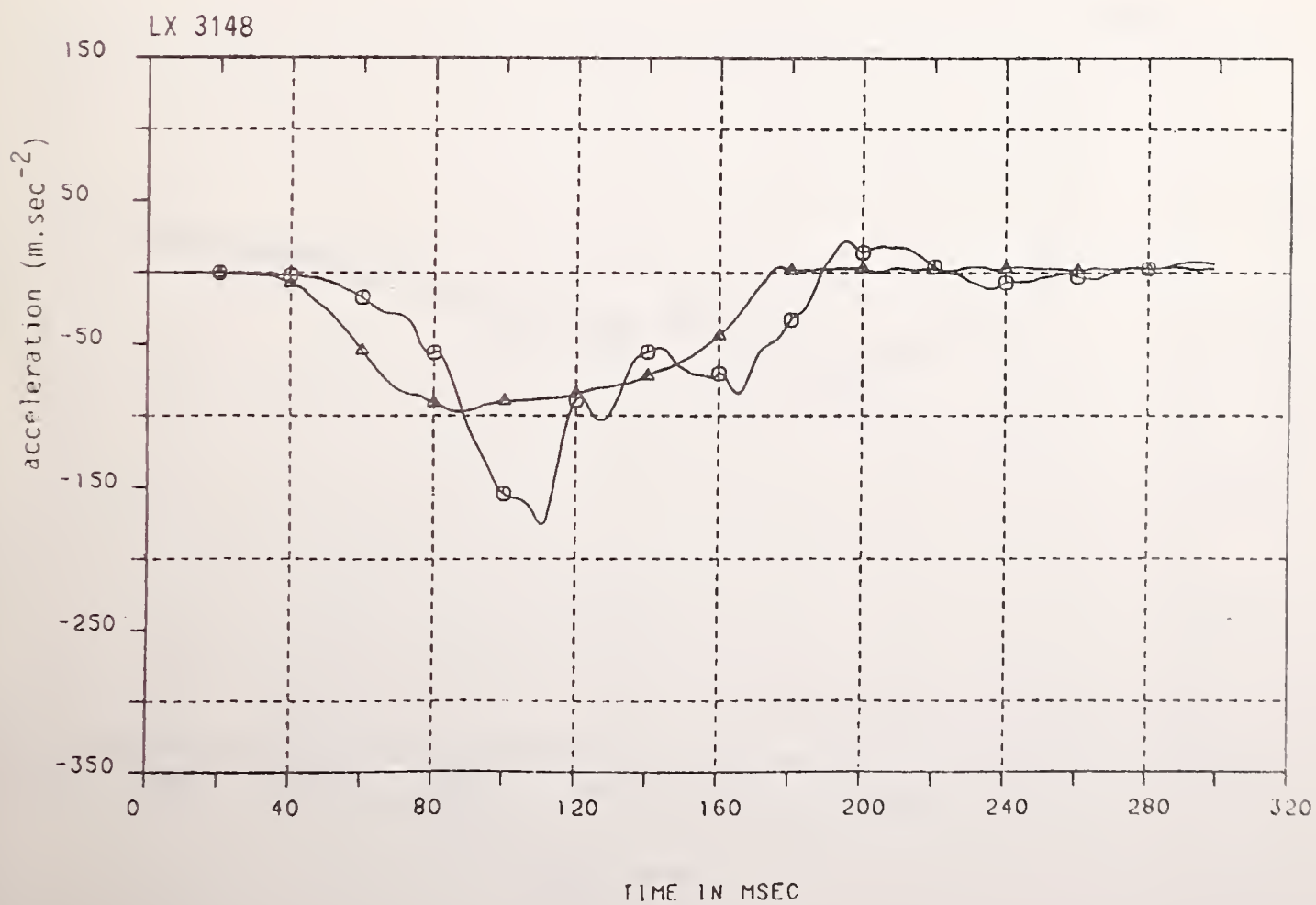
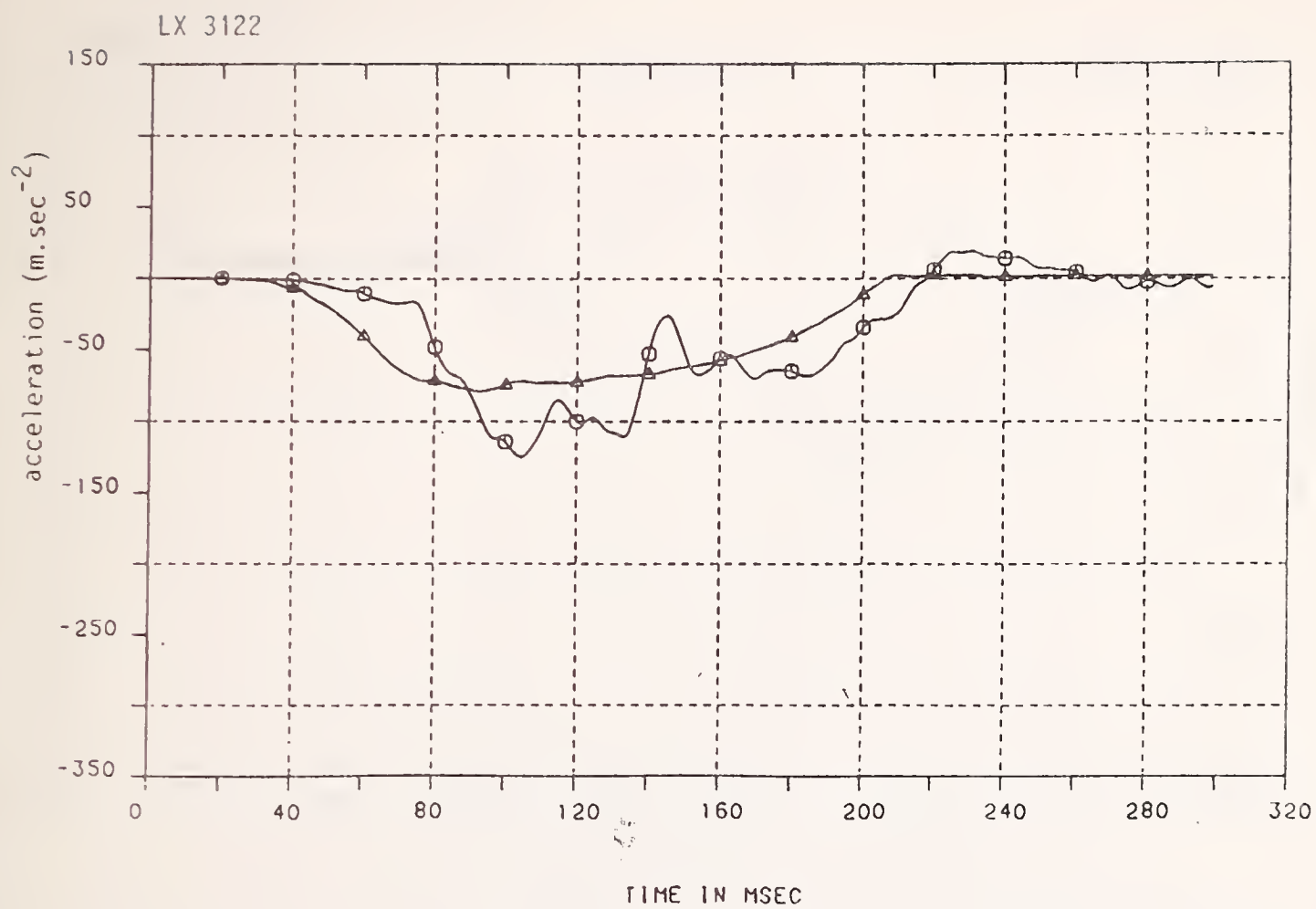


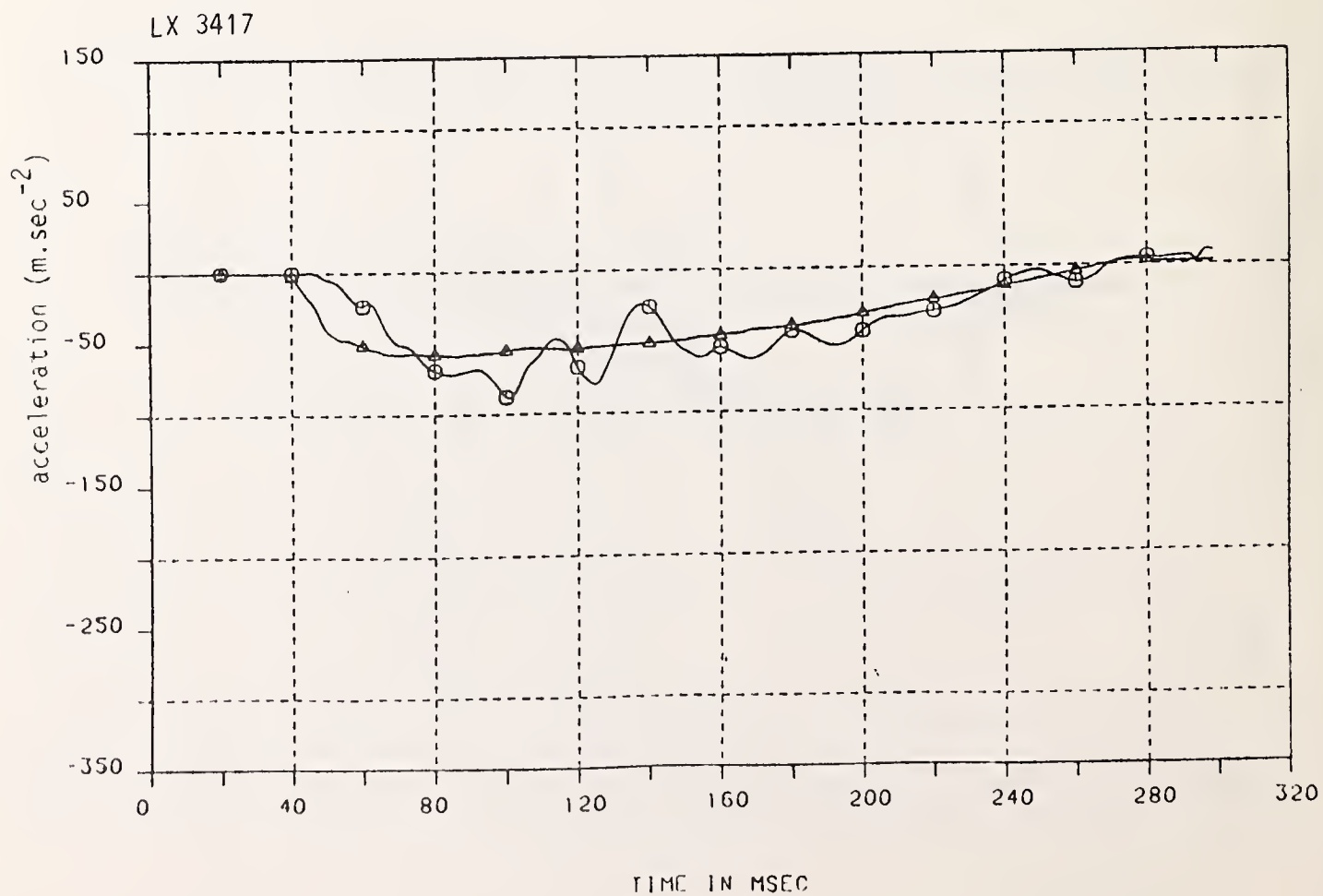
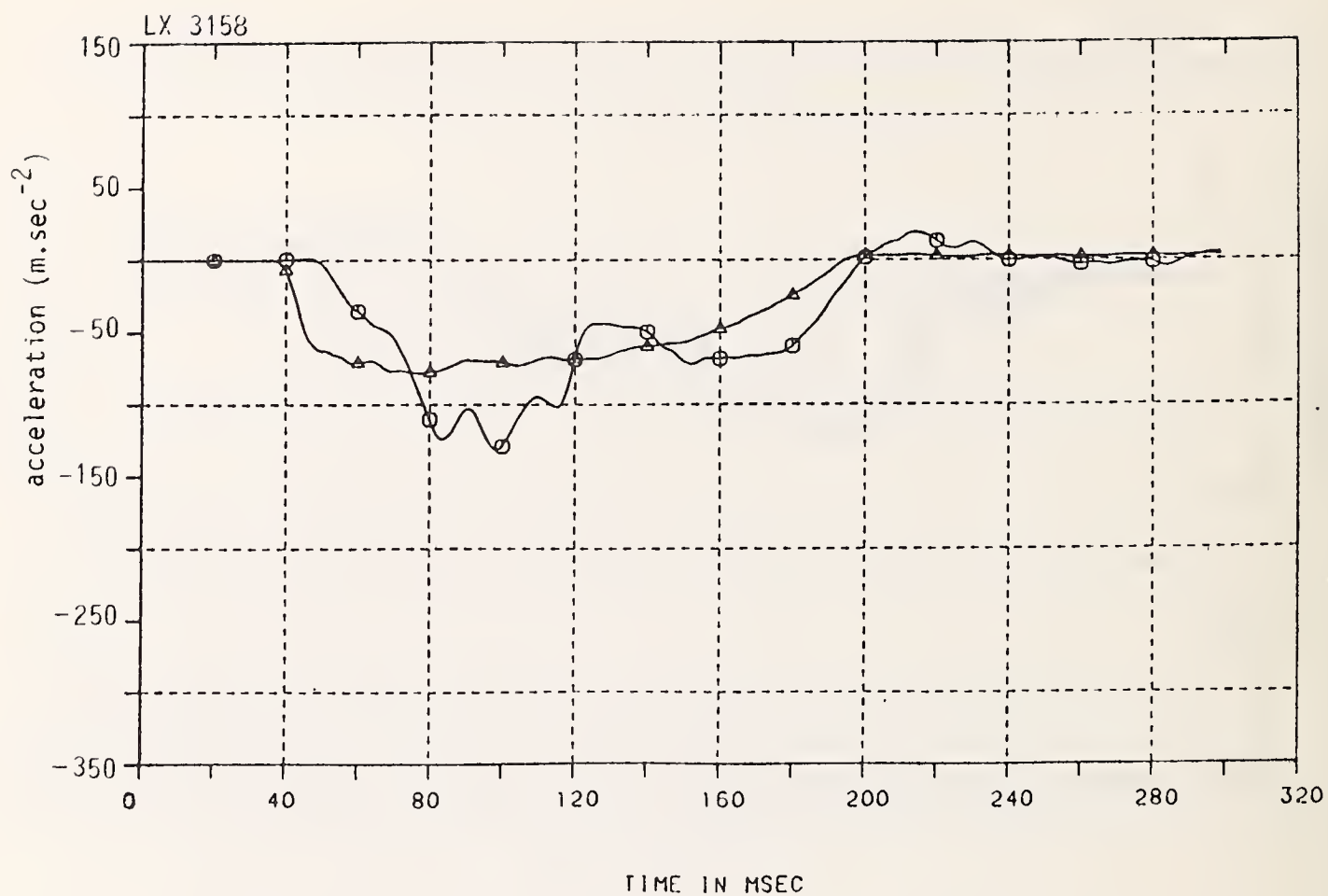






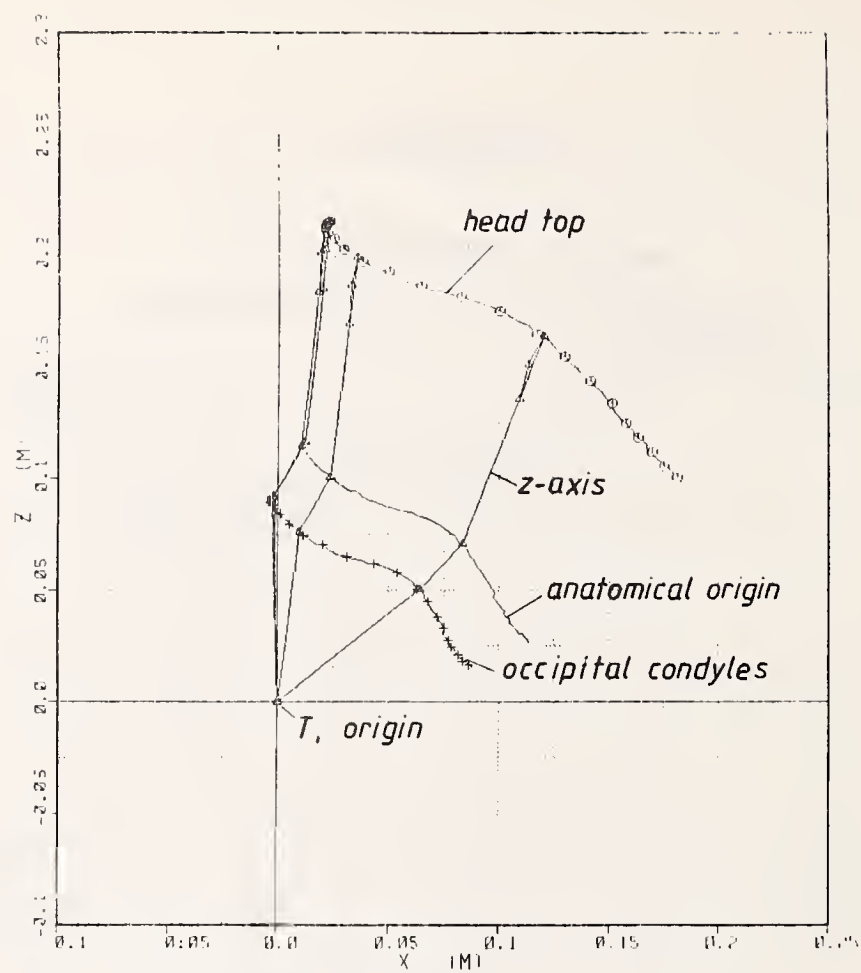




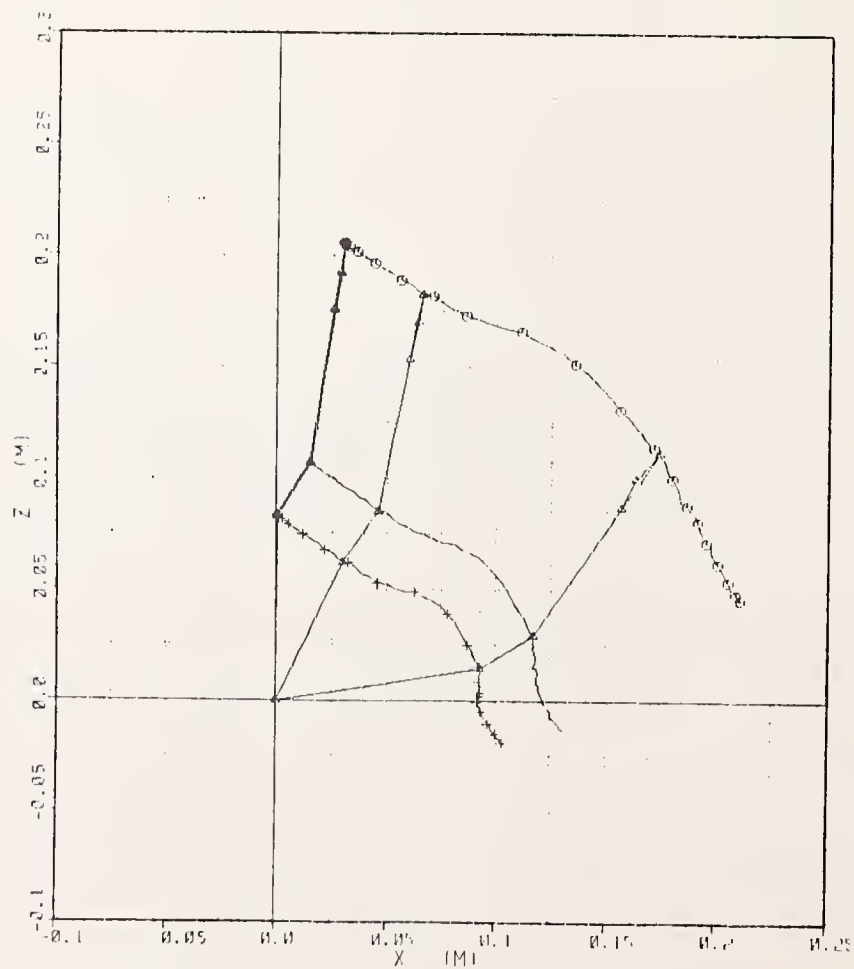


APPENDIX B

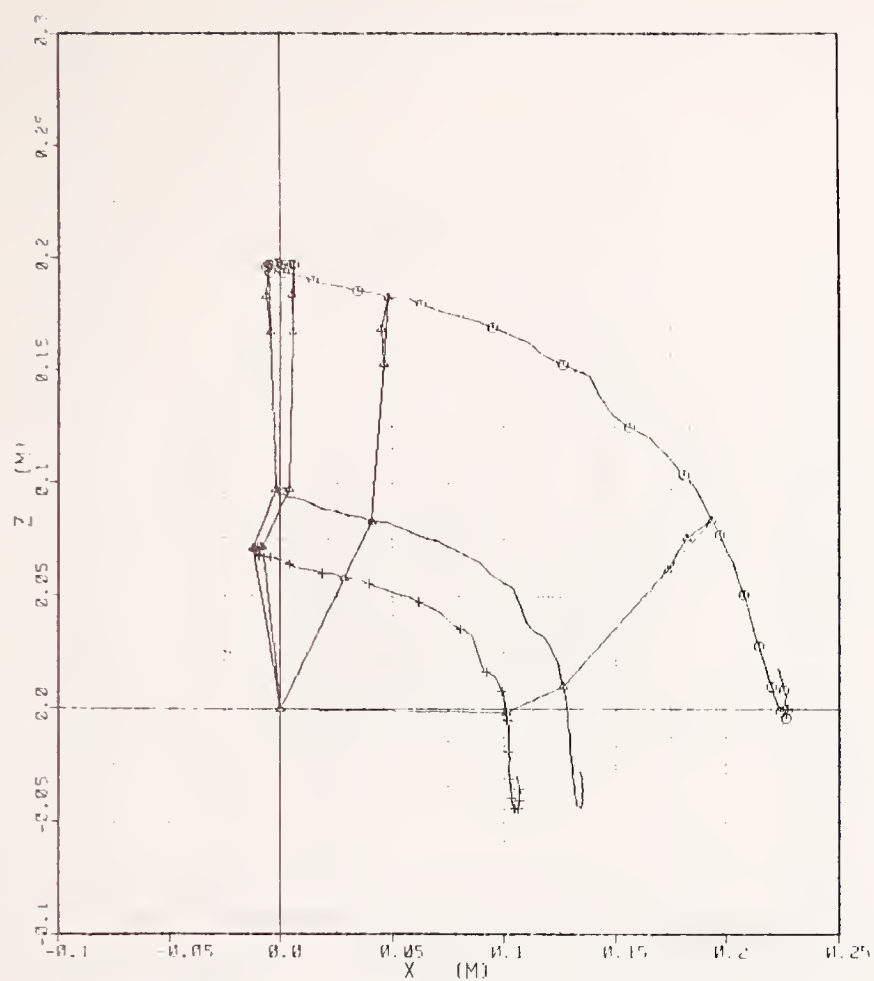
RELATIVE HEAD MOTIONS IN
30 SELECTED TESTS IN PLANE OF IMPACT



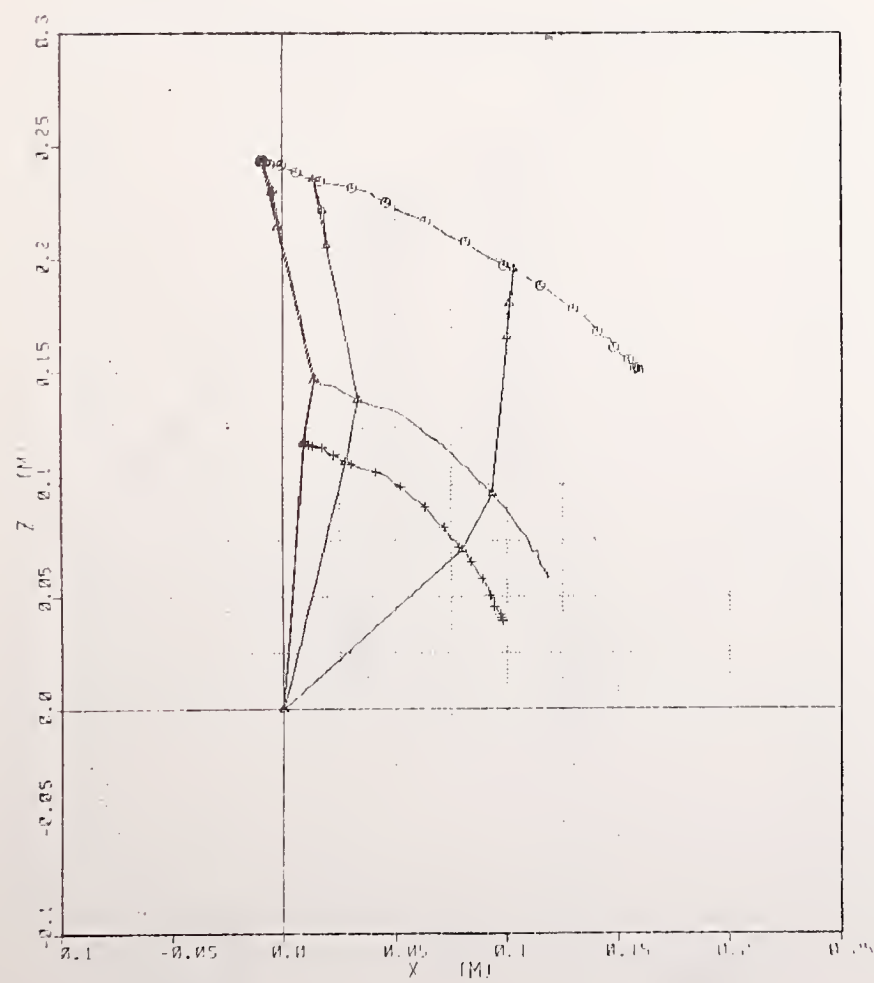
LX3530



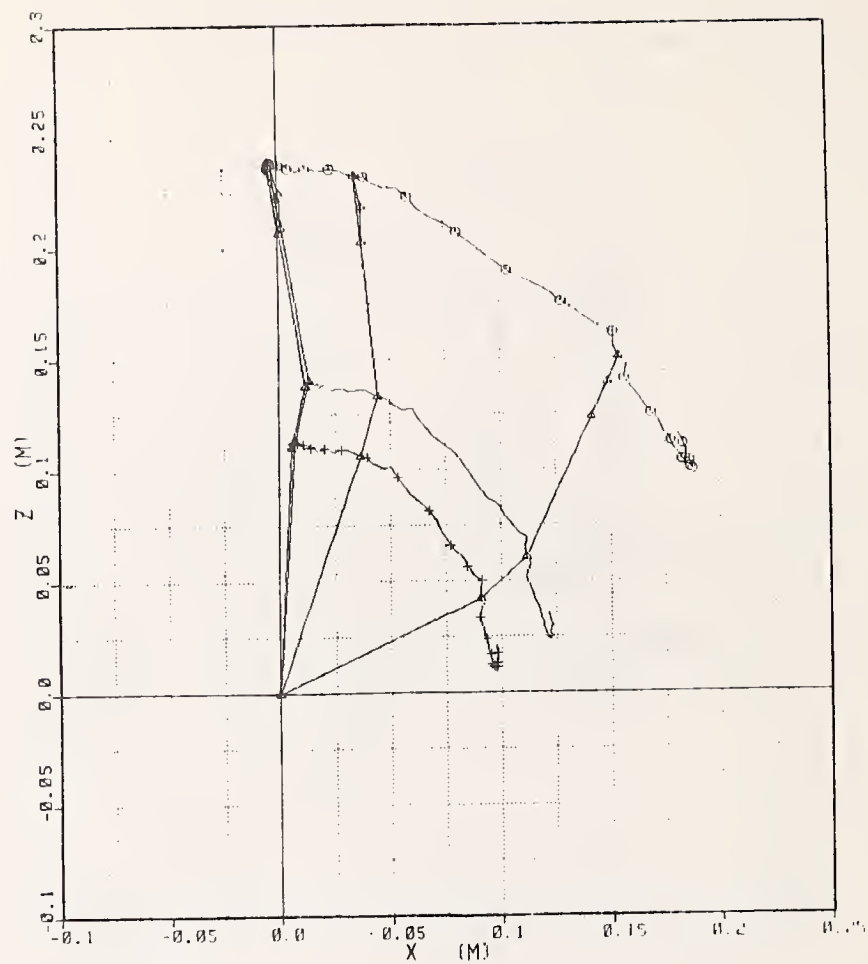
LX3536



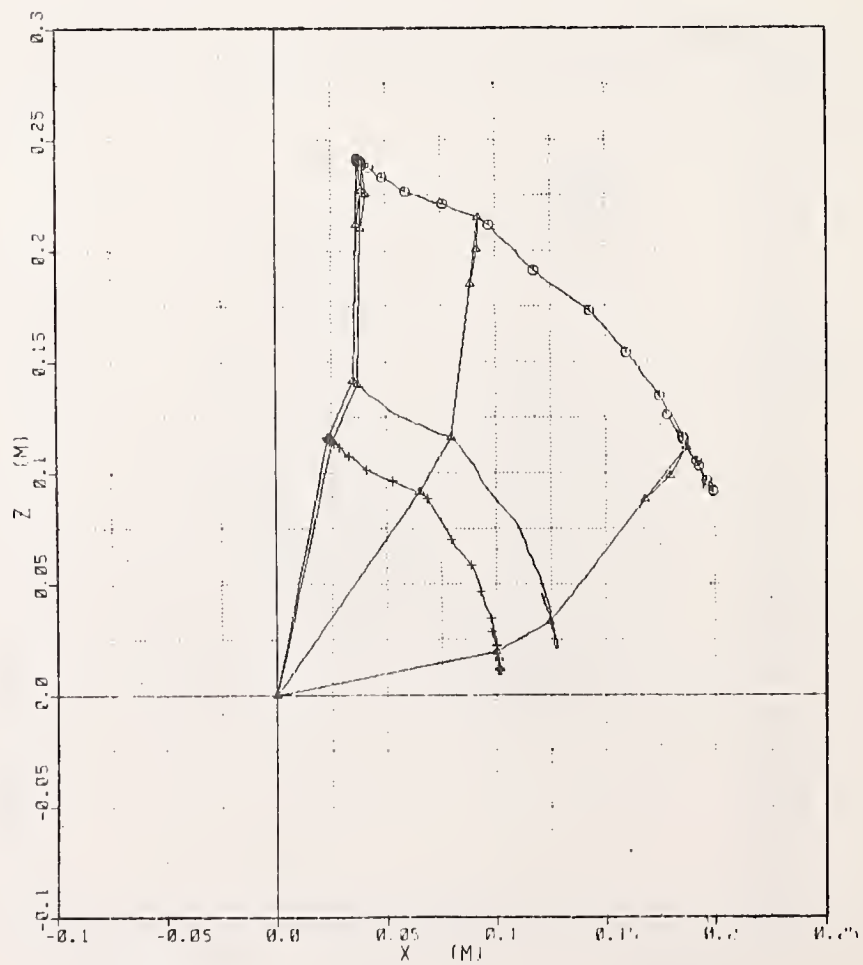
LX3544



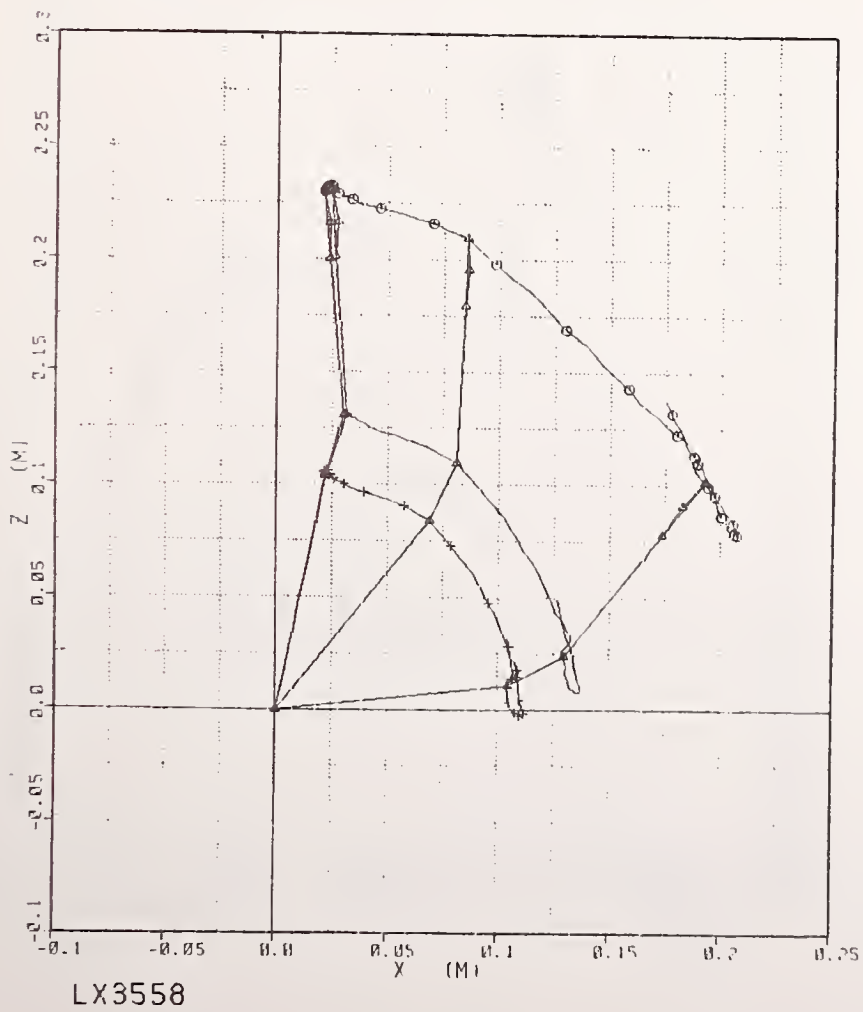
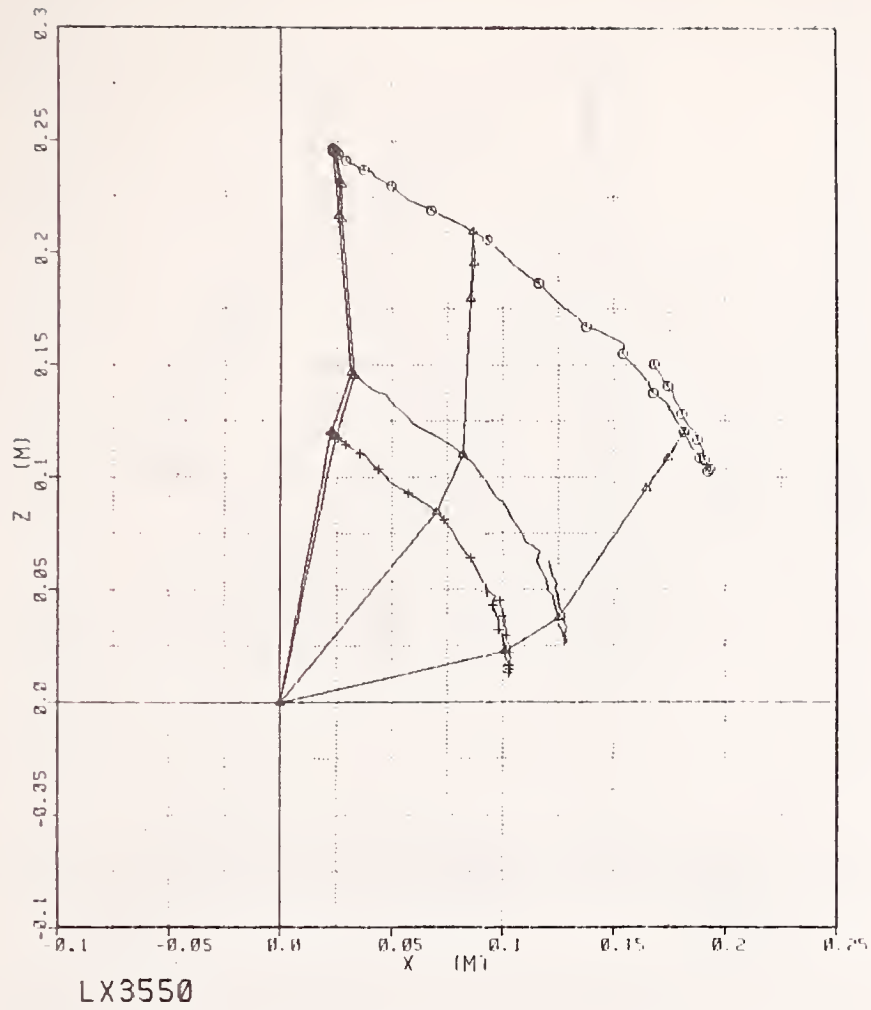
LX3531

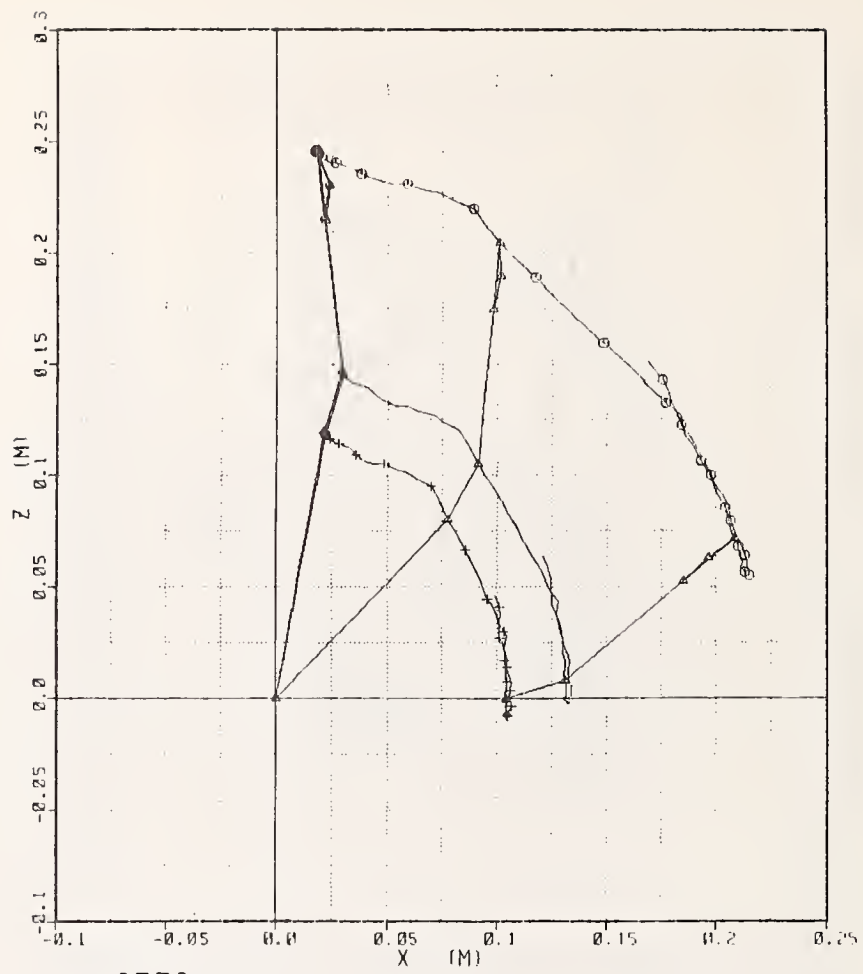


LX3537

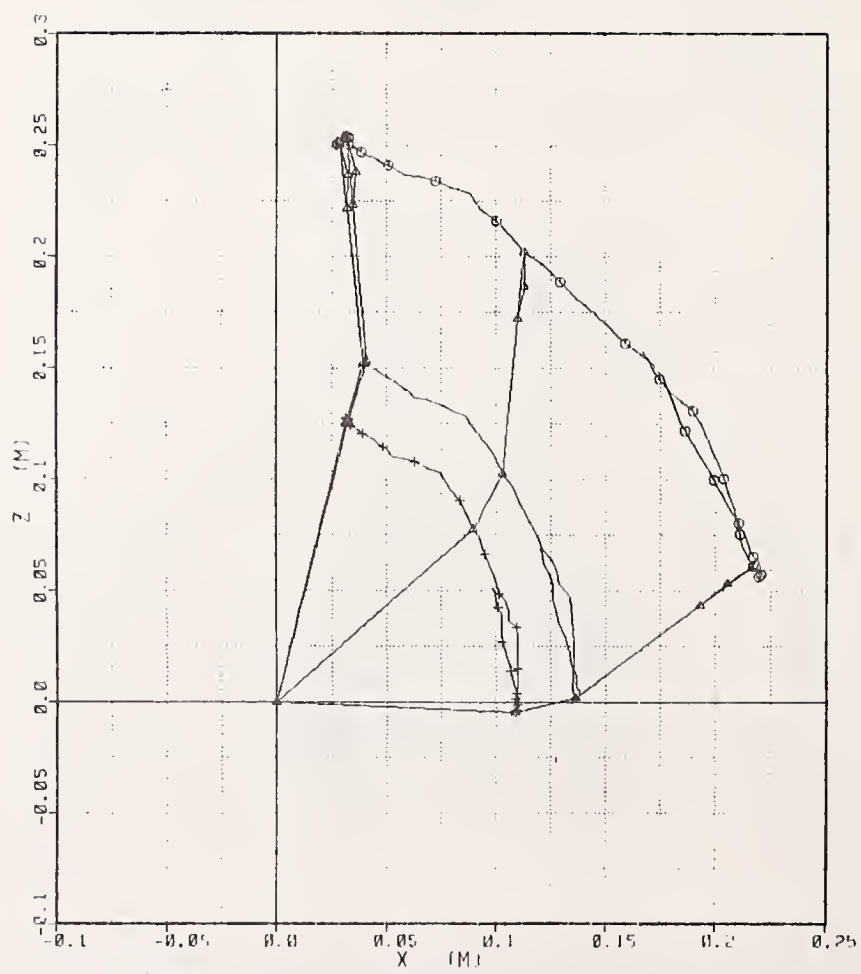


LX3548

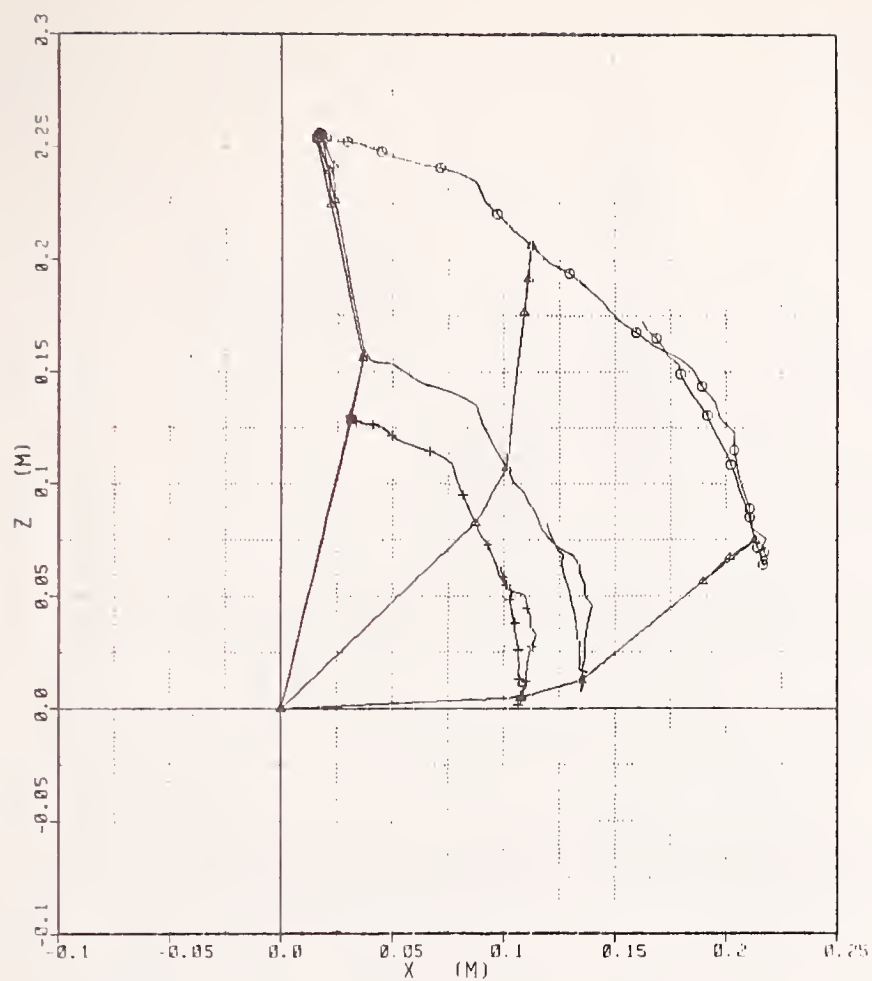




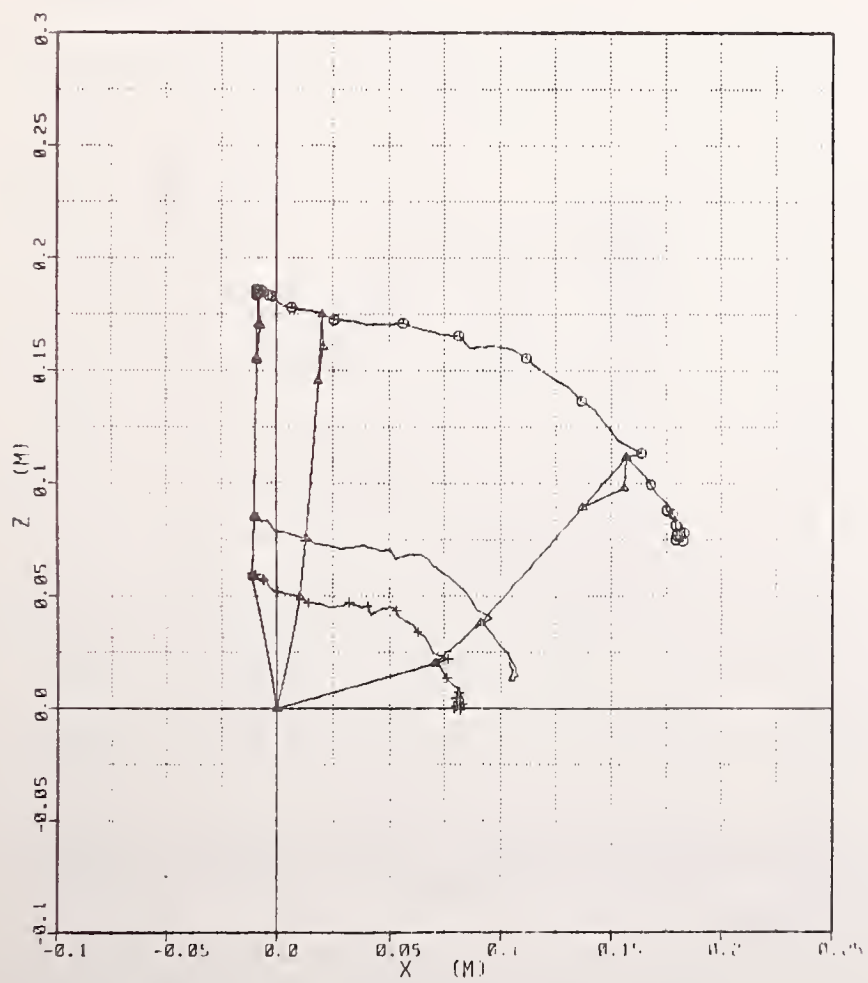
LX3578



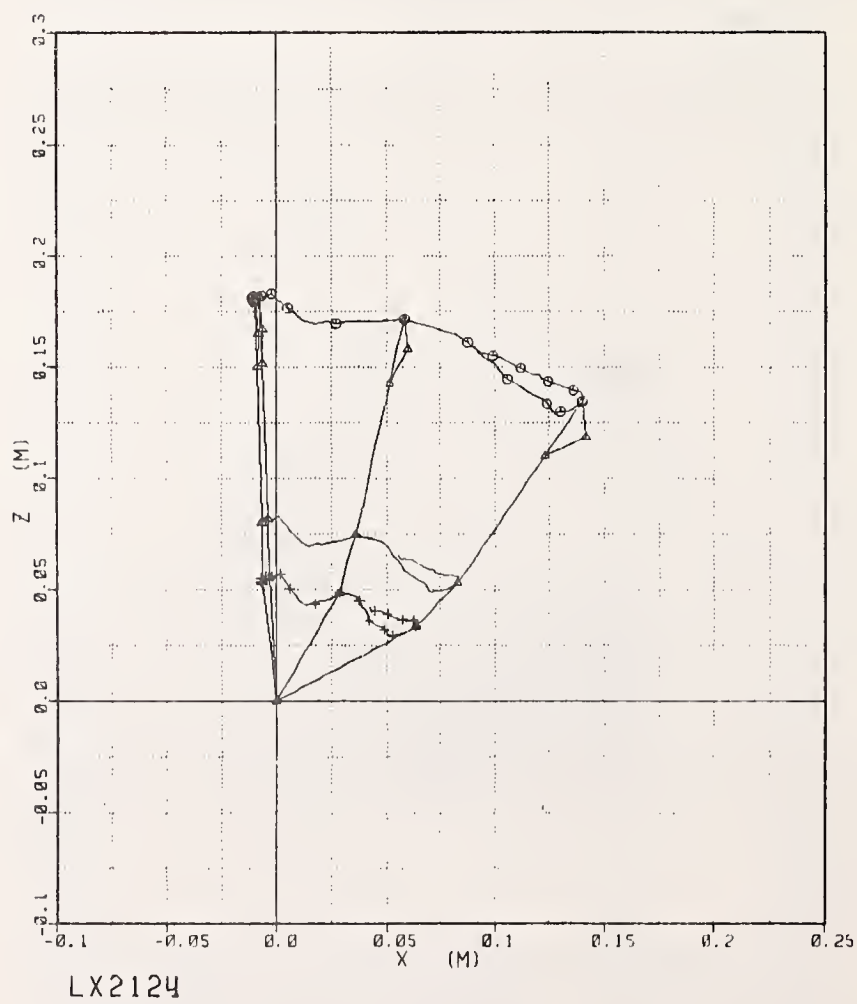
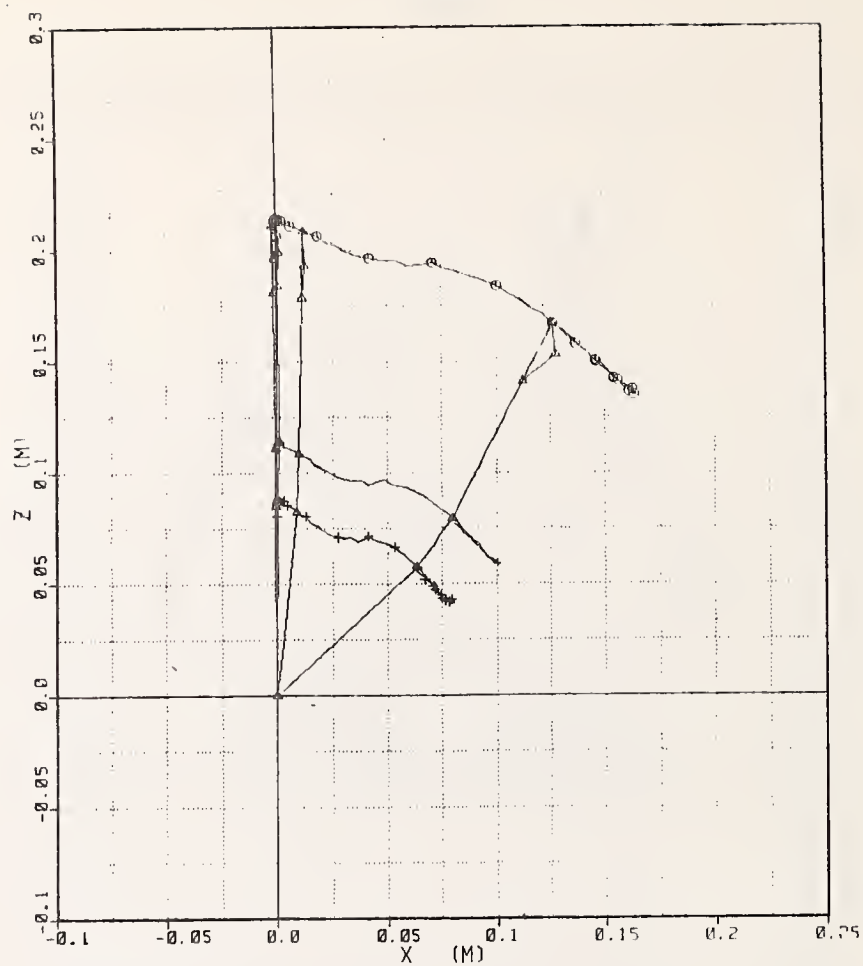
LX3583

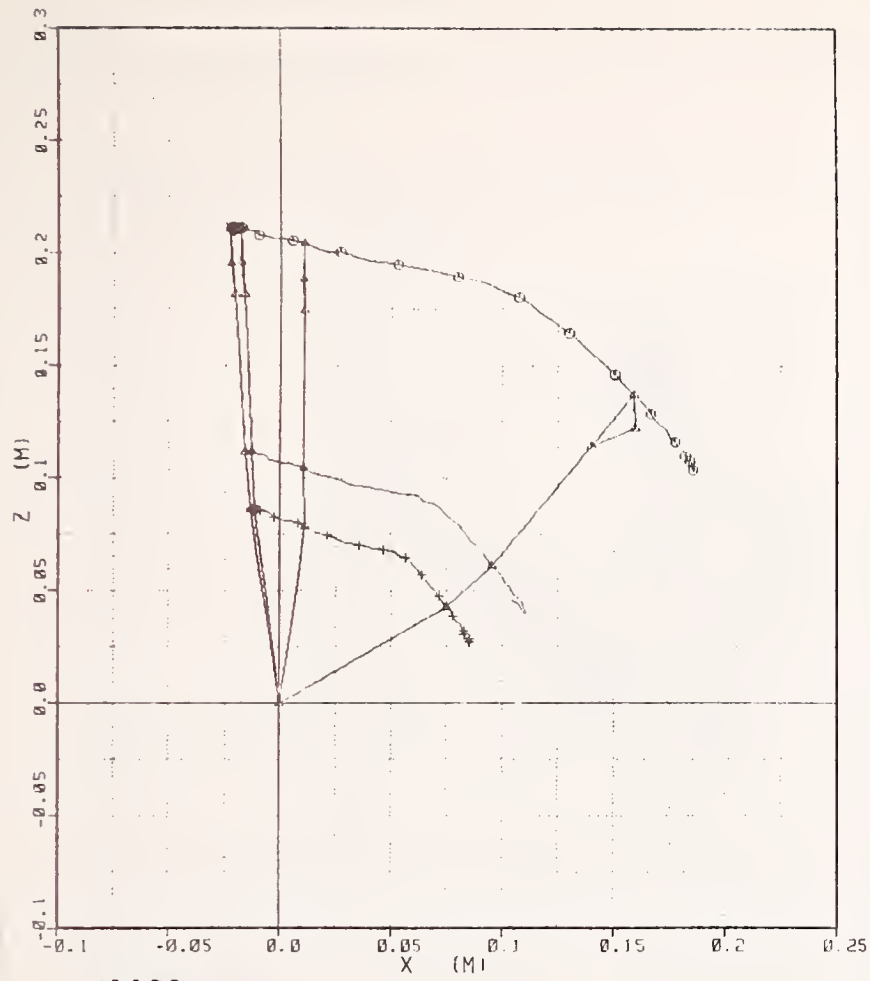


LX3616

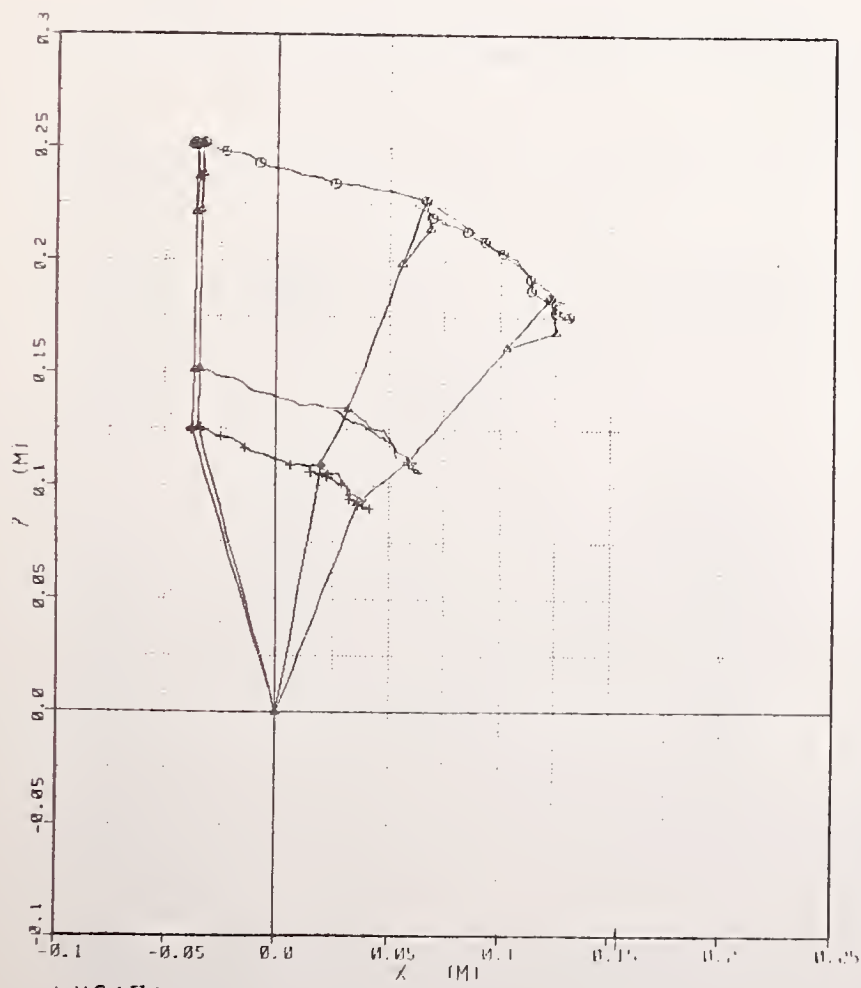


LX1831

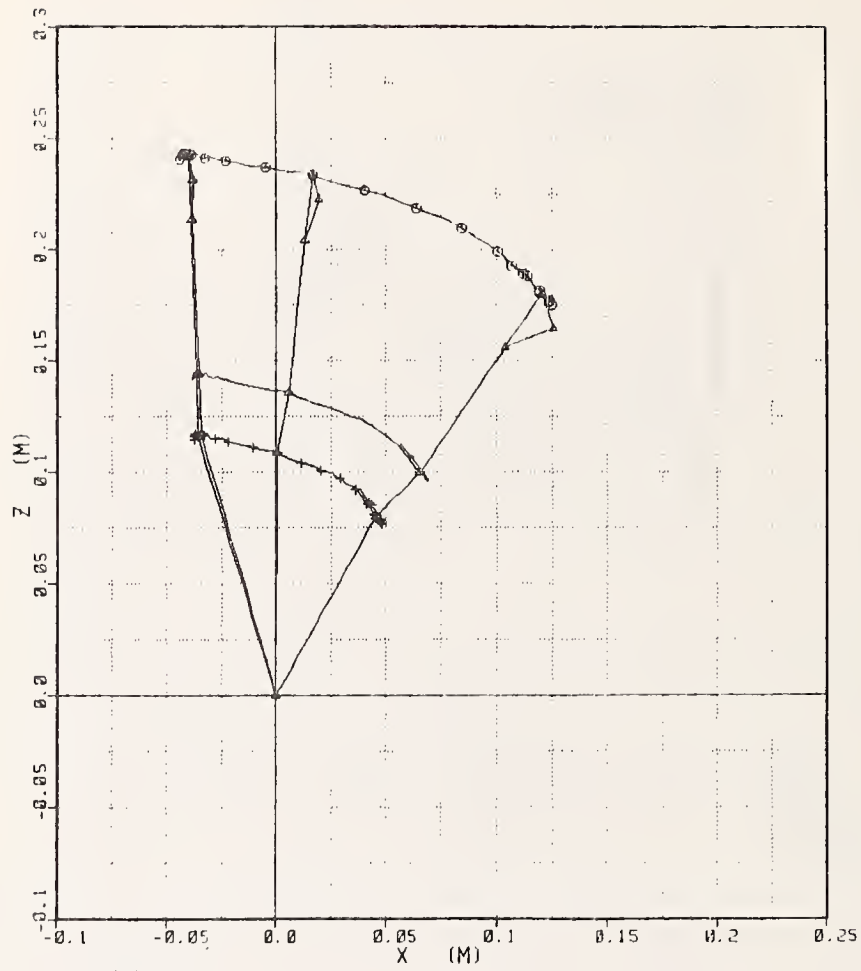




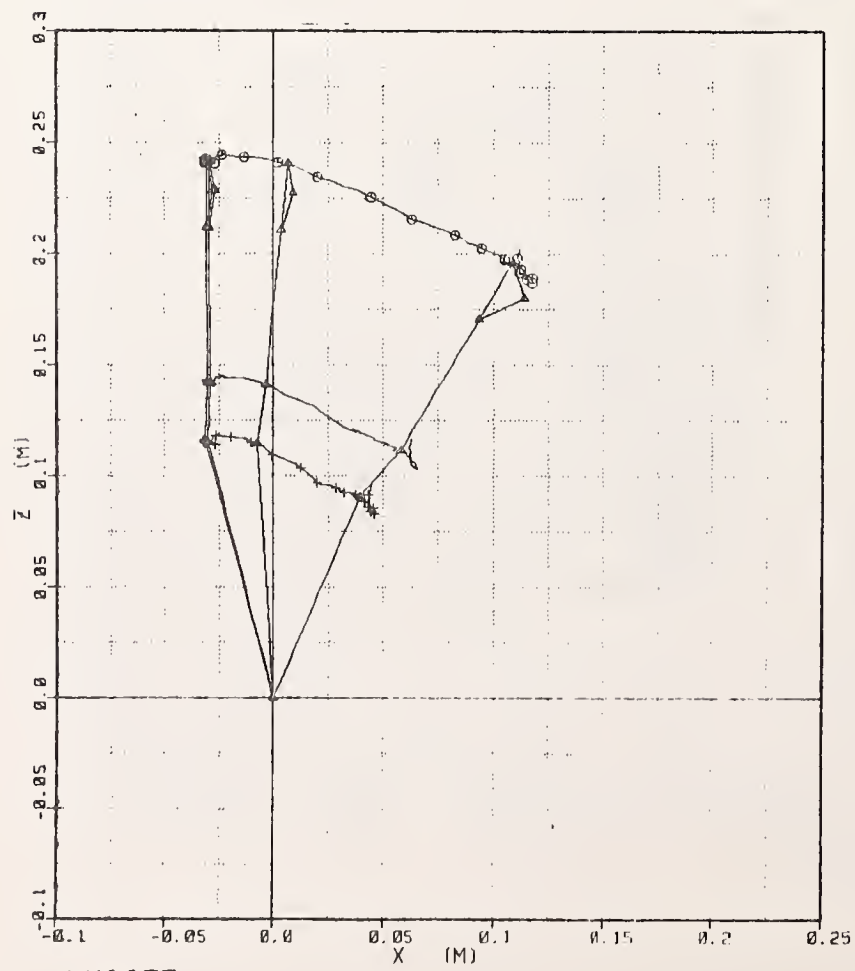
LX2302



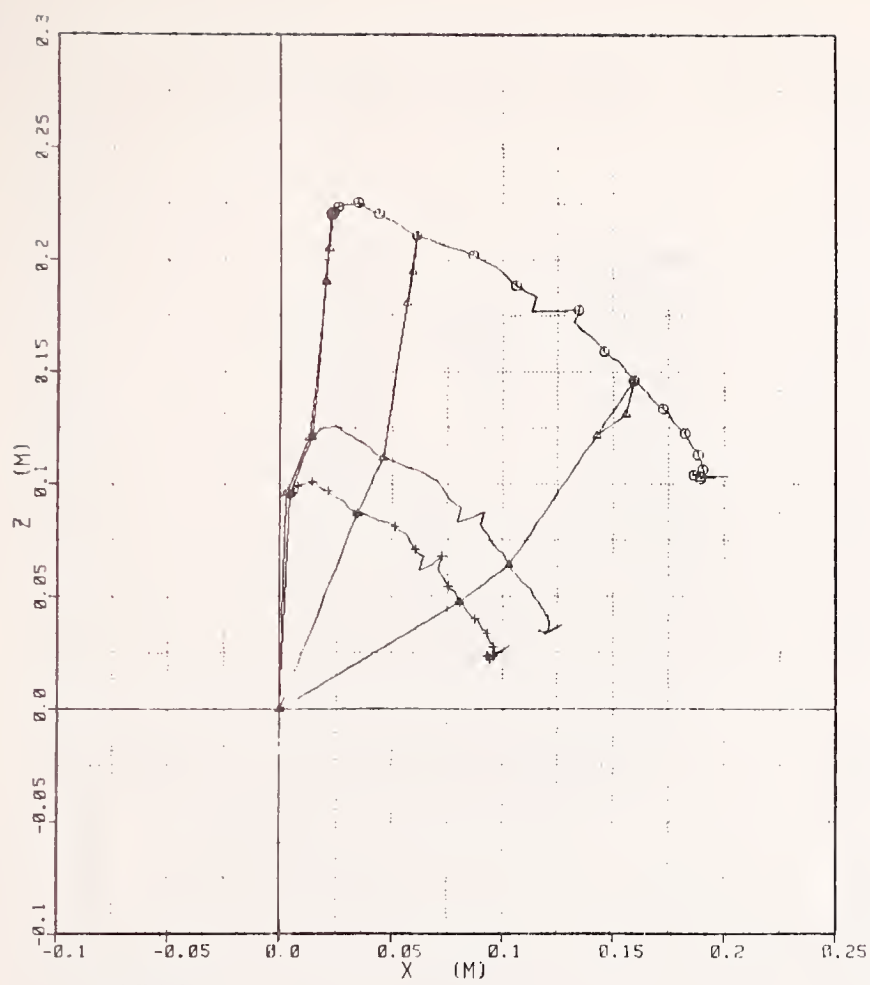
LX2151



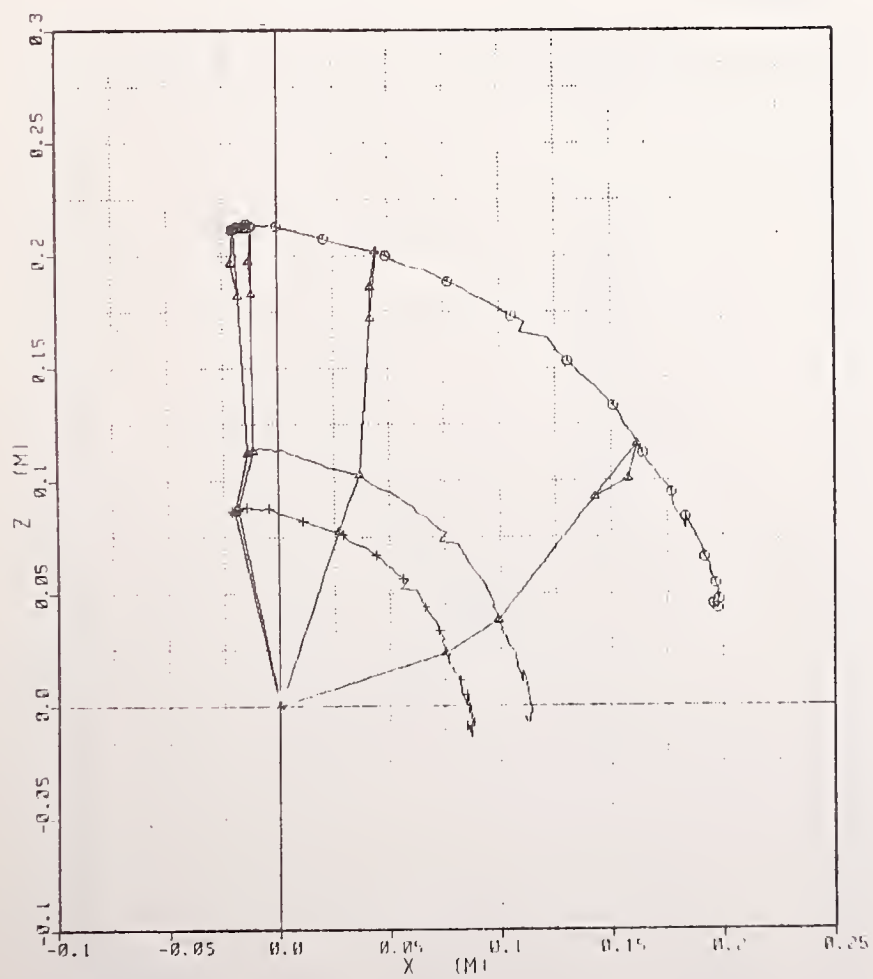
LX2326



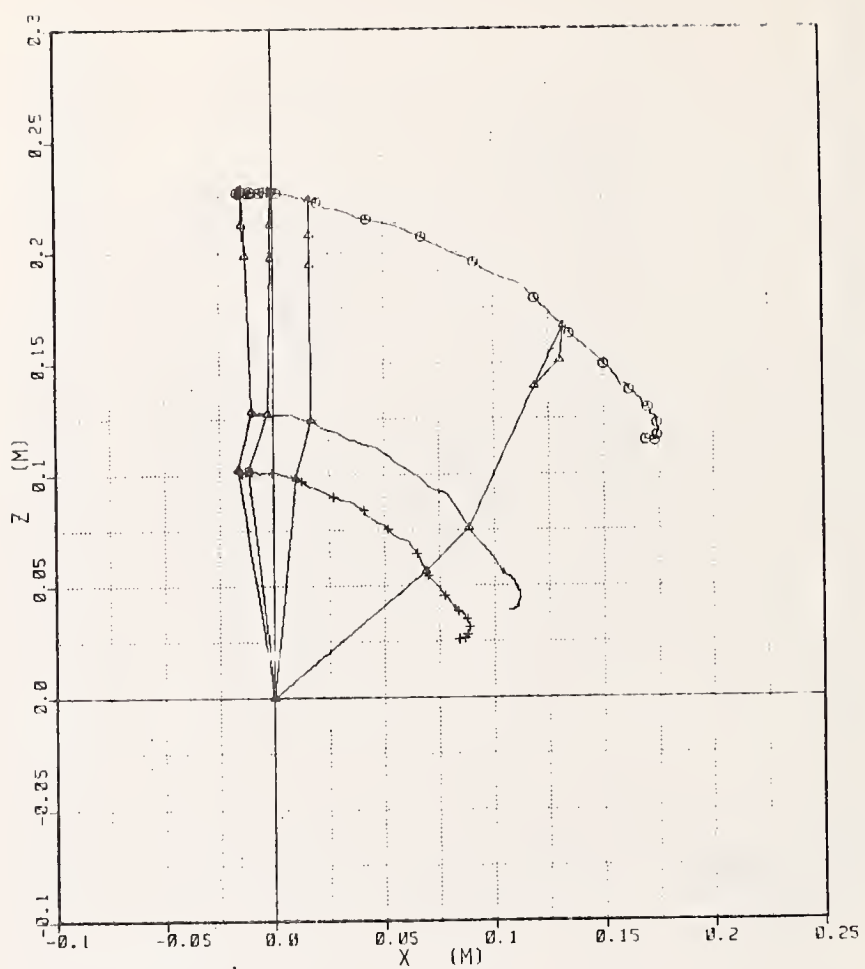
LX2355



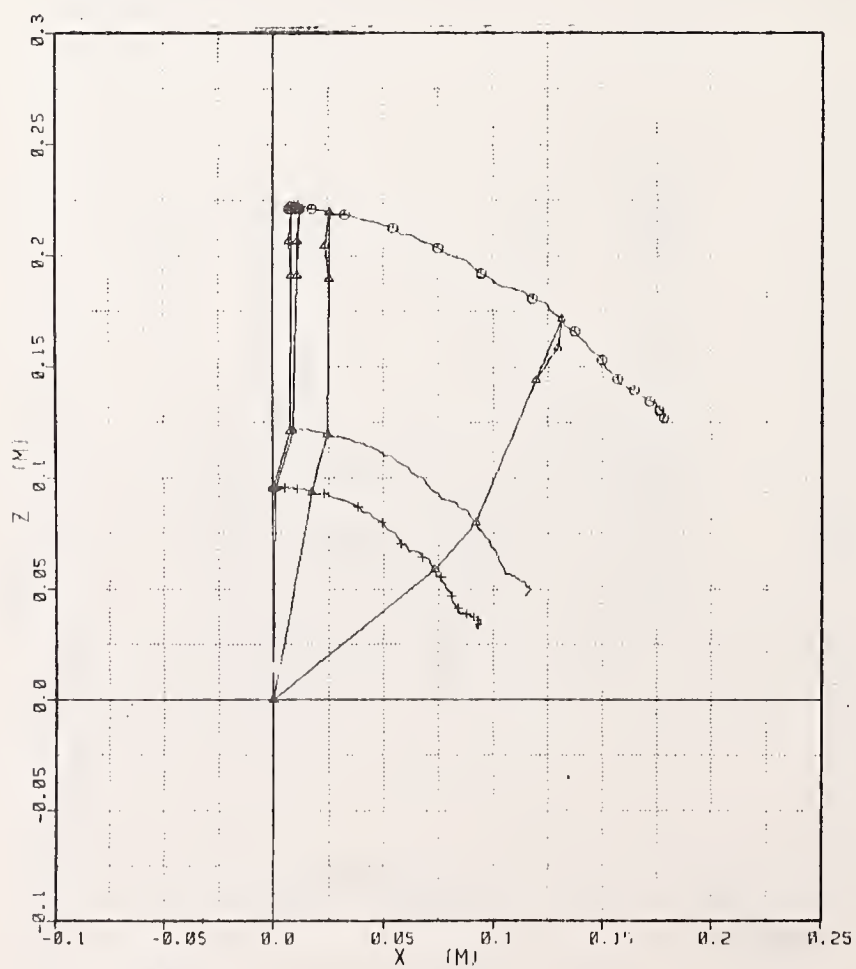
LX2786



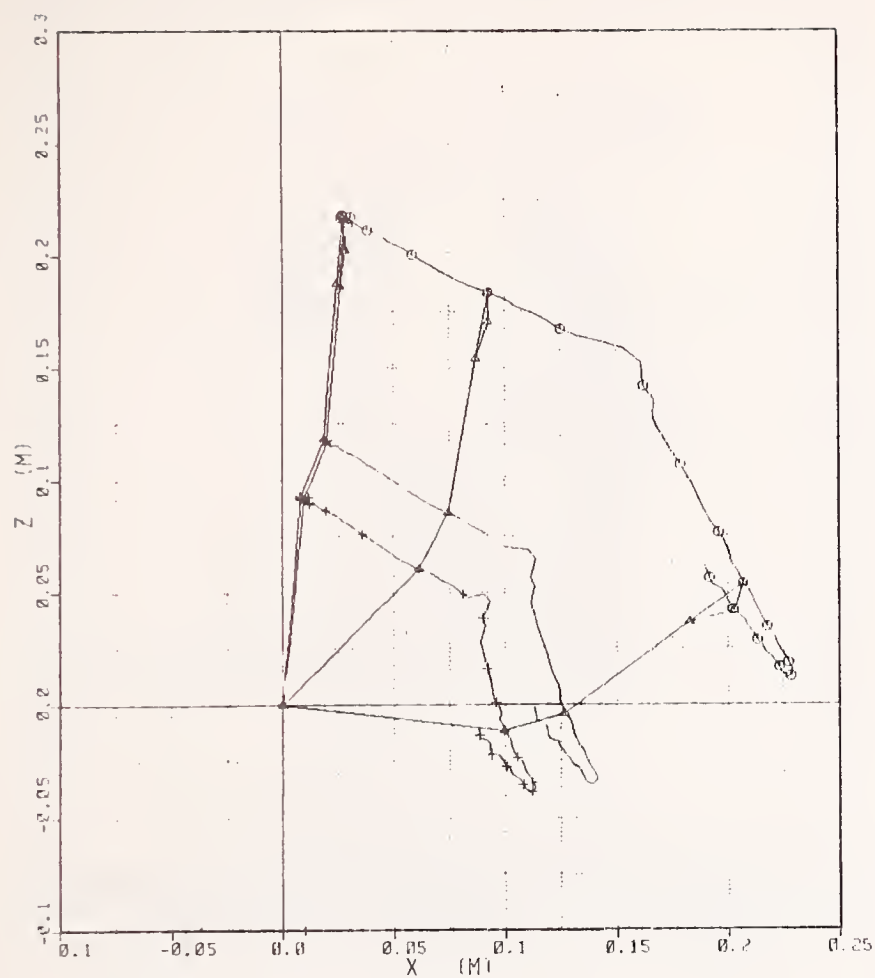
LX2872



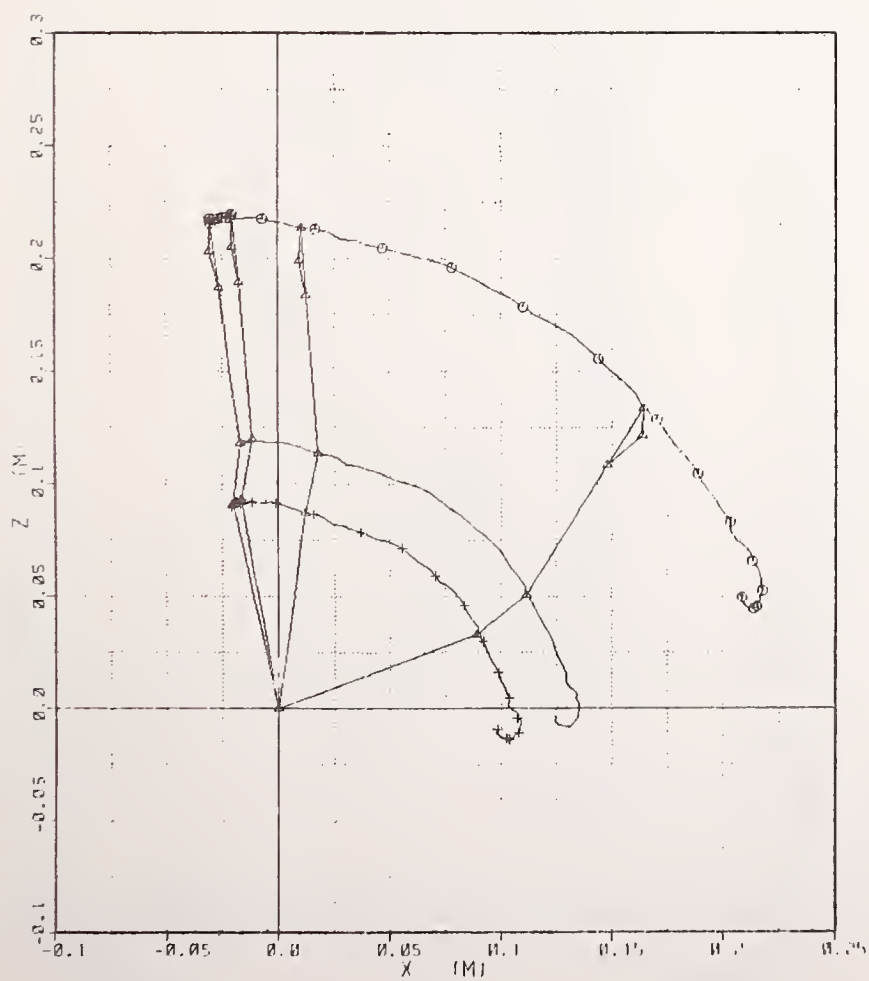
LX3093



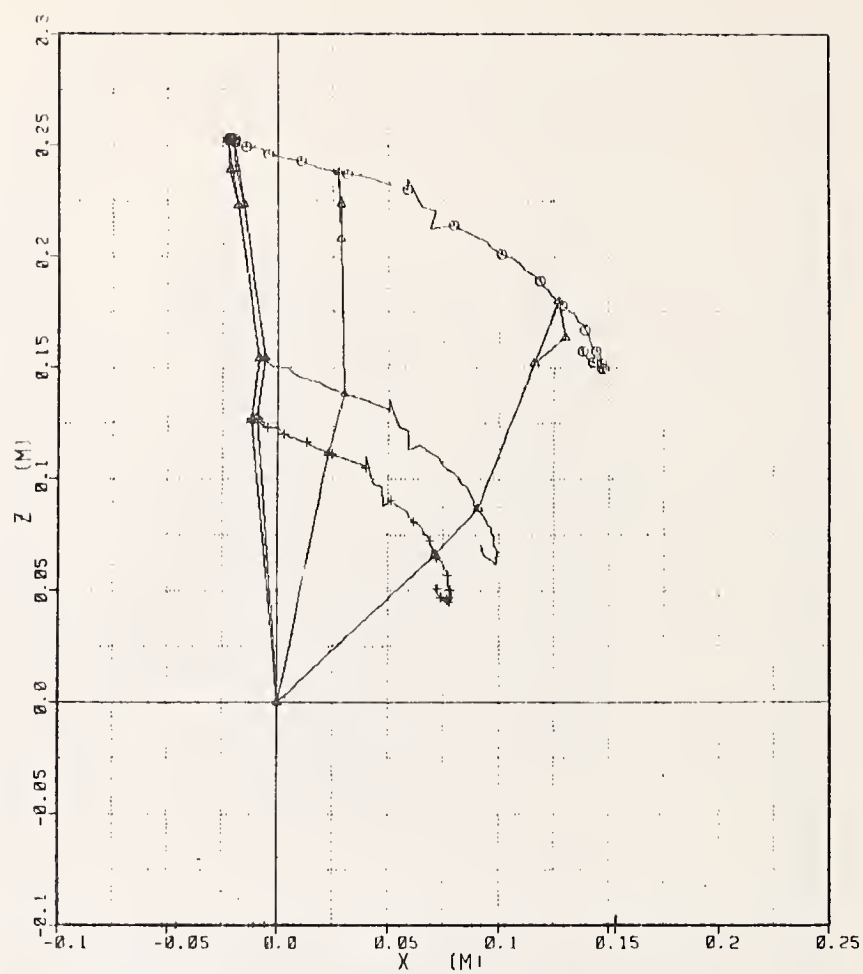
LX3102



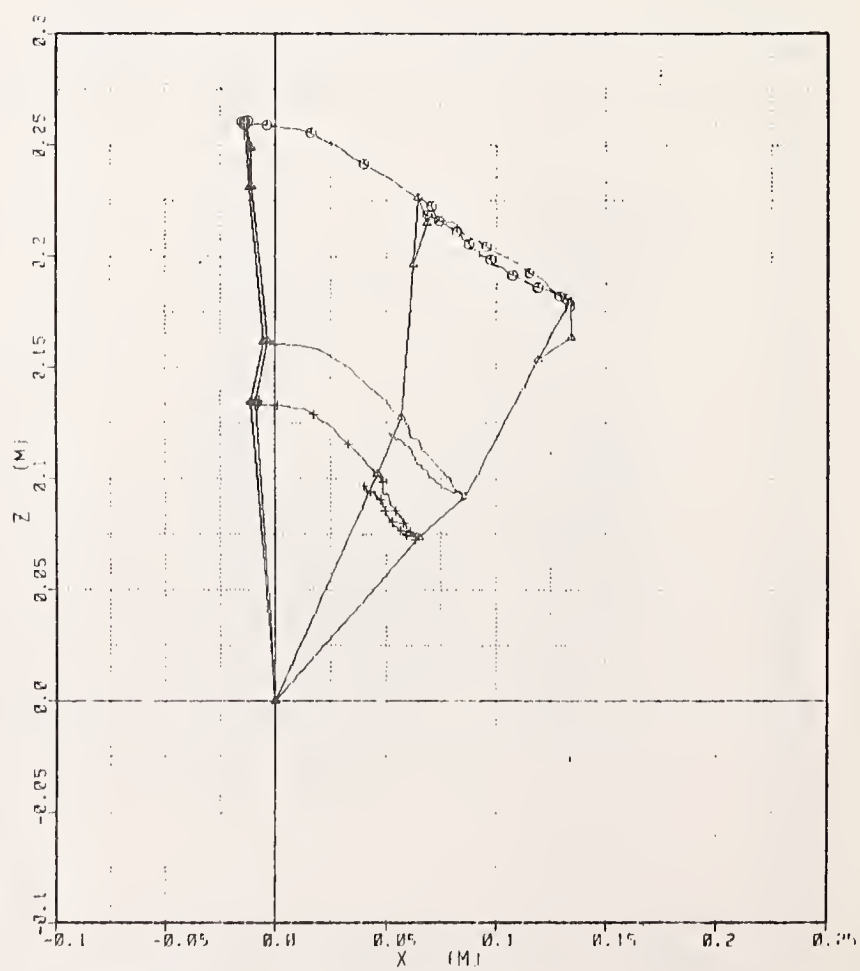
LX3153



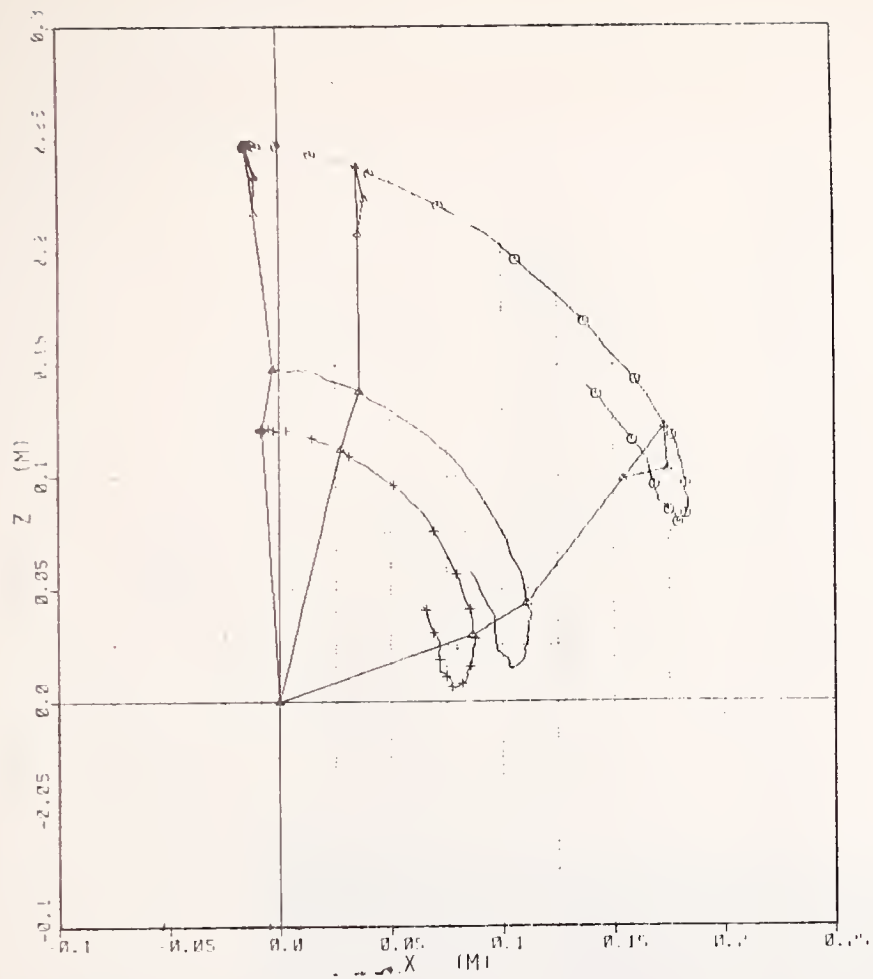
LX3133



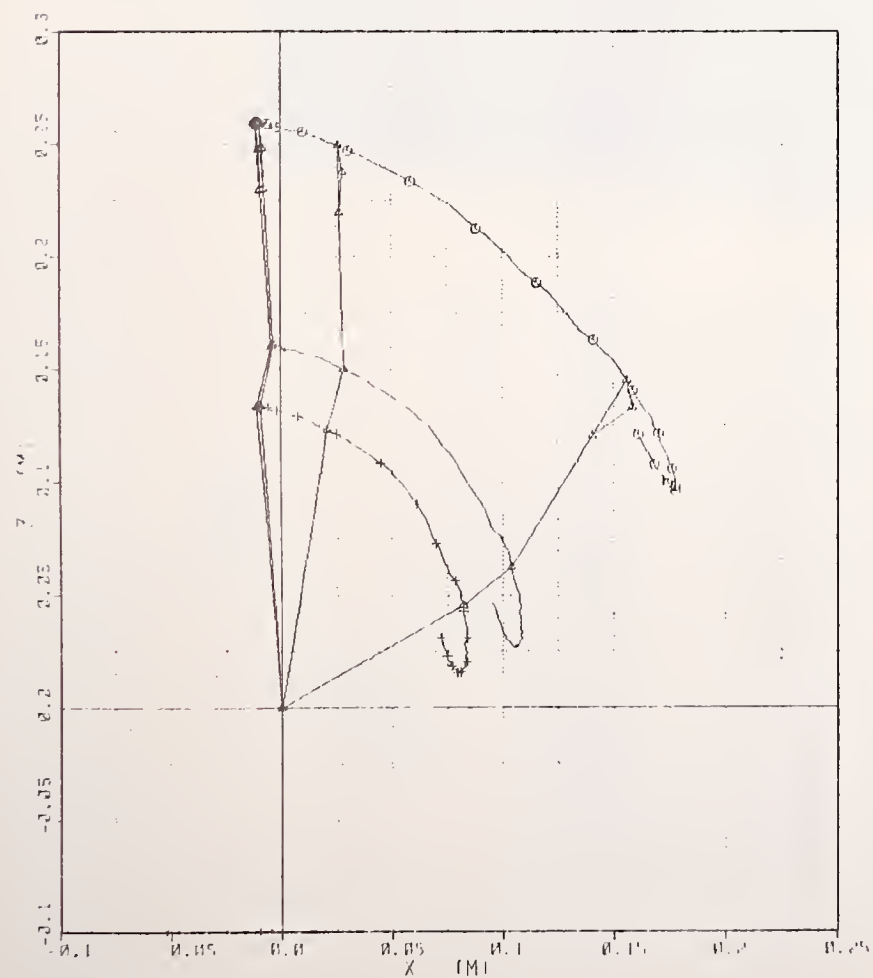
LX2784



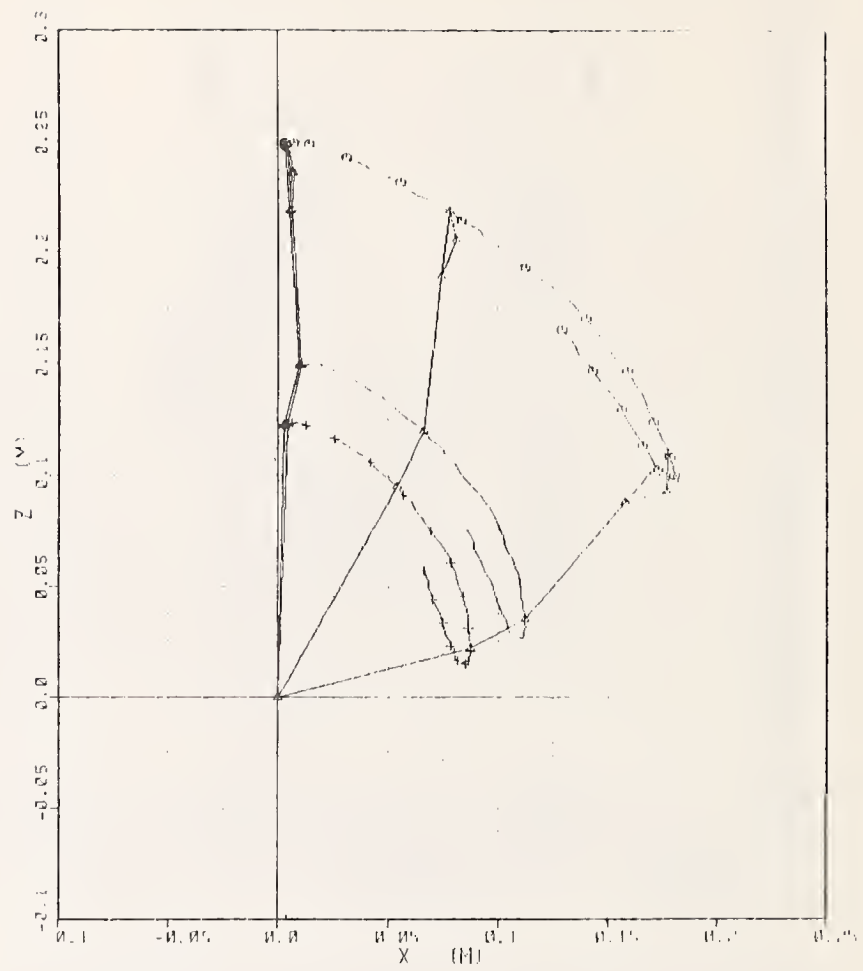
LX2843



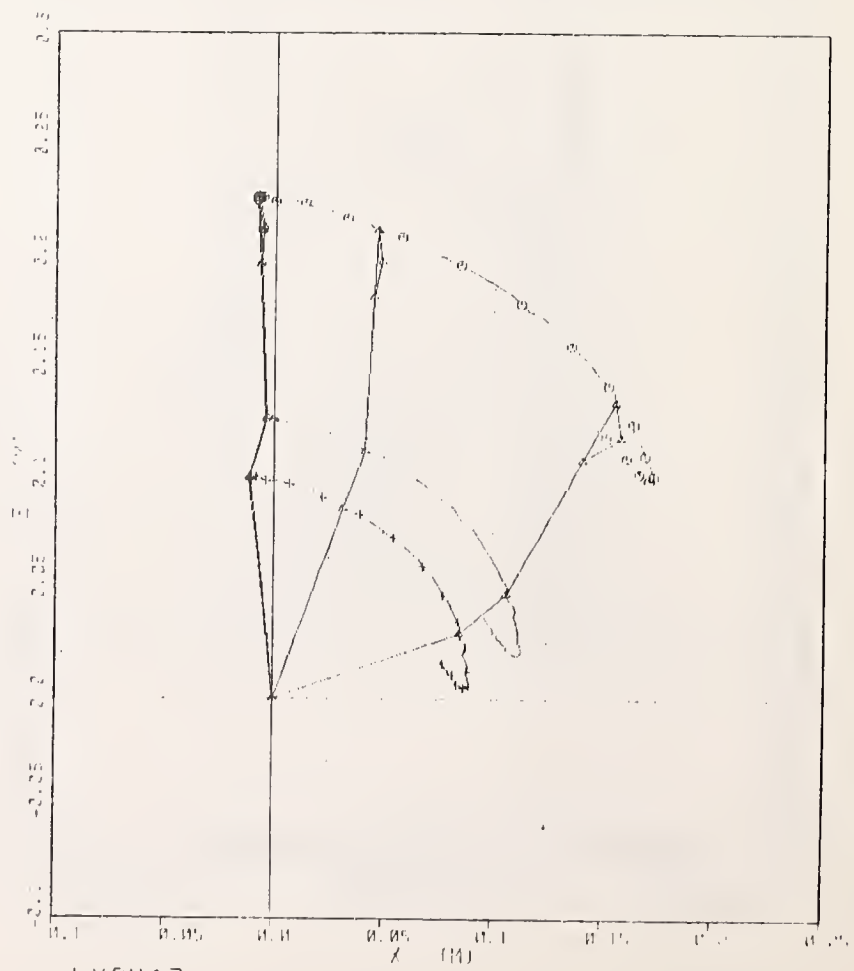
LX3148



LX3122



LX3158



LX3417

EPHONE	DATE
VPABEON	10/24/94
841-8384	

GPO 896-099

GP O 896-099

DOT LIBRARY



00177556